ELECTRONIC TUNING OF SITE SELECTIVITY AND SEMISYNTHESIS OF C2'-DEOXYAMPHOTERICIN B

BY

BRANDON C. WILCOCK

DISSERTATION

Submitted in partial fulfillment of the requirements
for the degree of Doctor of Philosophy in Chemistry
in the Graduate College of the
University of Illinois at Urbana-Champaign, 2013

Urbana, Illinois

Doctoral Committee:

Professor Martin D. Burke, Chair
Professor Wilfred A. van der Donk
Professor Scott K. Silverman
Professor Richard H. Perry

ABSTRACT

The small molecule Amphotericin B (AmB) is a natural product that is utilized in the treatment of systemic fungal infections. AmB is effective against a broad spectrum of fungi, and resistance to this potent antifungal agent is rare. However, the use of AmB is limited due to its high toxicity. All of the details of the mechanism of AmB have not yet been elucidated, and a molecular understanding of the mechanisms and interactions of AmB would be an asset in the improvement of the therapeutic index of this antimycotic and in the development of other antimicrobials that would be refractory to resistance development.

AmB is known to self-assemble into ion channels in phospholipid membranes containing sterol. The resulting membrane permeabilization has long been the leading hypothesis for the primary mechanism of antifungal activity. Three possible interactions involving the carboxylic acid and mycosamine appendages of AmB have been predicted to play important roles in the mechanism. To investigate the mode of action of AmB, derivatives of AmB lacking one or both of these appendages were synthesized and submitted to biophysical assays to determine their roles in the possible mechanistic interactions. It was found that the mycosamine was essential for antifungal activity, forming ion channels and mediating a direct interaction with ergosterol.

The discovery that AmB directly binds ergosterol pointed to two possible primary mechanisms, membrane permeabilization through channel formation or ergosterol sequestration. The C35 hydroxyl group on AmB has been predicted to be important in the stabilization of the ion channel complex via hydrogen-bonding. A C35-deoxyAmB derivative was synthesized and evaluated for its antifungal activity, channel forming ability, and sterol binding capacity. C35-deoxyAmB was unable to permeablize yeast cells but still retained the ability to bind sterol and displayed significant antifungal activity. These findings support the conclusion that the primary mechanism of AmB is ergosterol sequestration.

Investigation of the mycosamine-sterol interaction is needed to further elucidate the mechanism of AmB. The mycosamine subunit contains multiple functional groups that could be involved in the AmB-sterol binding event. The C2’ hydroxyl group has been implicated in a potential hydrogen-bond interaction with the sterol. Electronic tuning of site-selective acylation reactions was developed towards the synthesis of a C2’-deoxyAmB derivative. More electron-rich acyl donors create a less exothermic reaction in which the transition state is more product-

like according to the Hammond Postulate. This more product-like transition state magnifies the site-discriminating interactions between the acylating complex and the substrate thereby engendering greater selectivity. The site-selective acylation of the C2' hydroxyl group allowed this hydroxyl to be isolated and deoxygenated. In addition, a hybrid route with a higher yielding and streamlined protection-deprotection sequence was also developed to produce the C2'-deoxyAmB derivative.

Acknowledgements

I would like to thank my advisor Dr. Martin Burke for support and guidance over my graduate career. I also thank the people that have served on my committee, Dr. Martin Burke, Dr. Wilfred van der Donk, Dr. Scott Silverman, Dr. Neil Kelleher, and Dr. Richard Perry for their input and advice throughout my journey to obtain my PhD. Additionally, I extend my gratitude to the organic and chemical biology secretaries for all of the assistance they have provided over the years.

I would also like to express my appreciation to all the past and present Burke group members for the advice and collaborative work environment they provided. I especially would like to thank all the co-workers on the projects I have been involved in: Brice Uno, Gretchen Bromann, Matthew Clark, Thomas Anderson, Ian Dailey, Matthew Endo, Kaitlyn Gray, Daniel Palacios, and David Siebert.

This work has been made possible through support and funding from the University of Illinois at Urbana-Champaign, National Institutes of Health, and Howard Hughes Medical Institute. The amphotericin B that made this work possible was generously donated by Bristol-Myers Squibb.

Abbreviations

Ac	acetate
AIBN	azobiidobutyronitrile
Alloc	allyloxycarbonyl
AmB	amphotericin B
AmdeB	amphoteronolide B
AmE	amphotericin B methyl ester
C2'-deoxyAmB	C2'-deoxy-amphotericin B
C35-deOAmB	C35-deoxy-amphotericin B
CBS	Corey-Bakshi-Shibata

CSA	(±)-10-camphorsulfonic acid	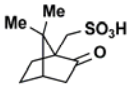
DDQ	2,3-dichloro-5,6-dicyano-1,4-benzoquinone	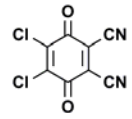
DIPEA	diisopropylethyl amine	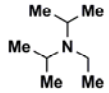
DEIPS	diethylisopropylsilyl	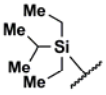
DMAP	4-(dimethylamino)-pyridine	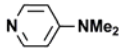
DMF	dimethyl formamide	
DMPC	1,2-dimyristoyl-sn-glycero-3-phosphocholine	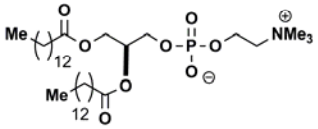
DMPU	1,3-dimethyl-3,4,5,6-tetrahydro2(1H)-pyrimidinone	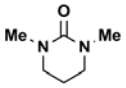
DMSO	dimethyl sulfoxide	
EYPC	egg yolk phosphatidylcholine	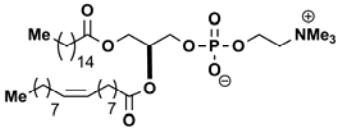
Fmoc	Fluorenylmethyloxycarbonyl	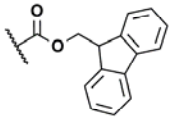
HPLC	high performance liquid chromatography	
ICC	iterative cross-coupling	
ITC	isothermal titration calorimetry	
LUV	large unilamellar vesicle	

MeAmB	C(41)-methyl amphotericin B
MeAmdeB	C(41)-methyl amphoteronolide B
MIC	minimum inhibitory concentration
MS	mass spectrometry
Ms	mesyl
NMR	nuclear magnetic resonance
PGA	penicillin G amidase
PMB	para-methoxybenzyl
PMP	para-methoxyphenyl
POPC	1-palmitoyl-2-oleoyl-sn-glycero-3-phosphocholine
Pyr	pyridine
TASF	tris(dimethylamino)sulfonium difluorotrimethylsilicate
TBAF	Tetra-n-butylammonium fluoride
TBS	t-butyldimethylsilyl
TES	triethylsilyl
THF	tetrahydrofuran

TLC	thin layer chromatography
TMSE	2-(trimethylsilyl)ethyl 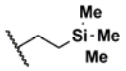
TIPS	triisopropylsilyl 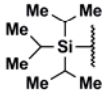
UV	ultraviolet

Table of Contents

Chapter 1

An Introduction to the Antimycotic Amphotericin B

This chapter discusses the importance of the polyene macrolide amphotericin B and the current understanding of the mechanism of its antifungal activity. As the last line of defense in the treatment of systemic fungal infections, amphotericin B is a critical therapeutic in the clinic despite its high toxicity. Amphotericin B also has a remarkable record of being refractory to resistance development. However, after over 50 years of study, many of the mechanistic details of how it functions are still unknown. The leading model and its hypothetical interactions are presented. Evaluation of the model and these interactions to gain a better understanding of the mechanism on a molecular level will be an asset in the improvement of the therapeutic index and design of resistance-refractory antimicrobials.

1-1 Amphotericin B is an Important Antimycotic

Amphotericin B (AmB, Figure 1.1) is an important antimicrobial agent used for the treatment of invasive fungal infections.[1-3] Systemic fungal infections represent a serious problem in human health. Systemic fungal infections afflict a large number of people, and the mortality rates are often quite high (Table 1.1).[4] This is especially true of immunocompromised patients who are particularly susceptible to contracting systemic fungal infections.[5] In addition, the incidence of systemic fungal infections is increasing.[6] AmB is a member of the class of antifungal agents known as the polyene macrolides. Isolated in the 1950's from *Streptomyces nodosus*,[7] AmB has been used in the clinic for over fifty years. It is effective across a broad range of fungi and yeast and is quite potent. Also, drug resistance to AmB is quite rare; this is in contrast to many other antimicrobials where drug resistance development is a growing problem and a major concern in the healthcare system.[8-10]

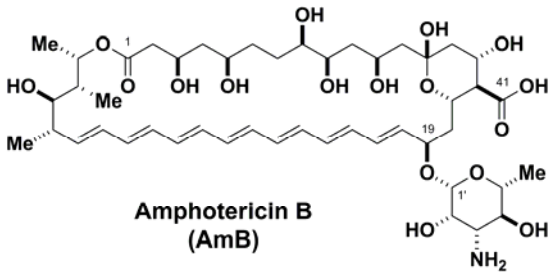

Figure 1.1. The polyene macrolide antimycotic amphotericin B.

AmB, however, does have drawbacks associated with it that limit its use, namely high toxicity and poor pharmacological properties.[11] Even after over fifty years of study, the mechanistic details of how AmB functions have yet to be fully elucidated.[12-14] A detailed understanding of how AmB operates on a molecular level would be beneficial to human health in terms of improving its therapeutic index and applying the underlying principles that bestow potency and resistance-refractory traits to the development of future antimicrobials.

Estimated World Incidence

Organism	Cases/year	Organism	Cases/year
Candida	~300,000	*Histoplasma*	~500,000
Aspergillus	~350,000	*Pneumocystis*	~200,000
Cryptococcus	~1,000,000	*Coccidioidomyces*	~300,000

Mortality Rates

Candida	~30-55%
Aspergillus	~50%
Cryptococcus	~60%

Table 1.1. Estimated world incidence and mortality rates of some systemic fungal infections.
Data from the Fungal Research Trust, How common are fungal diseases? Fungal Research Trust 20th Anniversary Meeting. June 18th **2011**.

1-2 Early studies and the Development of the Leading Model

Early studies with AmB and *A. laidlawii* cells that do not produce their own sterols demonstrated that the activity of AmB was sterol dependent. *A. laidlawii* cells that were grown without sterols were not susceptible to AmB; however, if the cells were grown in the presence of cholesterol that they could uptake, they were susceptible to AmB.[15] While the activity of AmB has been linked to a sterol dependence in the membrane, the exact function of the sterol is unknown. Additional studies with the *A. laidlawii* cells showed that when sterols are present in the membrane, AmB induces membrane permeability.[16] The sterol dependence of the activity and membrane permeabilization abilities of AmB has been shown in numerous other studies with cells, liposomes, and planar lipid bilayers.[17-26] Addition of extra sterols can diminish the efficacy of AmB.[18] While AmB caused increased permeability of ions and small solutes, increased permeability of glucose and larger molecules was not observed.[17] A significant advance came with the observation of single ion channels in planar lipid bilayers upon addition of AmB.[27,28] All of these early biophysical experiments created the foundation of the leading theory in which AmB associates with the membrane and self assembles into a channel complex with a 7-10

angstrom pore causing membrane permeabilization that leads to cell death. Other mechanisms based upon AmB-induced oxidative damage have also been proposed.[29]

The structure of the ion channel is not known. It is proposed that eight AmB molecules come together to forming a barrel-stave like structure with the polyol portion lining the inside and the polyene facing the lipid matrix (Figure 1.2).[30-32] The role of the sterol and whether it is directly bound or part of the channel complex has long been a matter of debate in the literature. In one model, there is a direct interaction with the sterol that stabilizes the channel structure. In the opposing model, the sterol doesn't associate with AmB but instead preorganizes the membrane to allow channel formation. While the activity of AmB has been shown to be

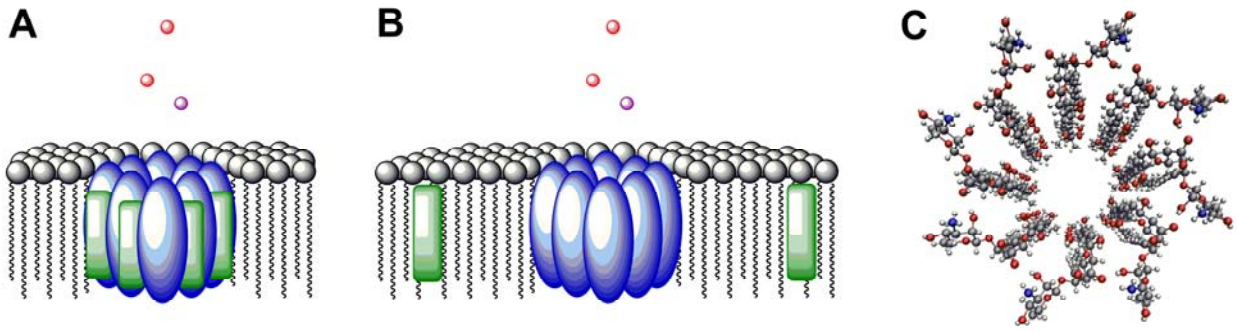

Figure 1.2. Hypothetical models of AmB ion channels. **A**. AmB (blue) assembled into an ion channel complex directly interacting with sterols (green). **B**. AmB ion channel formation supported by indirect membrane preorganization by sterols. **C**. Top down view of hypothetical AmB ion channel model.

dependent upon the specific sterol, experiments with different sterols and sterol derivatives are inconclusive when resolving the direct versus indirect models because the change in sterol can affect the direct binding event and/or change the global membrane properties. Several molecular modeling and computational studies have also been done to investigate possible properties of this channel model.[33-37]

1-3 Predicted Interactions of the Leading Model

Several interactions have been proposed to be active in the membrane permeability mechanism (Figure 1.3). These interactions are centered around two functional group appendages on the AmB macrolide, the C41 carboxylic acid and the C19 mycosamine sugar. These two groups are installed by enzymes post polyketide synthase construction of the macrocycle.[38] Under physiological conditions, the C41 acid exists as the carboxylate and the amine on the C19 mycosamine unit is protonated, making AmB zwitterionic. The first

interaction in the channel model involves a salt-bridge between the charged carboxylate of an AmB molecule and the protonated amine on the mycosamine of the adjacent AmB molecule in the complex.[33-37,39,42,43] This interaction would create a ring of stabilization around the channel complex. The second potential interaction is between the phospholipid headgroups and the carboxylate and/or mycosamine.[40,44,45] This interaction would play an important role anchoring the ion channel complex to the membrane. A possible third interaction is the direct binding of sterol to the carboxylate and/or mycosamine.[21,33-37,41,46,47]

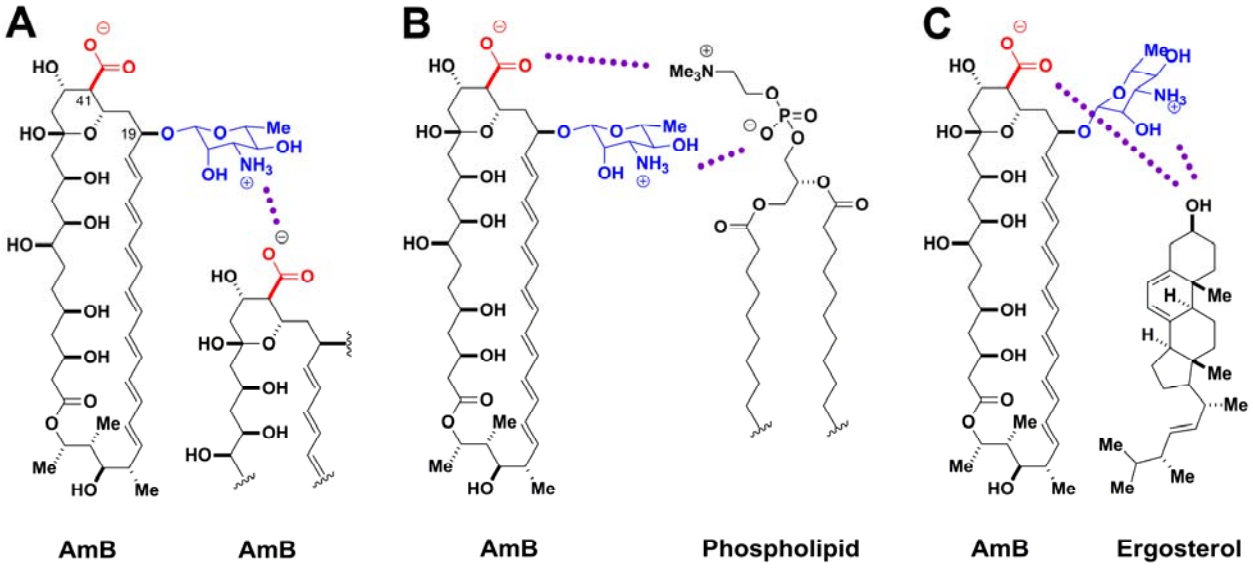

Figure 1.3. Possible interactions of the leading AmB ion channel model. **A**. Intermolecular AmB interaction between the C41 carboxylate and the C19 mycosamine. **B**. AmB binding to phospholipid headgroups **C**. Direct binding interaction between AmB and ergosterol. Figure adapted from ref. 48.

Insights into the possible mechanism of AmB can be obtained by probing the roles of these two functional appendages on the AmB macrolide skeleton through biophysical studies. The carboxylic acid and amine have unique reactivities that have been taken advantage of in the synthesis of derivatives of AmB that are covalently modified at these two positions.[12,13,14] However, the conclusions that can be made from biophysical experiments with these derivatives can be limited by the possible effects due to additional steric bulk being introduced and remaining abilities to hydrogen bond. Computer modeling has also been utilized to support the possibility of the existence of these mechanistic interactions.[33-37] Biophysical evaluation of AmB derivatives that lack the C41 carboxylate and/or the C19 mycosamine would be an effective way

to evaluate their contributions to the mechanism[48] in a similar fashion to alanine scanning in protein science.

1-4 References

1. Ellis, D. *J. Antimicrob. Chemother*. **2002**, *49*, 7-10.
2. Omura, S.; Tanaka, H. *Macrolide Antibiotics*. Acadaemic Press: Orlando, FL, **1984**.
3. Gibbs, W. J.; Drew, R. H.; Perfect, J. R. *Expert Rev. Anti-Infective Ther.* **2005**, *3*, 167-181.
4. Fungal Research Trust, How common are fungal diseases? Fungal Research Trust 20th Anniversary Meeting. June 18th **2011**.
5. Pfaller, M. A.; Diekema, D. *J. Crit. Rev. Microbiol.* **2010**, *36*, 1-53.
6. Martin, G. S.; Mannino, D. M.; Eaton, S.; Moss, M. *New Engl. J. Med.* **2003**, *348*, 1546-1554.
7. Donnovick, R.; Gold, W.; Pagano, J. F.; Stout, H. A. *Antibiot. Annu.* **1955**, *3*, 236-239.
8. Perea, S.; Patterson, T. F. *Clinical Infectious Diseases.* **2002**, *35*, 1073-1080.
9. Talbot, G. H.; Bradley, J.; Edwards, J. E.; Gilbert, D.; Scheld, M.; Bartlett, J. G. *Clinical Infectious Diseases.* **2006**, *42*, 657-668.
10. Kontoyiannis, D. P.; Lewis, R. E. *Lancet.* **2002**, *359*, 1135-1144.
11. Gallis, H. A.; Drew, R. H; Pickard, W. W. *Rev. Infect. Dis.* **1990**, *12*, 308-329.
12. Volmer, A. A.; Szpilman, A. M.; Carreira, E. M. *Nat. Prod. Rep.* **2010**, *27*, 1329-1349.
13. Cereghetti, D. M.; Carreira, E. M. *Synthesis.* **2006**, *6*, 914-942.
14. Bolard, J. *Biochim, Biophys. Acta.* **1986**, *864*, 257-304.
15. Feingold, D. S. *Biochem. Biophys. Res. Commun.* **1965**, *19*, 261.
16. de Kruijff, B.; Gerritsen, W. J.; Oerlemans, A.; Demel, R. A.; van Deenen, L. L. M. *Biochim. Biophys. Acta.* **1974**, *339*, 30-43.
17. Andreoli, T. E.; Dennis, V. W.; Weigl, A. M. *J. Gen. Physiol.* **1969**, *53*, 133-156.
18. Gottleib, D.; Carter, H. E.; Sloneker, J. H.; Amman, A. *Science.* **1958**, *128*, 361.
19. HsuChen, C.; Feingold, D. S. *Biochem. Biophys. Res. Commun.* **1973**, *51*, 972-978.
20. HsuChen, C.; Feingold, D. S. *Antimicrob. Agents Chemother.* **1973**, *4*, 309-315.
21. Kotler-Brajtburg, J.; Price, H. D.; Medoff, G.; Schlessinger, D.; Kobayashi, G. S. *Antimicrob. Agents Chemother.* **1974**, *5*, 377-382.
22. Kinsky, S.C.; *Biochim. Biophys. Res. Commun.* **1961**, *5*, 353.
23. Zygmunt, W. A. *Appl. Microbiol.* **1966**, *14*, 953-956.

24. Andreoli, T. E.; Monahan, M. *J. Gen. Physiol.* **1968**, *52*, 300-325.
25. Finkelstein, A. Krespi, V. *J. Gen. Physiol.* **1970**, *56*, 100-124.
26. Shigeru, M.; Murata, M. *Biochim. Biophys. Acta.* **2002**, *1564*, 429-434.
27. Ermishkin, L. N.; Kasumov, K. M.; Potzeluyev, V. M. *Nature*. **1976**, *262*, 698-699.
28. Borisova, M. P.; Ermishkin, L. N.; Silberstein, A. Y. *Biochim. Biophys. Acta.* **1979**, *553*, 450-459.
29. Kovacic, P.; Cooksy, A. *Med. Chem. Commun.* **2012**, *3*, 274-280.
30. de Kruijff, B.; Demel, R. A. *Biochim. Biophys. Acta*. **1974**, *339*, 57-70.
31. Finkelstein, A.; Holz, R. *Membranes. Lipid Bilayers and Antibiotics.* Eisemand, G.; Ed. Marcel Dekker: NewYork, **1973**.
32. Andreoli, T. E. *Ann. N. Y. Acad. Sci.* **1974**, *235*, 448-468.
33. Khutorsky, V. E.; *Biochim. Biophys. Acta.* **1992**, *1108*, 123-127.
34. Baginski, M.; Resat, H.; McCammon, J. A. *Mol. Pharm.* **1997**, *52*, 560-570.
35. Baginski, M.; Resat, H.; Borowski, E. *Biochim. Biophys. Acta.* **2002**, *1567*, 63-78.
36. Czub J.; Baginski, M. *J. Phys. Chem. B.* **2006**, *110*, 16743-16753.
37. Neumann, A.; Czub, J.; Baginski, M. *J. Phys. Chem. B.* **2009**, *113*, 15875-15885.
38. Caffery, P.; Lynch, S.; Flood, E.; Finnan S.; Oliynyk, M. *Chem. Biol.* **2001**, *8*, 713-723.
39. Kasumov, K. M.; Borisova, M. P.; Ermishkin, L. N.; Potseluyev, V. M.; Silberstein, A. Y. *Biochim. Biophys. Acta* **1979**, *551*, 229-237.
40. Balakrishnan, A. R.; Easwaran, K. *Biochemistry* **1993**, *32*, 4139-4144.
41. Herve, M.; Debouzy, J. C.; Borowski, E.; Cybulska, B.; Gary-Bobo, C. M. *Biochim. Biophys. Acta* **1989**, *980*, 261-272.
42. Schaffner, C. P.; Borowski, E. *Antibiot. Chemother.* **1961**, *11*, 724.
43. Mechlinski, W.; Schaffner, C. P. *J. Antibiot.* **1972**, *30*, 256-258.
44. Czub, J.; Borowski, E.; Baginski, M. Biochim. *Biophys. Acta* **2007**, *1768*, 2616-2626.
45. Minones, J. *Langmiur* **2002**, *18*, 2817-2827.
46. Baran, M.; Mazerski, M. *Biophys. Chem.* **2002**, *95*, 125-133.
47. Matsumori, N.; Sawada, Y.; Murata, M. *J. Am. Chem. Soc.* **2005**, *127*, 10667-10675.
48. Palacios, D. S.; Dailey, I.; Siebert, D. M.; Wilcock, B. C.; Burke, M. D. *Proc. Natl. Acad. Sci. U. S. A.* **2011**, *108*, 6733-6738.

Chapter 2

Discovery of a Critical Mycosamine-Mediated Sterol Interaction

This chapter details the investigation of the roles of the C41 carboxylate and the C19 mycosamine in the mechanism of amphotericin B. The synthesis of functional-group deficient derivatives and subsequent biophysical studies allowed the evaluation of hypothetical interactions in the leading model for amphotericin B antifungal activity. This resulted in the discovery that the mycosamine appendage of AmB is required for a direct interaction with ergosterol, channel formation, and antifungal activity. Dan Palacios developed the synthetic routes to the AmB derivatives. The AmB derivatives were prepared by Dan Palacios and Brandon Wilcock. Membrane binding and MIC experiments were performed by Dan Palacios and Dave Siebert. Voltage clamp and yeast potassium efflux experiments were done by Dan Palacios. ITC experiments were conducted by Dan Palacios and Ian Dailey. Portions of this chapter have been adapted from Palacios, D. S.; Dailey, I.; Siebert, D. M.; Wilcock, B. C.; Burke, M. D. *Proc. Natl. Acad. Sci. U. S. A.* **2011**, *108*, 6733-6738.

2-1 C41 Carboxylic Acid and C19 Mycosamine Functional-Group Deficient Derivatives

In order to provide clean experiments to investigate the hypothetical interactions pertaining to the roles of the carboxylic acid and mycosamine in the mechanism (see Chapter 1), derivatives of AmB where these groups are removed or "synthetically deleted" were envisioned. Removal of these groups would reveal if the groups were essential to the proposed interactions in the mechanistic model (Figure 1.3) without the complications of steric perturbations or remaining hydrogen-bonding ability. My colleague Dan Palacios therefore expanded upon previous degradative synthetic studies on AmB carried out by Nicolaou[1] and the Smith-Kline Beecham group[2] to develop a mild and modular synthesis of three derivatives of AmB: the C41-methyl amphotericin B (MeAmB) lacking oxidation at C41, amphoteronolide B (AmdeB) with no mycosamine sugar, and C41-methyl amphoteronolide B (MeAmdeB) missing both groups (Scheme 2.1). Dan Palacios and I were able to synthesize large quantities of these derivatives for biophysical studies conducted by my coworkers Dan Palacios, Ian Dailey, and David Siebert.[3]

Global protection of AmB via Fmoc protection of the amine, conversion of the hemi ketal to the methyl ketal, and silylation of the hydroxyl groups creates a common intermediate. The

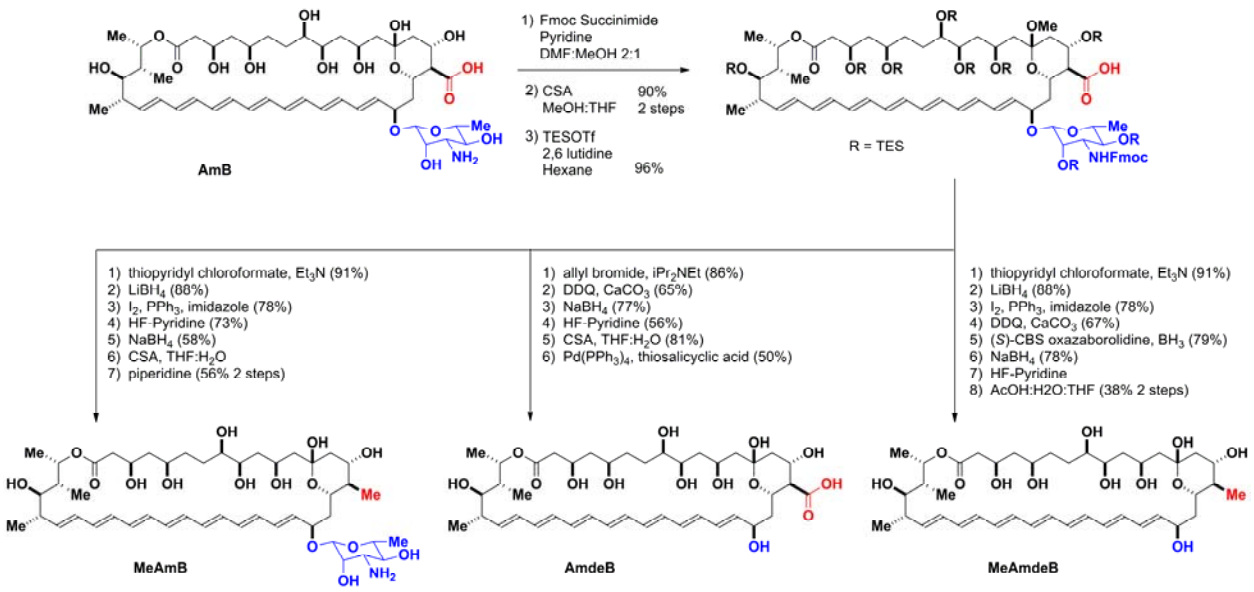

Scheme 2.1. Synthesis of C41-methyl amphotericin B (MeAmB), amphoteronolide B (AmdeB), and C41-methyl amphoteronolide B (MeAmdeB). Scheme adapted from ref. 3

C41 carboxylic acid can be reduced to an alcohol via activation as a thioester. The alcohol can then be transformed to an iodide and reductively displaced to create a methyl group at C41. The mycosamine can be removed, after acid protection, via oxidative cleavage. Subsequent reduction of the conjugated enone results in the allylic alcohol at C19. Employing one or both of these modules in conjunction with global deprotection allows for the synthesis of the functional-group deficient derivatives MeAmB, AmdeB, and MeAmdeB (Scheme 2.1).[3,4]

The consequences of deleting these groups on the antifungal activity was determined by the minimum inhibitory concentration (MIC) against the growth of two yeast strains, *S. cerevisiae* and the pathogenic *C. albicans* (Table 2.1).[3] It was discovered that MeAmB was equipotent to the natural product AmB. However, AmdeB was found to be inactive displaying no antifungal activity. This allows us to conclude that the carboxylic acid oxidation state at C41 is not required for antifungal activity and the mycosamine sugar is essential for antifungal activity. Further biophysical studies were undertaken to investigate the predicted interactions in order to determine what role the mycosamine was playing that caused the loss of activity.

MIC (μM)	AmB	MeAmdeB	AmdeB	MeAmB
S. cerevesiae	0.5	>50	>50	0.5
C. albicans	0.25	>50	>50	0.25

Table 2.1. MIC values for AmB and derivatives. Table adapted from ref. 3.

2-2 Membrane Permeabilization and Channel Formation

Membrane permeabilization via channel formation has long been a popular hypothesis as a main component of the antifungal activity for the mechanism of AmB. There are, however, some reports that question whether channel formation is the cause of cell death.[5-7] At physiological pH, the C41 acid exists as the carboxylate and the C3' amine on the mycosamine is protonated. One of the key predicted stabilizing interactions of the leading theoretical channel complex model is an electrostatic bond between these two charged groups. Computational modeling studies are in agreement with the existence of this interaction.[8-13]

Covalent derivatives of AmB have been employed to investigate this interaction. For instance, the C41 ester of AmB still displayed potent membrane permeabilization and antifungal activity against yeast.[14,15] However, acylating the amine results in a reduction in activity and membrane permeablization.[14,15] Caution must be exercised in the interpretation of these results due to the ester and amide derivatives still retain the ability to have a polar interaction. In addition, small molecule assembly is known to often be sensitive to steric effects, and the added steric bulk of these derivatives may be contributing to reduced capacity to self assemble into ion channels. We therefore decided to determine the channel forming and membrane permeabilization abilities of the functional-group deficient derivatives we synthesized.

I conducted some preliminary membrane permeabilization studies with AmB, AmdeB, and MeAmB. Potassium efflux experiments with egg yolk phosphatidylcholine (EYPC) large unilamellar vesicles (LUVs) containing 10% ergosterol were performed with a range of concentrations of the polyene macrolides to determine the required concentrations for membrane permeabilization. I found robust efflux was observed for AmB and MeAmB at 1 μM; in contrast, AmdeB showed no efflux. These membrane experiments were further continued and expanded into potassium efflux from yeast cells by Dan Palacios. The results from the yeast potassium efflux assays paralleled the LUV experiments with the compounds containing the mycosamine inducing membrane permeabilization and the compounds lacking the mycosamine causing no efflux (Figure 2.1 A, B).[3]

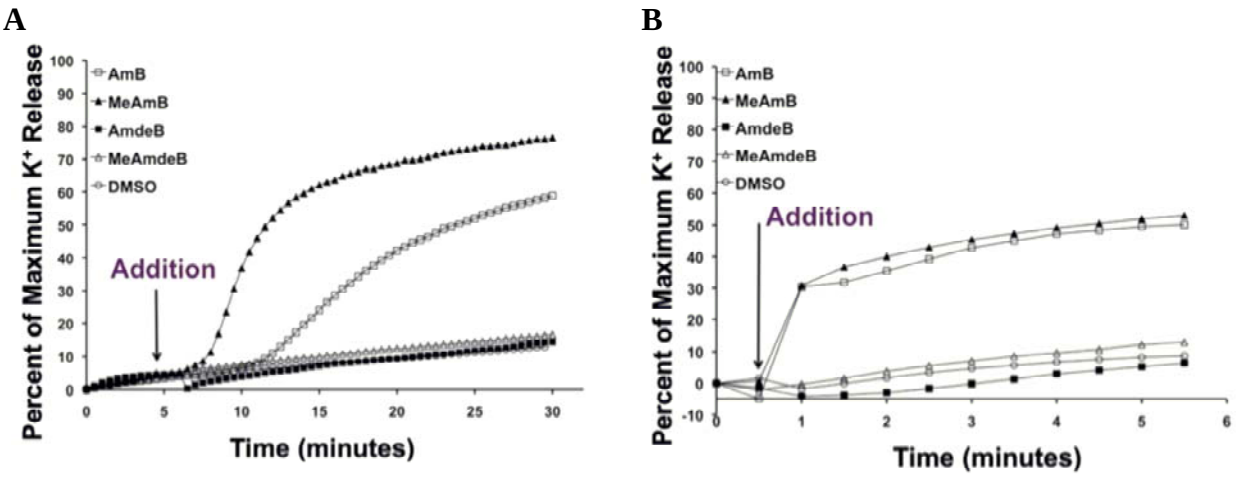

Figure 2.1. Membrane Permeabilization Studies. **A**. Potassium efflux in yeast (*S. cerevisiae*) after addition of polyene macrolides (3 μM). **B**. Potassium efflux in 10% ergosterol LUVs after addition of polyene macrolides (1 μM). Figure adapted from ref. 3.

To further investigate the channel forming capacity and confirm that the potassium efflux activity was due to channel formation and not indiscriminate membrane defects, Dan Palacios also conducted voltage clamp recordings with the polyene macrolides and planar lipid bilayers containing ergosterol (Figure 2.2).[3] These experiments showed single ion channel recordings for AmB and MeAmB and not for AmdeB or MeAmdeB. Collectively, efflux and voltage clamp experiments demonstrate the mycosamine is required for the channel formation of AmB. The

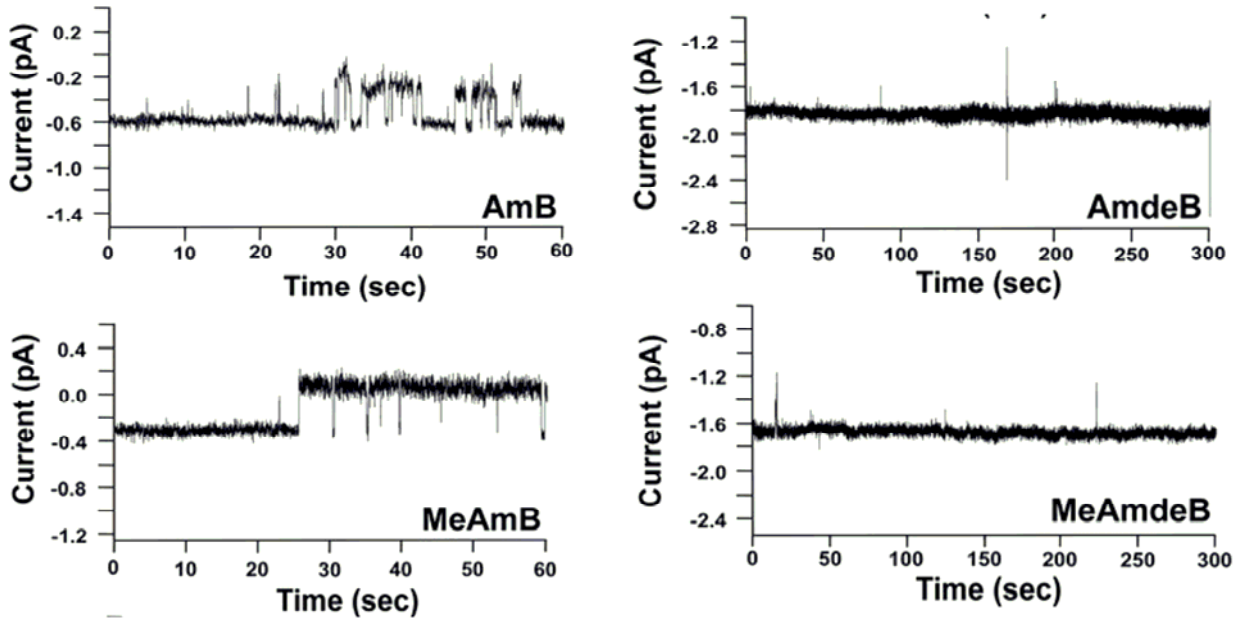

Figure 2.2. Voltage clamp recordings with planar lipid bilayers containing ergosterol after addition of polyene macrolides at an applied potential of 150 mV. AmB (10 nM), MeAmB (75 nM), AmdeB (100 nM), MeAmdeB (50 nM). Figure adapted from ref. 3.

fact that MeAmB, which lacks the carboxylate and thus is unable to create the stabilizing ring of electrostatic interactions with the C3' amine, forms channels supports the conclusion that the salt-bridge interaction is not necessary to stabilize the channel complex.

2-3 Membrane and Ergosterol Binding

Missing interactions with the phospholipid head groups could also underlie the observed lack of activity and channel formation of these mycosamine-deficient derivatives. Previous reports, including NMR and computational experiments, have suggested that AmB forms a complex with the lipids.[9-11,16-18] This interaction would play a crucial role in anchoring AmB and the complex to membrane and/or stabilizing the complex. This was investigated by David Siebert and Dan Palacios by determining the ability of the derivatives to bind LUVs containing ergosterol and yeast membranes. It was found that all the compounds incorporated and bound to both LUVs and yeast membranes indicating that neither the C41 carboxylic acid nor the mycosamine are essential for AmB to associate with membranes (Figure 2.3 A, B).[3]

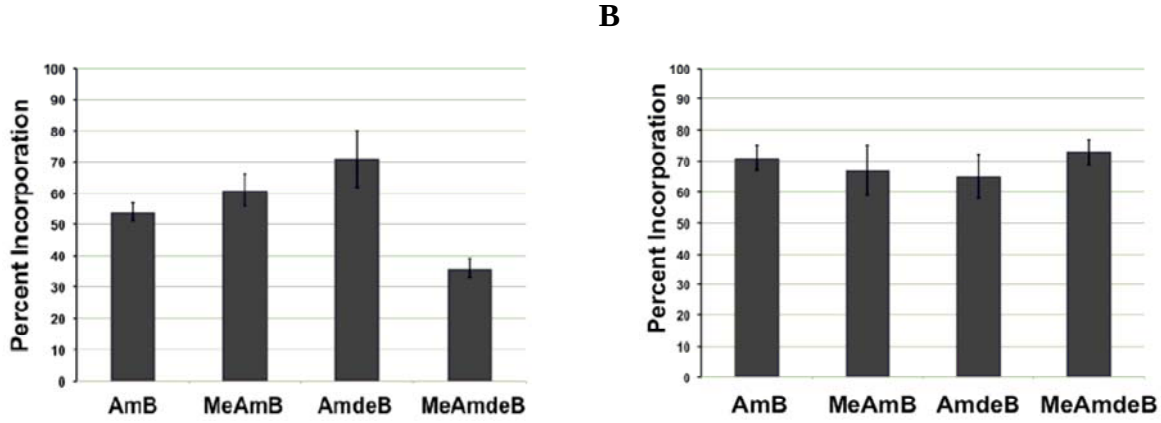

Figure 2.3. Polyene macrolide binding to phospholipid membranes. **A**. Binding to *S. cerevisiae*. **B**. Binding to 10% ergosterol LUVs. Figure adapted from ref. 3.

The roles of the sterol in the mechanism are poorly understood. There are reports supporting both indirect sterol effects and the direct binding of sterol.[10,12,16,19-26] In addition, there are also some reports of membrane permeabilization in sterol free membranes,[27-29] but these were done at super-physiological concentrations of AmB or with strained small liposome vesicles. To elucidate whether a direct binding event was occurring between AmB and the sterol, Ian Dailey and Dan Palacios conducted isothermal titration calorimetry (ITC) with the derivatives and both liposomes containing ergosterol and liposomes devoid of ergosterol.[3] The net isotherm was calculated from the isotherms of the ergosterol-containing liposomes and the ergosterol-free

liposomes. A significant exotherm was observed with AmB and MeAmB with the erosterol-containing liposomes indicating a direct binding event. AmdeB and MeAmdeB did not produce significant exotherms (Figure 2.4). The conclusion drawn from these experiments is that the mycosamine is required to meditate a direct interaction between the sterol and AmB. To investigate whether this exotherm was due to changes in global membrane properties, the same experiment was conducted with 10% lanosterol instead of 10% ergosterol LUVs. Lanosterol and ergosterol cause very similar changes in global membrane properties.[30-32] No significant net exotherm was observed with AmB and the lanosterol containing LUVs. This supports our previous conclusion of a direct binding event between AmB and ergosterol.

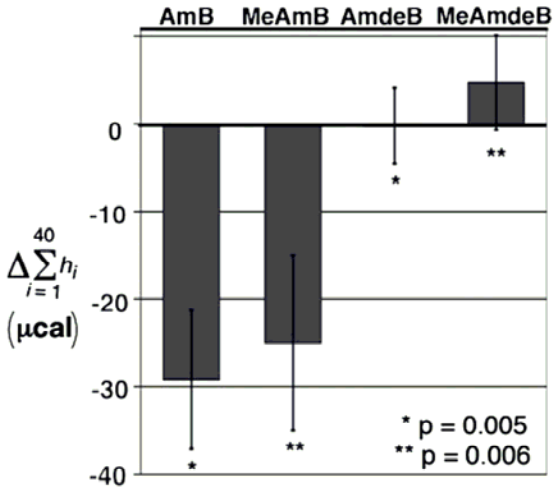

Figure 2.4. Net exotherm for polyene macrolides titrated with sterol-free LUVs followed by 10% ergosterol LUVs. Figure adapted from ref. 3.

2-4 Summary

The experiments we conducted elucidated some critical points of the mechanism of AmB: The mycosamine appendage is essential for antifungal activity, channel formation, and a direct binding event with ergosterol. However, these findings do not fully address the question of how AmB is achieving cell death, specifically, is the primary mode of action based in ergosterol sequestration through the direct binding event or cell gradient disruption driven by channel formation (Figure 2.5). In order to investigate this, a derivative of AmB that could still bind sterol but is incapable of forming ion channels is needed.

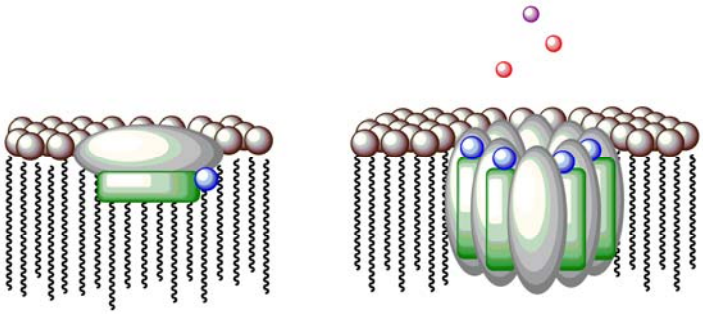

Figure 2.5. Two possible mechanisms of AmB, ergosterol sequestration and membrane permeabilization.

2-5 Experimental

The experimental section is adapted from ref. 3.

General Methods

Materials

Commercially available materials were purchased from Aldrich Chemical Co. (Milwaukee, WI), Fisher Scientific (Hampton, NH), Avanti Polar Lipids (Alabaster, AL), and Small Parts Inc. (Miramar, FL) and were used without further purification unless noted otherwise. Amphotericin B was a generous gift from Bristol-Myers Squibb and was purified by preparative RP-HPLC using an Agilent (Santa Clara, CA) 1100 series HPLC system equipped with a Waters (Milford, MA) Sunfire Prep C_{18} 30 x 150 mm column. Ergosterol and camphorsulfonic acid were recrystallized from ethyl acetate. Water was obtained from a Millipore (Billerica, MA) Gradient A10 water purification system.

Antifungal Assays

Growth Conditions for *S. cerevisiae*

S. cerevisiae was maintained with yeast peptone dextrose (YPD) growth media consisting of 10 g/L yeast extract, 20 g/L peptone, 20 g/L dextrose, and 20 g/L agar for solid media. The media was sterilized by autoclaving at 250 °F for 30 min. Dextrose was subsequently added as a sterile 40% w/v solution in water (dextrose solutions were filter sterilized). Solid media was prepared by pouring sterile media containing agar (20 g/L) onto Corning (Corning, NY) 100 x 20 mm polystyrene plates. Liquid cultures were incubated at 30 °C on a rotary shaker and solid cultures were maintained at 30 °C in an incubator.

Growth Conditions for *C. albicans*

C. albicans was cultured in a similar manner to *S. cerevisiae* except both liquid and solid cultures were incubated at 37 °C.

Broth Microdilution Minimum Inhibitory Concentration (MIC) Assay

The protocol for the broth microdilution assay was adapted from the Clinical and Laboratory Standards Institute document M27-A2.[33] 50 mL of YPD media was inoculated and

incubated overnight at either 30 °C (*S. cerevisiae*) or 37 °C (*C. albicans*) in a shaker incubator. The cell suspension was then diluted with YPD to an OD_{600} of 0.10 (~5 x 10^6 cfu/mL) as measured by a Shimadzu (Kyoto, Japan) PharmaSpec UV-1700 UV/Vis spectrophotometer. The solution was diluted 10-fold with YPD, and 195 μL aliquots of the dilute cell suspension were added to sterile Falcon (Franklin Lakes, NJ) Microtest 96 well plates in triplicate. Compounds were prepared either as 400 μM (AmB, MeAmB) or 2 mM (AmdeB, MeAmdeB) stock solutions in DMSO and serially diluted to the following concentrations with DMSO: 1600, 1200, 800, 400, 320, 240, 200, 160, 120, 80, 40, 20, 10 and 5 μM. 5 μL aliquots of each solution were added to the 96 well plate in triplicate, with each column representing a different concentration of the test compound. The concentration of DMSO in each well was 2.5% and a control well to confirm viability using only 2.5% DMSO was also performed in triplicate. This 40-fold dilution gave the following final concentrations: 50, 40, 30, 20, 10, 8, 6, 4, 1, 0.5, 0.25 and 0.125 μM. The plates were covered and incubated at 30 °C (*S. cerevisiae*) or 37 °C (*C. albicans*) for 24 hours prior to analysis. The MIC was determined to be the concentration of compound that resulted in no visible growth of the yeast. The experiments were performed in duplicate and the reported MIC represents an average of two experiments.

Potassium Efflux Assays

General Information

Ion selective measurements were obtained using a Denver Instruments (Denver, CO) Model 225 pH meter equipped with a Denver Instruments potassium selective electrode. The pH meter was connected to a desktop computer by an RS232 connection and the data were collected using Labtronics (Guleph, Ontario) Collect SL software. The electrode was conditioned in a 1000 ppm KCl standard solution overnight prior to ion selective measurements. Measurements were made on 15 mL solutions that were magnetically stirred in 40 mL I-Chem (Rockwood, TN) vials incubated in a 30 °C stirred water bath (*S. cerevisiae*) or at 23 °C (LUVs). The instrument was calibrated daily with KCl standard solutions to 10, 100, and 1000 ppm potassium. The potassium concentration was sampled every 30 seconds throughout the course of the efflux experiments.

Potassium Efflux from *S. cerevisiae*

The protocol to determine potassium efflux from *S. cerevisiae* was adapted from a similar experiment utilizing *C. albicans*.[34] An overnight culture of *S. cerevisiae* in YPD was centrifuged at 1200 g for 5 minutes at 4 °C. The supernatant was decanted and the cells were washed twice with sterile water. After the second wash step, the cells were suspended in 150 mM NaCl, 5 mM HEPES pH 7.4 (Na buffer) to an OD_{600} of 1.5 (~$1x10^9$ CFU/mL). A 15 mL sample of the cell suspension was then incubated in a 30 °C water bath with stirring for approximately 10 minutes before data collection. The probe was then inserted and data was collected for 5 minutes before adding 150 μL of the compound in question as a 300 μM solution in DMSO. The cell suspension was stirred and data were collected for 30 minutes and then 150 μL of a 1% aqueous solution of digitonin was added to effect complete potassium release and data were collected for an additional 15 minutes. The experiment was performed independently three times for each small molecule.

Data Analysis

The data from each run was normalized to the percent of total potassium release, from 0 to 100%. Thus for each experiment a scaling factor S was calculated using the following relationship:

$$\left[\frac{[K^+]_{final}}{[K^+]_{initial}} - 1\right] \cdot S = 100$$

Each concentration data point was then multiplied by S before plotting as a function of time.

Efflux from 10% ergosterol LUVs

LUV Preparation

Egg yolk phosphatidylcholine (EYPC) was obtained as a 10 mg/mL solution in $CHCl_3$ from Avanti Polar Lipids (Alabaster, AL) and was stored at -20 °C under an atmosphere of dry argon and used within 3 months. A 4 mg/mL solution of ergosterol in $CHCl_3$ was prepared monthly and stored at -20 °C under an atmosphere of dry argon. Prior to preparing a lipid film, the solutions were warmed to ambient temperature to prevent condensation from contaminating the solutions. A 13 x 100 mm test tube was charged with 1.6 mL EYPC and 230 μL of the ergosterol solution. The solvent was removed with a gentle stream of nitrogen and the resulting

lipid film was stored under high vacuum for a minimum of eight hours prior to use. The film was then hydrated with 1 mL of 150 mM KCl, 5 mM HEPES pH 7.4 (K buffer) and vortexed vigorously for approximately 1 minute to form a suspension of multilamellar vesicles (MLVs). The resulting lipid suspension was pulled into a Hamilton (Reno, NV) 1 mL gastight syringe and the syringe was placed in an Avanti Polar Lipids Mini-Extruder. The lipid solution was then passed through a 0.20 μm Millipore (Billerica, MA) polycarbonate filter 21 times, the newly formed large unilamellar vesicle (LUV) suspension being collected in the syringe that did not contain the original suspension of MLVs to prevent the carryover of MLVs into the LUV solution. To obtain a sufficient quantity of LUVs, three independent 1 mL preparations were pooled together for the dialysis and subsequent potassium efflux experiments. The newly formed LUVs were dialyzed using Pierce (Rockford, IL) Slide-A-Lyzer MWCO 3,500 dialysis cassettes. The samples were dialyzed three times against 600 mL of Na buffer. The first two dialyses were two hours long, while the final dialysis was performed overnight.

Determination of Phosphorus Content

Determination of total phosphorus was adapted from the report of Chen and coworkers.[35] The LUV solution was diluted tenfold with Na buffer and three 10 μL samples of the diluted LUV suspension were added to three separate 7 mL vials. Subsequently, the solvent was removed with a stream of N_2. To each dried LUV film, and a fourth vial containing no lipids that was used as a blank, was added 450 μL of 8.9 M H_2SO_4. The four samples were incubated open to ambient atmosphere in a 225 °C aluminum heating block for 25 min and then removed to 23 °C and cooled for 5 minutes. After cooling, 150 μL of 30% w/v aqueous hydrogen peroxide was added to each sample, and the vials were returned to the 225 °C heating block for 30 minutes. The samples were then removed to 23 °C and cooled for 5 minutes before the addition of 3.9 mL water. Then 500 μL of 2.5% w/v ammonium molybdate was added to each vial and the resulting mixtures were then vortexed briefly and vigorously five times. Subsequently, 500 μL of 10% w/v ascorbic acid was added to each vial and the resulting mixtures were then vortexed briefly and vigorously five times. The vials were enclosed with a PTFE lined cap and then placed in a 100 °C aluminum heating block for 7 minutes. The samples were removed to 23 °C and cooled for approximately 15 minutes prior to analysis by UV/Vis spectroscopy. Total phosphorus was determined by observing the absorbance at 820 nm and comparing this value to

a standard curve obtained through this method and a standard phosphorus solution of known concentration.

Determination of Ergosterol Content

Ergosterol content was determined spectrophotometrically. The LUV solution was diluted tenfold with Na buffer, and 50 μL of the dilute LUV suspension was added to 450 μL 2:18:9 hexane:isopropanol:water (v/v/v). Three independent samples were prepared and then vortexed vigorously for approximately one minute. The solutions were then analyzed by UV/Vis spectroscopy and the concentration of ergosterol in solution was determined by the extinction coefficient of 10400 L mol^{-1} cm^{-1} at the UV_{max} of 282 nm and was compared to the concentration of phosphorus to determine the percent sterol content. The extinction coefficient was determined independently in the above ternary solvent system. LUVs prepared by this method contained between 7 and 14% ergosterol.

Efflux from LUVs

The LUV solutions were adjusted to 1 mM in phosphorus using Na buffer. 15 mL of the 1 mM LUV suspension was added to a 40 mL I-Chem vial and the solution was gently stirred. The potassium ISE probe was inserted and data were collected for one minute prior to the addition of the compound. Then, 150 μL of a 100 μM DMSO solution of the compound in question was added and data were collected for five minutes. Then to effect complete potassium release, 150 μL of a 10% v/v solution of triton X-100 was added and data were collected for an additional five minutes. The experiment was duplicated with similar results.

Data Analysis

The data from each run were analyzed in the same manner as the efflux data from *S. cerevisiae.*

Planar Lipid Bilayer Experiments

General Information

All data were acquired using a Warner Instruments (Hamden, CT) BC-535 amplifier and the data were filtered using a built in 4 pole Bessel filter with a cutoff frequency of 5 kHz. The

headstage and delrin cell were housed within a Warner Instruments model FC-1 Faraday cage. The solutions were stirred using a Warner Instruments SUNstir-3 stirplate. The signal was passed through a Warner Instruments low pass 8 pole Bessel filter with a frequency cutoff of 1 kHz. The filtered data were sampled at a rate of 10 kHz using a Molecular Devices (Sunnyvale, CA) Digidata 1440 data acquisition system and the data were analyzed using Molecular Devices pClamp 10 software. Following acquisition, the data were digitally filtered to 20 Hz. Salt bridges were prepared monthly and were fabricated from 1.5 mm OD, 0.86 mm ID borosilicate capillary tubing and were filled with 1 M aqueous KCl with 2.5% agar. Prior to a day's experiments, silver electrodes were plated by submerging in commercial bleach for 15 to 30 minutes. The electrodes were plated periodically throughout the day.

Preparation of Teflon® Sheets

Prior to use, Teflon® sheets of 125 μM thickness (Small Parts Inc, Miramar, FL) were washed sequentially with 10 mM tribasic sodium phosphate, 1% HCl and then MilliQ water. Pores of approximately 100-150 μm in diameter were formed with the spark method[36] using a home built sparking apparatus. The Teflon® sheet was scored with a sewing needle and then the sheet was placed on a grounded sheet of copper and the Teflon® was sparked 10 times. The sheet was then flipped over and sparked an additional 10 times. Pore sizes were analyzed via light microscopy.

Preparation of Lipid Solution

Lipids were obtained from Avanti Polar Lipids as 10 mg/ml solutions in $CHCl_3$. The solutions were stored at -20 °C under dry argon and used within 3 months. A 4 mg/mL solution of ergosterol in $CHCl_3$ was prepared monthly and stored at -20 °C under dry argon. Lipid films were prepared by charging a 12 x 75 mm test tube with 40 μL porcine brain phosphatidylcholine, 20 μL porcine brain phosphatidylethanolamine and 3.8 μL ergosterol. The solvent was removed with a gentle stream of nitrogen. The lipid film was then dissolved in 30 μL *n*-decane to give the 20 mg/ml solution of lipids used for the electrophysiology experiments. The decane solutions were used within 3 hours of preparation.

Formation of planar lipid bilayers

Teflon® sheets were cut to approximately 1 cm^2 and adhered to a home fabricated delrin cell[37] using Dow Corning (Midland, MI) high vacuum grease. The area around the hole was then primed with the decane lipid solution. The primed sheet was left to stand for approximately 10 minutes such that some of the decane evaporated. Then 3.5 mL of 2 M KCl, 10 mM potassium phosphate pH 7.0 buffer was added to each chamber. The membrane was formed by sequential vertical swabs across the hole using a flame polished glass applicator that had been previously dipped into the lipid solution. The formation of a membrane was detected by a reduction in the current to 0 pA. The integrity of this membrane was confirmed by applying a potential of 150 mV for approximately one minute. If the current increased by >1 pA upon voltage introduction, the membrane was rejected. Membranes were between 20 and 45 pF in size.

Interrogating Channel Formation

If the membrane was acceptable, 3.5 μL of a compound in DMSO was added to both chambers and the solutions were stirred with zero applied potential for 10 minutes. After 10 minutes the stirring was stopped, and 150 mV of potential was applied across the membrane. The formation of single AmB channels under similar conditions has been well documented.[38-45] The concentration of AmB and MeAmB required to observe channel activity varied based upon the lot number and age of the lipids used to make the membrane. For AmB, single channel formation was observed at concentrations between 0.5 and 5 nM while MeAmB displayed single channel activity between 30 and 80 nM. The concentration of MeAmdeB was raised to 1000 nM without observing any channel activity. At concentrations greater than 100 nM MeAmdeB and AmdeB tended to grossly destroy the membrane, as evidenced by an abrupt change from zero current to an offscale reading. To verify the inability of MeAmdeB and AmdeB to form channels, 5 independent experiments were performed at concentrations ranging from 50 to 100 nM, each with 15 minutes of applied potential. In every case, AmdeB and MeAmdeB failed to produce channel activity. These same conditions consistently led to channel formation with AmB and MeAmB.

Yeast Binding Assay

Determination of Binding

The yeast binding assay was adapted from the report by Kobayashi and coworkers that

demonstrated binding of AmB to intact *S. cerevisiae* cells.[46] 10 mL of an overnight culture of *S. cerevisiae* in YPD was centrifuged at 1200 g for 5 min at 4 °C. The supernatant was decanted, and the cells were washed twice with sterile water using the same centrifuge conditions. The washed cells were then suspended in sterile water to an OD_{600} of 0.10 (~$5x10^6$ CFU/mL), and 990 µl of this suspension was added to a 1.5 mL microcentrifuge tube. 10 µL of a 200 µM solution of compound in DMSO was added to the suspension, which was vortexed for approximately 10 seconds and then incubated at 30 °C for 15 minutes. The samples were subsequently centrifuged at 5000 RPM with a Savant HSC10K Speedfuge for 5 min to pellet the cells. The concentration of AmB in such aqueous solutions cannot be accurately determined because of aggregate formation.[47,48] Thus, 950 µL of the supernatant was removed and incubated at -20 °C for approximately 20 minutes before being lyophilized overnight. The lyophilized sample was dissolved in 400 µL of MeOH and the concentration of compound in solution was determined by UV/Vis analysis using the known extinction coefficent of each compound. This analysis gives the percent recovery, the percent incorporation being equal to 1-(percent recovery). The samples were prepared in triplicate and the entire experiment was duplicated. The values represent the average of 5 or 6 trials plus or minus the standard deviation.

Recovery Control

To ensure that the compounds were not binding to the walls of the microcentrifuge tube or decomposing during the course of the experiment, a control was run using the experimental protocol outlined above but substituting pure water for the *S. cerevisiae* suspension. Greater than 90% recovery was achieved with all four compounds.

LUV Binding Assay

Preparation of LUVs

LUVs were prepared as described in Section III except dialysis was not performed and the newly extruded vesicles were purified via size exclusion chromatography using Sephadex G50-150 resin as the stationary phase and K buffer as the mobile phase. The concentration of phosphorus and the sterol content of the LUVs were determined as described in Section III.

LUV Binding

The partitioning of AmB into both sterol-containing[49-51] and sterol-free[52-54] LUVs has been previously demonstrated. While many prior methods relied upon a measureable change of a physical property (such as electronic absorption spectra) upon the interaction of AmB with a phospholipid bilayer, the SEC based method is advantageous because it physically separates bound from unbound compound, and thereby avoids assumptions regarding the underpinnings of the observed spectral changes.[55] A LUV solution of known phosphorus concentration was diluted to a concentration of 2.05 mM using K buffer, and the solution was gently vortexed. Then, a 975 μL sample of the LUV suspension was added to a 7 mL screw cap vial. Subsequently, 25 μL of a 0.8 mM DMSO solution of the compound under investigation was added and the sample was gently vortexed. The sample was then incubated at 30 °C for one hour. The sample was then purified via size exclusion chromatography using a 1.5 x 30 cm Sephadex G50-150 column, with K buffer as the mobile phase (LUVs typically eluted from the column between 9 and 11 ml of eluent). After the LUVs eluted from the column, the column was flushed with 100 mL of K buffer to remove any small molecules left on the resin.

The concentration of the purified LUVs was then determined through analysis of phosphorus content, as described above. The concentration of compound within the lipid bilayer was determined by dissolving triplicate 50 μL samples of the LUV solution in 450 μL of 2:18:9 hexane:isopropanol:water (v/v/v) and analyzing the sample by UV/Vis spectroscopy. The amount of compound incorporation was determined by comparing the final ratio of lipid to compound to the theoretical max of 100:1. The experiments were performed in quadruplicate for each compound; thus, the reported values represent the average of four runs plus or minus the standard deviation. The binding to sterol-free vesicles was determined in similar fashion except no ergosterol was added to the initial lipid film. AmB, MeAmB, AmdeB and MeAmdeB readily partition into sterol-free vesicles.

LUV-free Control Studies

As a control, the same procedure described above was repeated without LUVs to determine the amount of compound that elutes from the column at the approximate elution volume of the LUVs (the LUVs typically eluted between 9 and 11 mL). Five fractions of 5 mL elution volume were collected, frozen and lyophilized overnight. Then, the resulting solid was suspended in 1 mL of MeOH and vortexed vigorously for approximately two minutes. The

samples were then centrifuged at 4000 rpm with a Savant HSC10K Speedfuge for approximately 30 minutes to pellet the inorganic salts. The supernatant was removed and analyzed by UV/vis spectroscopy to determine the amount of compound in solution. For all compounds, less than 10% of the compound loaded onto the column eluted at the retention time of the LUVs. The measurement was performed in duplicate.

Isothermal Titration Calorimetry

General Information

Experiments were performed using a VP-ITC isothermal titration calorimeter (MicroCal Inc., Piscataway, NJ). Solutions of the compounds to be tested were prepared by diluting a 5.0 mM stock solution of the compound in DMSO to 50 μM with K buffer. The final DMSO concentration in the solution was 1% v/v. LUVs were prepared and phosphorus and ergosterol content was quantified as described in above. Ergosterol and lanosterol were also incorporated into POPC LUVs. The LUV solutions were diluted with buffer and DMSO to give a final phospholipid concentration of 8.0 mM in a 1% DMSO/K buffer solution. Immediately prior to use, all solutions were degassed under vacuum at 17 °C for 10 minutes. The reference cell of the instrument was filled with a solution of 1% v/v DMSO/K buffer.

Titration Experiment

Titrations were performed by injecting the LUV suspension at ambient temperature into the sample cell (volume = 1.4399 mL or 1.4495 mL) which contained the 50 μM solution of the compound in question at 25 °C. The volume of the first injection was 1 μL. Consistent with standard procedure,[56] due to the large error commonly associated with the first injection of ITC experiments, the heat of this injection was not included in the analysis of the data. Next, forty 5 μL injections of the LUV suspension were performed. The injection duration was 2.1 seconds and 10.3 seconds for the 1 μL and 5 μL injections, respectively. The spacing between each injection varied between 240 seconds and 480 seconds and was adjusted to allow the instrument to return to baseline before the next injection was made. The rate of stirring for each experiment was 300 or 310 rpm.

Data Analysis

ORIGIN software (MicroCal, Inc.) was used for baseline determination and integration of the injection heats, and Microsoft Excel was used for subtraction of dilution heats and the calculation of overall heat evolved. To approximate the dilution heats, the final integrated heat from each run was subtracted from all the data for that particular experiment.[57] The overall heat evolved during the experiment was calculated using the following formula:

$$\mu\text{cal}_{overall} = \sum_{i=1}^{n} (\Delta h^{i}_{injection} - \Delta h^{n}_{injection})$$

Where i = injection number, n = total number of injections, $\Delta h^{i}_{injection}$ = heat of the i^{th} injection, $\Delta h^{n}_{injection}$ = the heat of the final injection of the experiment.

2-6 References

1. Nicolaou, K. C.; Chakraborty, T. K.; Ogawa, Y.; Daines, R. A.; Simpkins, N. S.; Furst, G. T. *J. Am. Chem. Soc.* **1988**, *110*, 4660-4672.
2. MacPherson, D. T.; Corbett, D. F.; Costello, B. C.; Driver, M. J.; Greenless, A. R.; Maclachlan, W. S.; Shanks, C. T.; Taylor, A. W. *Recent Advances in the Chemistry of Anti-Infective Agents*; Bently, P. H.; Ponsford, R. Ed.; Royal Society of Chemistry: Cambridge, **1993**; No. 119, 205-222.
3. Palacios, D. S.; Dailey, I.; Siebert, D. M.; Wilcock, B. C.; Burke, M. D. *Proc. Natl. Acad. Sci. U. S. A.* **2011**, *108*, 6733-6738.
4. Palacios, D. S.; Anderson, T. M.; Burke, M. D. *J. Am. Chem. Soc.* **2007**, *129*, 13804-13805.
5. HsuChen C.; Feingold, D. S. *Nature* **1974**, *251*, 656-659.
6. Brajtburg, J.; Powderly, W. G.; Kobayashi, G. S.; Medoff, G. *Antimicrob. Agents Chemother.* **1990**, *34*, 183-188.
7. Temple, M. E.; Brady , M. T.; Koranyi, K. I.; Nahata, M. C. *Pharmacotherapy* **2001**, *21*, 351-354.
8. Khutorsky, V. E.; *Biochim. Biophys. Acta.* **1992**, *1108*, 123-127.
9. Baginski, M.; Resat, H.; McCammon, J. A. *Mol. Pharm.* **1997**, *52*, 560-570.
10. Baginski, M.; Resat, H.; Borowski, E. *Biochim. Biophys. Acta.* **2002**, *1567*, 63-78.
11. Czub J.; Baginski, M. *J. Phys. Chem. B.* **2006**, *110*, 16743-16753.
12. Neumann, A.; Czub, J.; Baginski, M. *J. Phys. Chem. B.* **2009**, *113*, 15875-15885.

13. Baran, M.; Mazerski, M. *Biophys. Chem.* **2002**, *95*, 125-133.
14. Schaffner, C. P.; Borowski, E. *Antibiot. Chemother.* **1961**, *11*, 724.
15. Mechlinski, W.; Schaffner, C. P. *J. Antibiot.* **1972**, *30*, 256-258.
16. Balakrishnan, A. R.; Easwaran, K. *Biochemistry* **1993**, *32*, 4139-4144.
17. Minones, J. *Langmiur* **2002**, *18*, 2817-2827.
18. Matsuoka, S.; Ikeuchi, H.; Umegawa, Y.; Matsumori, N.; Murata, M. *Bioorg. Med. Chem.* **2006**, *14*, 6608-6614.
19. HsuChen, C.; Feingold, D. S. *Biochem. Biophys. Res. Commun.* **1973**, *51*, 972-978.
20. Kotler-Brajtburg, J.; Price, H. D.; Medoff, G.; Schlessinger, D.; Kobayashi, G. S. *Antimicrob. Agents Chemother.* **1974**, *5*, 377-382.
21. Herve, M.; Debouzy, J. C.; Borowski, E.; Cybulska, B.; Gary-Bobo, C. M. *Biochim. Biophys. Acta* **1989**, *980*, 261-272.
22. Matsumori, N.; Sawada, Y.; Murata, M. *J. Am. Chem. Soc.* **2005**, *127*, 10667-10675.
23. Matsumori, N.; Tahara, K.; Yamamoto, H.; Morooka, A.; Doi, M.; Oishi, T.; Murata, M. *J. Am. Chem. Soc.* **2009**, *131*, 11855-11860.
24. Paquet, M.; Fournier, I.; Barwicz, J.; Tancrede, P.; Auger, M. *Chem. Phys. Lipids* **2002**, *119*, 1-11.
25. Nezil, F.; Bloom, M. *Biophys. J.* **1992**, *61*, 1176-1183.
26. Zumbuehl, A.; Stano, P.;Heer, D.; Walde, P.; Carreira, E. M. *Org. Lett.* **2004**, *6*, 3683-3686.
27. Whyte, B. S.; Peterson,R. P.; Hartsel, S.C. *Biochem. Biophys. Res. Commun.* **1989**, *164*, 609-614.
28. Cotero, B. V.; Rebolledo-Antunez, S.; Ortega-Blake, I. *Biochim. Biophys. Acta* **1998**, *1375*, 43-51.
29. Venegas, B.; Gonzalez-Damian, J.; Celis, H.; Ortega-Blake, I. *Biophys. J.* **2003**, *85*, 2323-2332.
30. Urbina, J. A.; Pekerar, S.; Le, H. B.; Patterson, J.; Montez, B.; Oldfield, E. *Biochim. Biophys. Acta* **1995**, *1238*, 163-176.
31. Henriksen, J. *Biophys. J.* **2006**, *90*, 1639-1649.
32. Hsueh, Y.; Chen, M.; Patty, P.; Code, C.; Cheng, J.; Frisken, B.; Zuckermann, M.; Thewalt, J. *Biophys. J.* **2007**, *92*, 1606-1615.

33. Clinical and Laboratory Standards Institute. Reference Method for Broth Dilution Antifungal Susceptibility Testing, M27-A2, Approved Standard 2nd Ed. Vol. 22, Number 15, **2002**.
34. Hammond, S. M.; Lambert, P. A.; Klinger, B. N. *J. Gen. Microbiol.* **1974**, *81*, 325-330.
35. Chen, P. S. T. Y. Toribara, H. Warner, *Anal.Chem.* **28**, 1756-1758 (1956).
36. W. R. Schule, W. Hanke, *Planar Lipid Bilayers* **1993**, Academic Press, London
37. Mayer, M.; Kriebel, M. J. K.; Tosteson, M. T.; Whitesides, G. M. *Biophys J.* **2003**, *85*, 2684-2695.
38. Ermishkin, L. N.; Kasumov, K. N.; Potzeluyev, V. M. *Nature* **1976**, *262*, 698-699.
39. Ermishkin, L. N.; Kasumov, K. N.; Potzeluyev, V.M. *Biochim. Biophys. Acta* **1977**, *470*, 357-367.
40. Kasumov, K. M.; Borisova, M. P.; Ermishkin, L. N.; Potzeluyev, V. M.; Silberstein, A. Y.; Vainshtein, V. A. *Biochim. Biophys. Acta* **1979**, *551*, 229-237.
41. Borosova, M. P.; Ermishkin, L. N.; Silberstein, A. Y. *Biochim. Biophys. Acta* **1979**, *553*, 450-459.
42. Borosova, M. P.; Brutyan, R. A.; Ermishkin, L. N. *J. Membrane Biol.* **1986**, *90*, 13-20.
43. Mickus, D. E.; Levitt, D. G.; Rychnovsky, S. R. *J. Am. Chem. Soc.* **1992**, *114*, 359-360.
44. Brutyan, R. A.; McPhie, P. *J. Gen. Physiol.* **1996**, *107*, 69-78.
45. Ibragimova, V.; Alieva, I.; Kasumov, K.; Khutorsky, V. *Biochim. Biophys. Acta* **2006**, *1758*, 29-37.
46. Kotler-Brajtburg, J.; Medoff, G.; Schlessinger, D.; Kobayashi, G. S. *Antimicrob. Agents Chemother.* **1974**, *6*, 770-776.
47. Millié, P.; Langlet, J.; Bergés, J.; Caillet, J.; Demaret, J. *J. Phys. Chem. B.* **1999**, *103*, 10883-10891.
48. Shervani, Z.; Etori, H.; Taga, K.; Yoshida, T.; Okabayashi, H. *Colloid Surface. B* **1996**, *7*, 31-38.
49. Mouri, R.; Konoki, K.; Matsumori, N.; Oishi, T.; Murata, M. *Biochemistry* **2008**, *47*, 7807-7815.
50. Fujii, G.; Chang, J.; Coley, T.; Steere, B. *Biochemistry* **1997**, *36*, 4959-4968.
51. Vertut-Croquin, A.; Bolard, J.; Chabbert, M.; Gary-Bobo, C. *Biochemistry* **1983**, *22*, 2939-2944.

52. Paquet, M.; Fournier, I.; Barwicz, J.; Tancrède, P.; Auger, M. *Chem. Phys. Lipids* **2002**, *119*, 1-11.
53. Milhaud, J.; Michels, B. *Chem. Phys. Lipids* **1999**, *101*, 223-235.
54. Milhaud, J.; Hartmann, M.; Bolard, J. *Biochimie* **1989**, *71*, 49-56.
55. White, S. H.; Wimley, W.C.; Ladokhin, A. S.; Hristova, K. *Method. Enzymol.* **1998**, *295*, 62-87.
56. Heerklotz, H.; Seelig, J. *Biochim. Biophys. Acta* **2000**, *1508*, 69-85.
57. te Welscher, Y. M.; *et al*. *J. Biol. Chem.* **2008**, *283*, 6393-6401.

Chapter 3

Elucidation of Ergosterol Binding as the Primary Mechanism of Amphotericin B

This chapter describes the synthesis and biophysical evaluation of C35-deoxyamphotericin B. This derivative retains the ability to bind ergosterol but lacks the capacity to form ion channels. Separation of these two functions of amphotericin B resulted in the discovery that amphotericin B primarily kills yeast cells by binding ergosterol, and channel formation is a complimentary second mechanism that enhances the antifungal potency. C35-deoxyamphotericin B was produced by Kaitlyn Gray, Dan Palacios, Ian Dailey, Matt Endo, Brice Uno, and Brandon Wilcock. Natamycin aglycone was prepared by Kaitlyn Gray. Dan Palacios and Matt Endo performed the potassium efflux assays. Dan Palacios, Matt Endo and Kaitlyn Gray conducted MIC experiments. Quantification of amphotericin B and ergosterol at the MIC concentration was done by Dan Palacios and Matt Endo. Portions of this chapter were adapted from Gray, K. C.; Palacios, D. S.; Dailey, I.; Endo, M. M.; Uno, B. E.; Wilcock, B. C.; Burke, M. D. *Proc. Natl. Acad. Sci. U. S. A.* **2012**, *109*, 2234-2239.

3-1 The Role of the C35 Hydroxyl

The hydroxyl group at C35 on AmB has been hypothesized to perform an essential function in the formation of the ion channel. There are two main proposed structures for the ion complex,[1] the double barrel model and the single barrel model (Figure 3.1). The length of AmB is roughly one half the thickness of the phospholipid bilayer membrane. In the double barrel model, two AmB complexes align in a tail to tail fashion to span the entire bilayer membrane. The two barrels are proposed to be held together through hydrogen

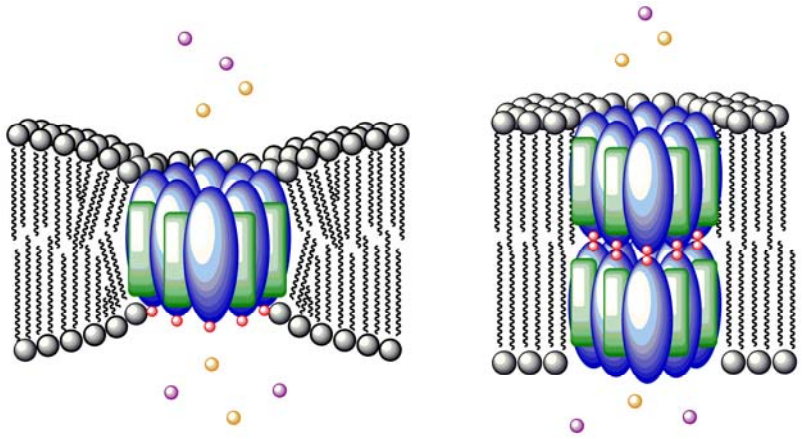

Figure 3.1. Single and double barrel models of the AmB ion channel. The C35 hydroxyl (red) is proposed to stabilize the complex through hydrogen bonding interactions between to barrels in the double barrel model and to the phospholipid head groups in the single barrel model.

bonding of the C35 hydroxyl groups on the AmBs. In the single barrel model, the membrane is pinched in, and the polar phospholipid head groups interact with the C35 hydroxyl to create a stable pore. In both cases, the C35 hydroxyl is predicted to be important for channel formation. If the predictions are correct, removal of this group would lead to diminished channel forming ability.

The methyl ester of a C35-deoxyAmB derivative was synthesized by the Carreira group and showed impaired ability to cause potassium efflux in liposomes and reduced antifungal activity in comparison to AmB methyl ester (AmE).[2] We hypothesized that LUVs might be more sensitive than yeast membranes to permeabilization. Also, the AmE (a derivative with net positive charge) might have different membrane permeabilization capabilities than AmB. Matthew Endo investigated this and found that, at the elevated concentrations of 30 μM, AmE was able to permeablize LUVs containing no sterol while AmB was unable to permeablize the LUVs.[3] This shows that AmE has different membrane permeabilization capacities than AmB and caution should be taken interpreting Carreira's results. We also found that AmdeB, which doesn't bind sterol or have antifungal activity, also permeablized the LUVs, but was incapable of permeablizing yeast membranes. This demonstrates that LUVs are more sensitive than the yeast membranes towards permeabilization. Given these results and the fact that no sterol binding studies were performed, we undertook the synthesis of C35-deoxyAmB (C35deOAmB) to test its sterol binding properties and channel forming capacity in yeast.

3-2 The Synthesis of C35-deoxyAmB

The strategy for the synthesis of C35-deoxyAmB was based upon a hybrid approach utilizing new iterative cross-coupling methodology[4,5] being developed in our group (Figure 3.2). Iterative cross coupling (ICC) relies on the ligand *N*-methyliminodiacetic acid (MIDA) attenuating the reactivity of boronic acids. MIDA imparts stability to the building blocks and is mildly deprotected with aqueous base. This allows a bifunctional MIDA-protected haloboronic acid to be coupled via a Suzuki-Miyaura reaction and subsequently deprotected to undergo an additional coupling. To employ this strategy, a hybrid synthesis with three building blocks was envisioned (Figure 3.2). The main building block comprising over half of the AmB skeleton was to be obtained from the degradation of AmB; the synthesis of this building block was based on previous degradative studies by Murata and Nicolaou.[6,7] This building block was coupled to a

polyene building block developed in our group.[8] The final building block consisted of the remaining fragment of the AmB skeleton with a methylene at the C35 position.[3]

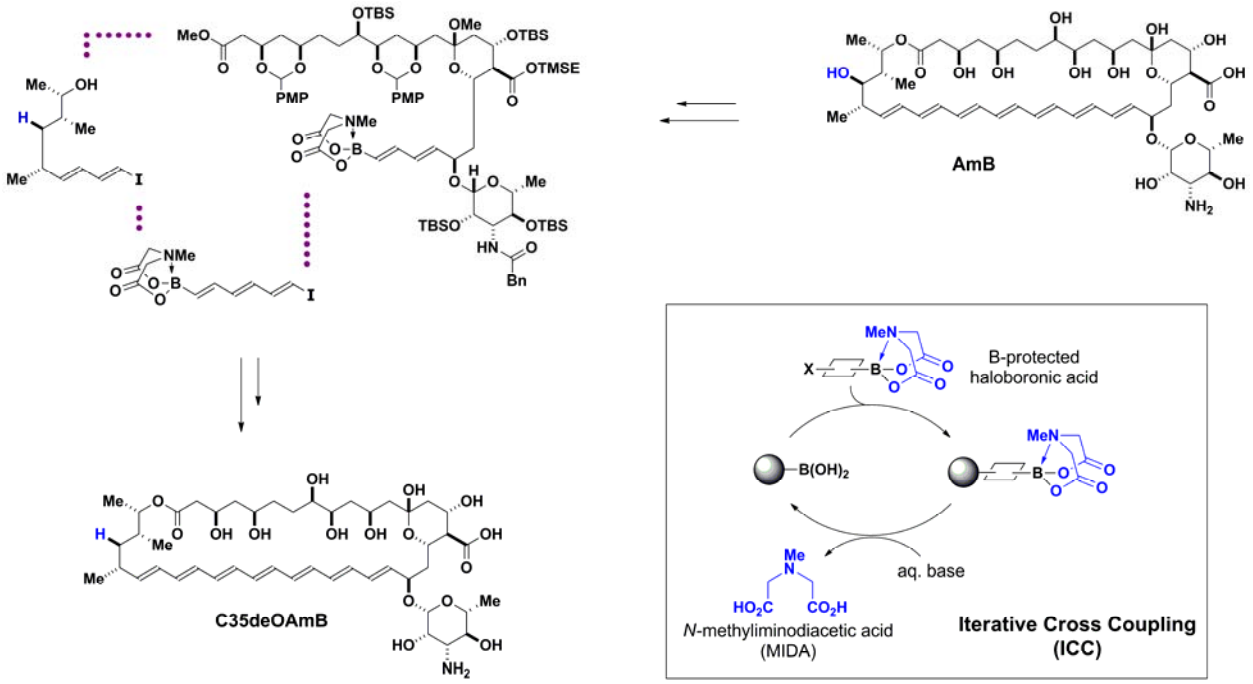

Figure 3.2. Iterative-cross-coupling based hybrid strategy for the synthesis of C35-deoxyAmB. AmB is protected and degraded to form the main building block. Iterative cross coupling with a polyene and a deoxy building block followed by macrocyclization and global deprotection gives C35-deoxyAmB. Figure was adapted from ref. 3.

The hybrid synthesis of C35-deoxyAmB (Scheme 3.1) was pioneered by Kaitlyn Gray and Dan Palacios with support from Brice Uno, Matt Endo, Ian Dailey and I. First, AmB was globally protected. The amine was protected as the phenylacetyl amide, and the hemi ketal was converted to the methyl ketal. Para-methoxybenzylidene acetals were installed on the polyol portion of AmB, and the acid was transformed into the TMSE ester after silylation of the remaining hydroxyl groups. The polyene portion of this protected intermediate was removed by ozonolysis. Takai olefination and cleavage of the ester at C1 completed the removal of half of the AmB skeleton. The resulting iodide from the Takai olefination was coupled to generate the AmB-derived, MIDA-protected building block. ICC with the remaining two building blocks created the linear C35-deoxyAmB skeleton. Macrolactonization followed by global deprotection generated the final C35-deoxyAmB compound.[3]

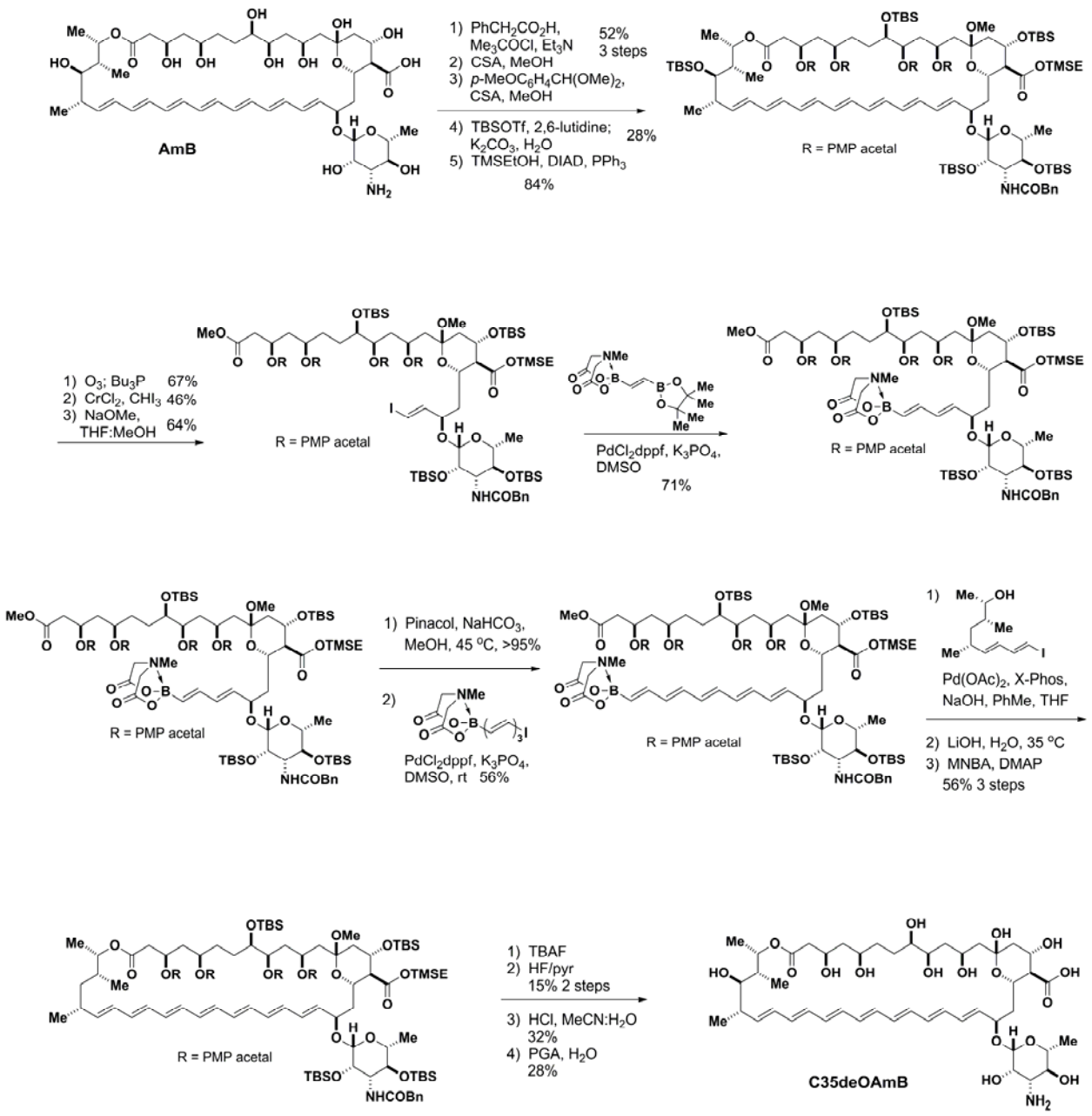

Scheme 3.1. The synthesis of C35-deoxyAmB. Scheme adapted from ref. 3.

One of the important aspects in the synthesis of AmB derivatives is the protecting group selection. The protecting groups must be orthogonal and/or robust enough to survive the chemistry conditions in the route yet be able to be mildly removed from the sensitive AmB framework. Finding an amine protecting group that meets these requirements was a challenge in this setting. AmB is sensitive to strong acid and hydrogenation conditions, and the group needed to be orthogonal to the nucleophilic/basic conditions of the ester cleavage and palladium/phosphines of the cross-coupling. These restrictions eliminated most of the

conventional choices for amine protecting groups. I envisioned utilizing a robust and stable acyl group to protect the amine as an amide. The deprotection of amides generally requires conditions that would be incompatible with AmB such as refluxing strong acid or base. However, amide bonds are commonly cleaved in nature by enzymes. For example, the phenylacetyl amide of penicillin G is transformed to the amine by the enzyme penicillin G amidase (PGA). In fact, this reaction is performed on large scale in industry to generate semi-synthetic penicillins.[9] I therefore decided to investigate the prospect of protecting the amine on AmB as the phenylacyl amide. The phenylacetyl protecting group would be robust enough to survive the synthetic route and potentially be removed under mild conditions with PGA (Scheme 3.2).

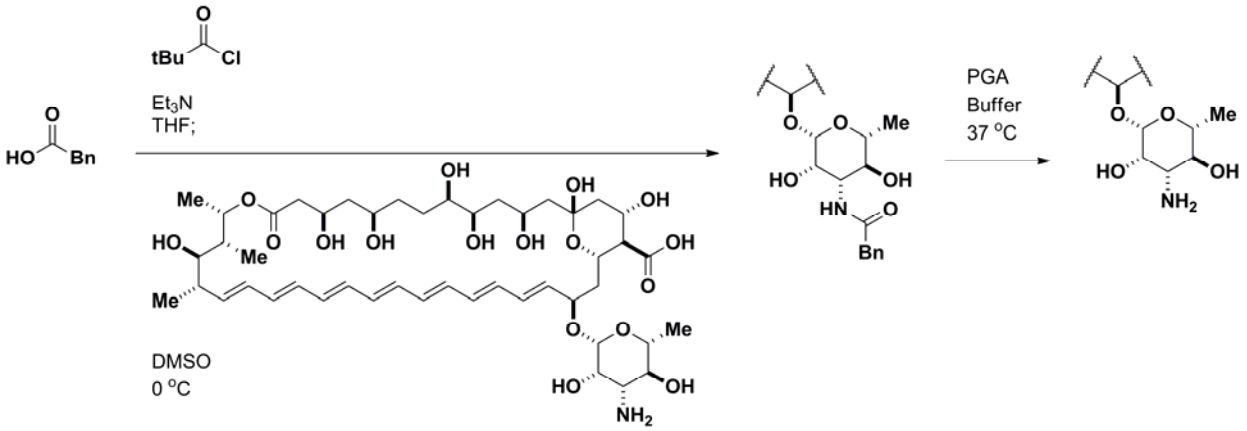

Scheme 3.2. Installation and removal of the phenylacetyl protecting group on the C3' amine of AmB.

I was able to successfully install the phenylacyl group selectively on the amine by generating the mixed anhydride and acylating at 0 °C. For removal of the phenylacyl group, I initially screened immobilized PGA sources on a variety of polymer backbones. I found these immobilized PGA reagents to be highly problematic. AmB had very poor solubility in the aqueous solutions the reaction requires and tended to aggregate and bind to the polymer supports. This complication made purification attempts to isolate clean product in good yields unsuccessful. However, crude PGA solution was obtained commercially, and I was able to adapt a PGA purification protocol[10] to arrive at pure PGA solutions for the deprotection. The best results were obtained in the pH range of 7.2-7.4 with very low buffer concentrations and a high concentration of PGA. I eventually obtained up to 60% conversion to the desired product, AmB. The conversion was hindered by the poor solubility of the AmB substrate and product; however, the remaining *N*-phenylacetyl AmB could be isolated and resubmitted to the reaction conditions. These results suggested that the phenylacetyl group was viable for the synthetic route.

3-3 Biophysical Evaluation of C35-deoxyAmB

Kaitlyn Gray, Daniel Palacios, Ian Dailey, Matthew Endo, Brice Uno and I were able to produce milligram quantities of C35-dexoyAmB for biophysical testing conducted by my colleagues. In addition to AmB and C35-deoxyAmB, we also included AmdeB as a control and another antifungal polyene macrolide, natamycin, as well as the natamycin aglycone (Figure 3.3). Natamycin displays antifungal activity but is incapable of forming membrane permeablizing channels and has been shown to directly bind sterol.[11]

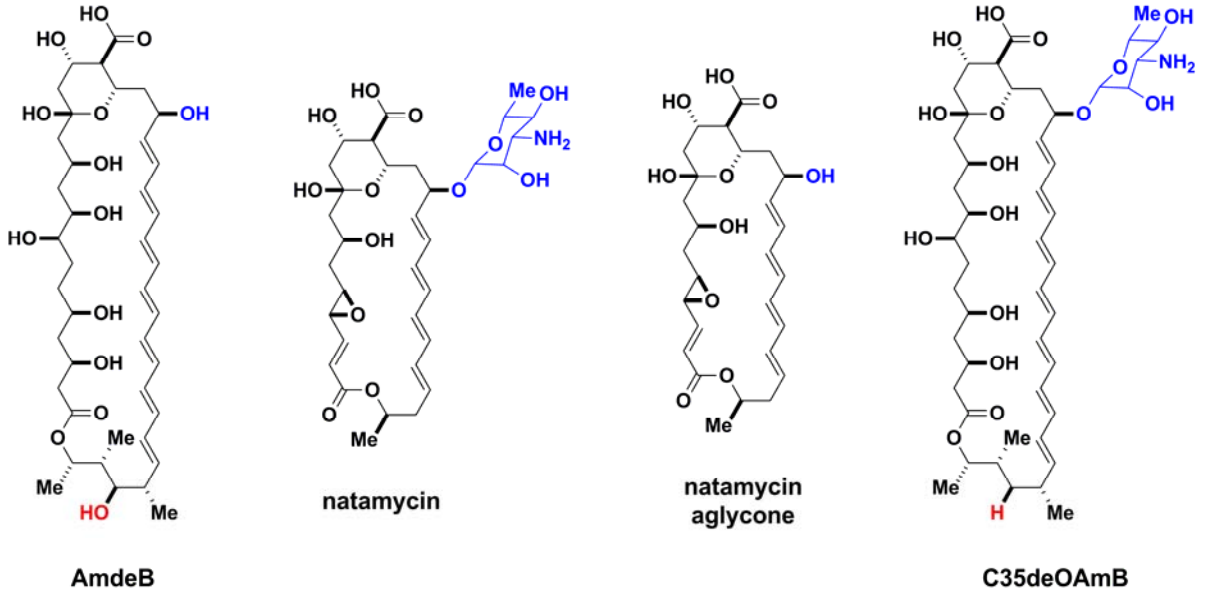

Figure 3.3. Polyene macrolide probes for the investigation of the contributions of ergosterol binding and membrane permeabilization to the mechanism of antifungal activity. Figure adapted from ref. 3.

To evaluate whether C35-deoxyAmB bound ergosterol or not, ITC was performed.[3] A significant net exotherm from sterol-free vs. ergosterol-containing liposomes revealed that the direct binding event still occurs (Figure 3.4). When potassium efflux experiments were conducted in yeast cells, it

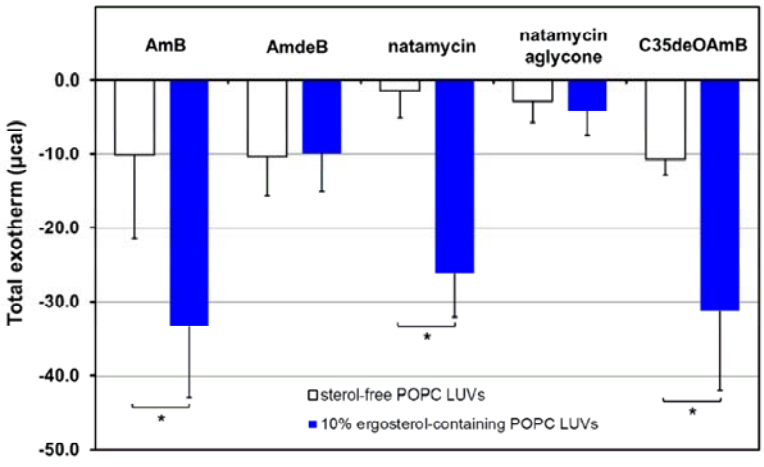

Figure 3.4. ITC exotherms with polyene macrolides and sterol-free and 10% ergosterol LUVs. Figure adapted from ref. 3.

was found that C35-deoxyAmB did not permeablize the membranes (Figure 3.5).[3]

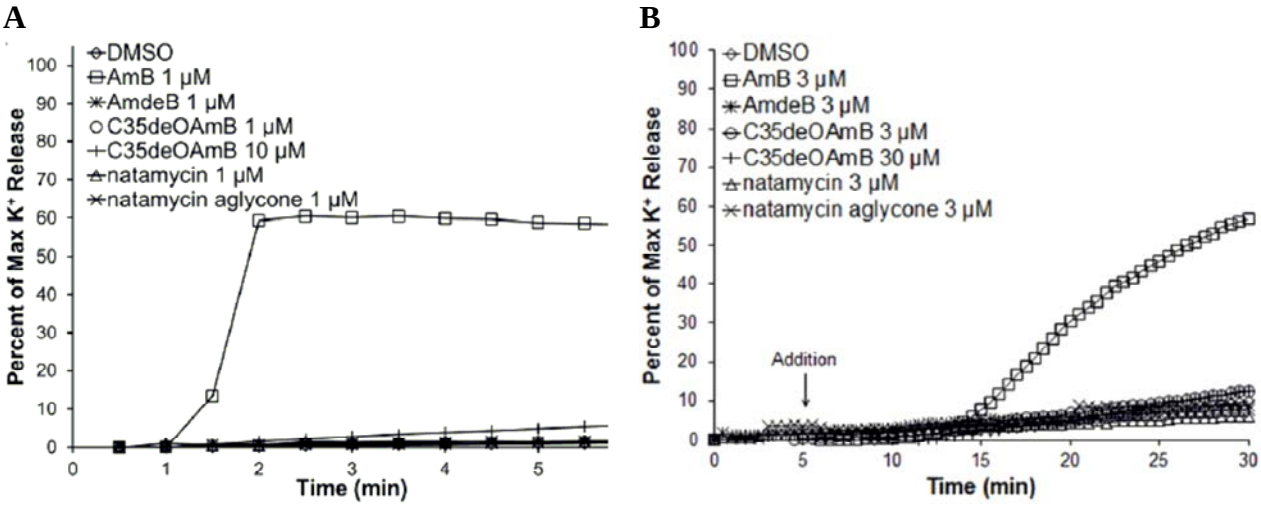

Figure 3.5. Membrane permeabilization with polyene macrolides. **A**. LUVs containing 10% ergosterol. **B**. *S. cerevisiae* yeast cells. Figure adapted from ref. 3.

Potassium efflux was also done with LUVs to ensure that the lack of efflux from yeast membranes was not due to an inability of C35-deoxyAmB to pass the cell wall. The antifungal activity of C35-deoxyAmB was compared to AmB in a MIC assay, and C35-deoxyAmB was determined to be only six times less active against *S. cerevisiae* despite its inability to permeablize membranes (Table 3.1). It is also notable that C35-deoxyAmB has a very similar MIC to natamycin, suggesting that sterol binding is the operative mechanism of antifungal activity.

MIC (μM)	AmB	AmdeB	natamycin	natamycin aglycone	C35deOAmB
S. cerevisiae	0.5	> 500	2	> 500	3
C. albicans	0.25	> 500	4	> 500	4

Table 3.1. MIC for polyene macrolides against *S. cerevisiae* and *C. albicans*. Table adapted from ref. 3.

The data gathered from these experiments supports the conclusion that a dual mechanism is operative in the case of AmB. The primary mechanism is ergosterol sequestration, and a secondary mechanism of membrane permeabilization gives a moderate boost in antifungal activity. To further add support to this conclusion, the ratio of AmB to ergosterol at the MIC concentrations was determined (Figure 3.6). For sterol sequestration to be the primary mechanism, a significant amount of the ergosterol must be bound by the AmB in order to disrupt cell function. At the MIC, we found that there is approximately a ten-fold excess of AmB over ergosterol to accomplish the sequestration.[3] It is also conceivable that ergosterol sequestration

could be a cause of cell death. Ergosterol plays important roles in the cell including membrane compartmentalization, endocytosis, vacuole fusion, and the function of membrane proteins.[12-15]

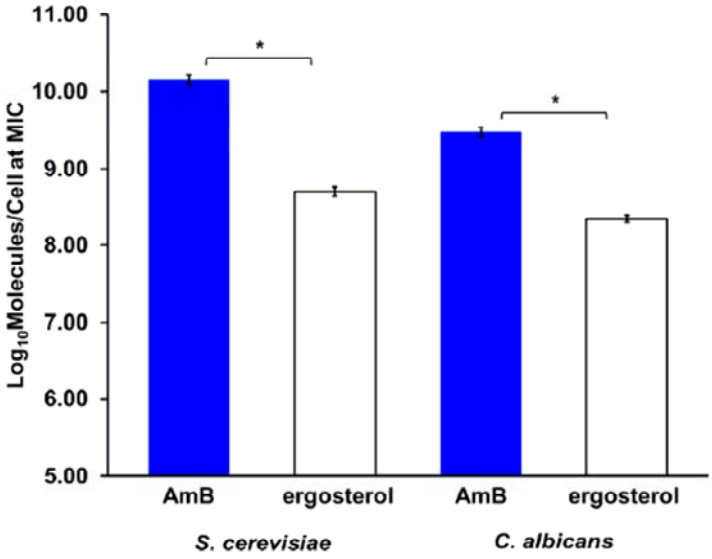

Figure 3.6. Comparison of the number of molecules of AmB to ergosterol at the MIC concentration against *S. cerevisiae* and *C. albicans*. Figure adapted from ref. 3.

3-4 Summary

The discovery that ergosterol binding is the primary mechanism by which AmB kills yeast cells overturns the leading line of thought on the antifungal mechanism of AmB that has been in place for fifty years. If the toxicity to humans is caused by an analogous binding of cholesterol, research towards improving AmB as a therapeutic can now be focused on modulating its sterol binding properties instead of its channel forming properties. Since the ergosterol binding event is mediated by the mycosamine subunit, AmB derivatives lacking functional groups on the mycosamine are needed to further study the mechanism in order to provide insight for the design of better therapeutics.

3-5 Experimental

The experimental section is adapted from ref. 3.

General Methods

Materials

Commercially available materials were purchased from Sigma-Aldrich, Alfa Aesar, Strem, Avanti Polar Lipids, Fisher Scientific or Julich, and were used without further purification unless stated otherwise. Amphotericin B was a generous gift from Bristol-Myers Squibb Company. Iodoform (methanol), camphorsulfonic acid (ethyl acetate), and triphenylphosphine (hexanes) were recrystallized from the indicated solvents prior to use. All solvents were dispensed from a solvent purification system that passes solvents through packed columns

according to the method of Pangborn and coworkers[16] (THF, Et_2O, CH_2Cl_2, toluene, dioxane, hexanes : dry neutral alumina; DMSO, DMF, CH_3OH : activated molecular sieves). 2,6-Lutidine and pyridine were freshly distilled under nitrogen from CaH_2. EtOAc and EtOH were freshly distilled under nitrogen from activated molecular sieves. Water was doubly distilled or obtained from a Millipore MilliQ water purification system. Ozone was generated using an ozone solutions ozone generator.

Reactions

Due to the light and air sensitivity of polyenes, all manipulations of polyenes were carried out under low light conditions and compounds were stored under an argon atmosphere. All reactions were performed in oven- or flame-dried glassware under an atmosphere of argon unless otherwise indicated. Reactions were monitored by analytical thin layer chromatography performed using the indicated solvent on E. Merck silica gel 60 F_{254} plates (0.25mm). Compounds were visualized using a UV (λ_{254}) lamp or stained by an acidic solution of *p*-anisaldehyde or $KMnO_4$. Alternatively, reactions were monitored by RP-HPLC using an Agilent 1100 series HPLC system equipped with a Symmetry® C_{18} 5 micron 4.6 x 150 mm column (Waters Corp. Milford, MA) with UV detection at 406 nm and the indicated eluent and flow rate.

Purification and Analysis

Flash chromatography was performed as described by Still and coworkers[17] using the indicated solvent on E. Merck silica gel 60 230-400 mesh. ^{1}H NMR spectra were recorded at 23 °C on one of the following instruments: Varian Unity 400, Varian Unity 500, Varian Unity Inova 500NB. Chemical shifts (δ) are reported in parts per million (ppm) downfield from tetramethylsilane and referenced internally to the residual protium in the NMR solvent ($CHCl_3$, δ = 7.26, $CD_3C(O)CHD_2$, δ = 2.04, center line) or to added tetramethylsilane. Data are reported as follows: chemical shift, multiplicity (s = singlet, d = doublet, t = triplet, q = quartet, p = pentet, sext = sextet, sept = septet, dd = doublet of doublets, ddd = doublet of doublet of doublets, td = triplet of doublets, m = multiplet, b = broad, app. = apparent), coupling constant (*J*) in hertz (Hz) and integration. ^{13}C spectra were recorded at 23 °C with a Varian Unity 500. Chemical shifts (δ) are reported downfield of tetramethylsilane and are referenced to the carbon resonances in the NMR solvent ($CDCl_3$, δ = 77.0, center line, $CD_3C(O)CD_3$, δ = 29.8, center line) or to added

tetramethylsilane. Carbons bearing boron substituents were not reported (quadrapolar relaxation). ^{11}B NMR were recorded using a General Electric GN300WB instrument and referenced to an external standard of $BF_3 \cdot Et_2O$. High resolution mass spectra (HRMS) were obtained at the University of Illinois mass spectrometry facility. All synthesized compounds gave HRMS within 5 ppm of calculated values. Infrared spectra were collected from a thin film on NaCl plates or as a KBr pellet on a Mattson Galaxy Series FTIR 5000 spectrometer with internal referencing. Absorption maxima (ν_{max}) are reported in wavenumbers (cm^{-1}).

Extinction Coefficient Determination

General procedure

A sample of dried compound was massed in a tared vial using a Mettler Toledo MT5 microbalance. This sample was then dissolved in DMSO to create a concentrated stock solution. A portion of this concentrated stock solution was diluted by a factor of five with DMSO to create a dilute stock solution. To achieve the final concentration for UV/Vis experiments, 5 μL of the dilute stock solution was diluted with 450 μL MeOH. For each compound, UV/vis experiments were performed using five different final concentrations and each concentration was prepared three times to obtain an average absorbance. The average absorbance was plotted against the concentration. The data was fitted with a linear least squares fit using Excel and the slope of the fitted line was used as the extinction coefficient. The extinction coefficients were as follows: AmB (ε_{406} = 164,000), AmdeB (ε_{406} = 102,000), C35deOAmB (ε_{404} = 78,000), natamycin (ε_{317} = 76,000), and natamycin aglycone (ε_{303} = 38,000).

Isothermal Titration Calorimetry

General Information

Experiments were performed using a NanoITC isothermal titration calorimeter (TA Instruments, Wilmington, DE). Solutions of the compounds to be tested were prepared by diluting a 15.0 mM stock solution of the compound in DMSO to 150 μM with K buffer (5.0 mM HEPES/KHEPES, pH = 7.4). The final DMSO concentration in the solution was 1% v/v. POPC LUVs were prepared and phosphorus and ergosterol content was quantified as described below. The LUV solutions were diluted with buffer and DMSO to give a final phospholipid concentration of 8.0 mM in a 1% DMSO/K buffer solution. Immediately prior to use, all

solutions were degassed under vacuum at 20 °C for 10 minutes. The reference cell of the instrument (volume = 0.190 mL) was filled with a solution of 1% v/v DMSO/K buffer.

LUV Preparation

Palmitoyl oleoyl phosphatidylcholine (POPC) was obtained as a 20 mg/mL solution in $CHCl_3$ from Avanti Polar Lipids (Alabaster, AL) and was stored at -20 °C under an atmosphere of dry argon and used within 1 month. A 4 mg/mL solution of ergosterol in $CHCl_3$ was prepared monthly and stored at 4 °C under an atmosphere of dry argon. Prior to preparing a lipid film, the solutions were warmed to ambient temperature to prevent condensation from contaminating the solutions. A 13 x 100 mm test tube was charged with 1.2 mL POPC and 350 μL of the ergosterol solution. For sterol-free liposomes, a 13 x 100 mm test tube was charged with 1.2 mL POPC. The solvent was removed with a gentle stream of nitrogen and the resulting lipid film was stored under high vacuum for a minimum of eight hours prior to use. The film was then hydrated with 1 mL of 5 mM HEPES pH 7.4 (K buffer) and vortexed vigorously for approximately 3 minutes to form a suspension of multilamellar vesicles (MLVs). The resulting lipid suspension was pulled into a Hamilton (Reno, NV) 1 mL gastight syringe and the syringe was placed in an Avanti Polar Lipids Mini-Extruder. The lipid solution was then passed through a 0.20 μm Millipore (Billerica, MA) polycarbonate filter 21 times, the newly formed large unilamellar vesicle (LUV) suspension being collected in the syringe that did not contain the original suspension of MLVs to prevent the carryover of MLVs into the LUV solution.

Determination of Phosphorus Content

Determination of total phosphorus was adapted from the report of Chen and coworkers.[18] Three 10 μL samples of the LUV suspension were added to three separate 7 mL vials. Subsequently, the solvent was removed with a stream of N_2. To each dried LUV film, and a fourth vial containing no lipids that was used as a blank, was added 450 μL of 8.9 M H_2SO_4. The four samples were incubated open to ambient atmosphere in a 225 °C aluminum heating block for 25 min and then removed to 23 °C and cooled for 5 minutes. After cooling, 150 μL of 30% w/v aqueous hydrogen peroxide was added to each sample, and the vials were returned to the 225 °C heating block for 30 minutes. The samples were then removed to 23 °C and cooled for 5 minutes before the addition of 3.9 mL water. Then 500 μL of 2.5% w/v ammonium molybdate

was added to each vial and the resulting mixtures were then vortexed briefly and vigorously five times. Subsequently, 500 μL of 10% w/v ascorbic acid was added to each vial and the resulting mixtures were then vortexed briefly and vigorously five times. The vials were enclosed with a PTFE lined cap and then placed in a 100 °C aluminum heating block for 7 minutes. The samples were removed to 23 °C and cooled for approximately 15 minutes prior to analysis by UV/Vis spectroscopy. Total phosphorus was determined by observing the absorbance at 820 nm and comparing this value to a standard curve obtained through this method and a standard phosphorus solution of known concentration.

Determination of Ergosterol Content

Ergosterol content was determined spectrophotometrically. A 50 μL portion of the LUV suspension was added to 450 μL 2:18:9 hexane:isopropanol:water (v/v/v). Three independent samples were prepared and then vortexed vigorously for approximately one minute. The solutions were then analyzed by UV/Vis spectroscopy and the concentration of ergosterol in solution was determined by the extinction coefficient of 10400 L mol^{-1} cm^{-1} at the UV_{max} of 282 nm and was compared to the concentration of phosphorus to determine the percent sterol content. The extinction coefficient was determined independently in the above ternary solvent system. LUVs prepared by this method contained between 7 and 14% ergosterol.

Titration Experiment

Titrations were performed by injecting the LUV suspension at ambient temperature into the sample cell (volume = 0.191 mL) which contained the 150 μM solution of the compound in question at 25 °C. The volume of the first injection was 0.23 μL. Consistent with standard procedure,[19] due to the large error commonly associated with the first injection of ITC experiments, the heat of this injection was not included in the analysis of the data. Next, nineteen 2.52 μL injections of the LUV suspension were performed. The spacing between each injection was 240 seconds to ensure that the instrument would return to a stable baseline before the next injection was made. The rate of stirring for each experiment was 300 rpm.

Data Analysis

NanoAnalyze software (TA Instruments) was used for baseline determination and

integration of the injection heats, and Microsoft Excel was used for subtraction of dilution heats and the calculation of overall heat evolved. To correct for dilution and mixing heats, the heat of the final injection from each run was subtracted from all the injection heats for that particular experiment.[20] By this method, the overall heat evolved during the experiment was calculated using the following formula:

$$\mu\text{cal}_{overall} = \sum_{i=1}^{n} (\Delta h^{i}_{injection} - \Delta h^{n}_{injection})$$

Where i = injection number, n = total number of injections, $\Delta h^{i}_{injection}$ = heat of the i^{th} injection, $\Delta h^{n}_{injection}$ = the heat of the final injection of the experiment. Values represent the mean ± SD of at least three experiments.

Potassium Efflux Assays

General Information

Ion selective measurements were obtained using a Denver Instruments (Denver, CO) Model 225 pH meter equipped with a World Precision Instruments (Sarasota, FL) potassium selective electrode inside a Faraday cage. The electrode filled with 1000 ppm KCl standard solution and conditioned in a 1000 ppm KCl standard solution for 30 minutes prior to ion selective measurements. Measurements were made on 3 mL solutions that were magnetically stirred in 7 mL Wheaton vials incubated in a 30 °C aluminum block (*S. cerevisiae*) or at 23 °C (LUVs). The instrument was calibrated daily with KCl standard solutions to 10, 100, and 1000 ppm potassium. The potassium concentration was sampled every 30 seconds throughout the course of the efflux experiments.

Growth Conditions for *S. cerevisiae*

S. cerevisiae was maintained with yeast peptone dextrose (YPD) growth media consisting of 10 g/L yeast extract, 20 g/L peptone, 20 g/L dextrose, and 20 g/L agar for solid media. The media was sterilized by autoclaving at 250 °F for 30 min. Dextrose was subsequently added as a sterile 40% w/v solution in water (dextrose solutions were filter sterilized). Solid media was prepared by pouring sterile media containing agar (20 g/L) onto Corning (Corning, NY) 100 x 20 mm polystyrene plates. Liquid cultures were incubated at 30 °C on a rotary shaker and solid cultures were maintained at 30 °C in an incubator.

Potassium Efflux from *S. cerevisiae*

The protocol to determine potassium efflux from *S. cerevisiae* was adapted from a similar experiment utilizing *C. albicans*.[21] An overnight culture of *S. cerevisiae* in YPD was centrifuged at 300 g for 5 minutes at 23 °C. The supernatant was decanted and the cells were washed twice with sterile water. After the second wash step, the cells were suspended in 150 mM NaCl, 5 mM HEPES pH 7.4 (Na buffer) to an OD_{600} of 1.5 (~$1x10^9$ CFU/mL) as measured by a Shimadzu (Kyoto, Japan) PharmaSpec UV-1700 UV/Vis spectrophotometer. A 3 mL sample of the cell suspension was then incubated in a 30 °C aluminum block with stirring for approximately 10 minutes before data collection. The probe was then inserted and data was collected for 5 minutes before adding 30 μL of the compound in question as a 0.3 mM or 3.0 mM solution in DMSO. The cell suspension was stirred and data were collected for 30 minutes and then 30 μL of a 1% aqueous solution of digitonin was added to effect complete potassium release and data were collected for an additional 15 minutes. The experiment was performed independently three times for each small molecule.

Data Analysis

The data from each run was normalized to the percent of total potassium release, from 0 to 100%. Thus for each experiment a scaling factor S was calculated using the following relationship:

$$\left[\frac{[K^+]_{final}}{[K^+]_{initial}} - 1\right] \cdot S = 100$$

Each concentration data point was then multiplied by S before plotting as a function of time.

Efflux from 10% ergosterol LUVs

LUV Preparation

Palmitoyl oleoyl phosphatidylcholine (POPC) was obtained as a 25 mg/mL solution in $CHCl_3$ from Avanti Polar Lipids (Alabaster, AL) and was stored at -20 °C under an atmosphere of dry argon and used within 3 months. A 4 mg/mL solution of ergosterol in $CHCl_3$ was prepared monthly and stored at 4 °C under an atmosphere of dry argon. Prior to preparing a lipid film, the

solutions were warmed to ambient temperature to prevent condensation from contaminating the solutions. A 13 x 100 mm test tube was charged with 640 μL POPC and 230 μL of the ergosterol solution. The solvent was removed with a gentle stream of nitrogen and the resulting lipid film was stored under high vacuum for a minimum of eight hours prior to use. The film was then hydrated with 1 mL of 150 mM KCl, 5 mM HEPES pH 7.4 (K buffer) and vortexed vigorously for approximately 3 minutes to form a suspension of multilamellar vesicles (MLVs). The resulting lipid suspension was pulled into a Hamilton (Reno, NV) 1 mL gastight syringe and the syringe was placed in an Avanti Polar Lipids Mini-Extruder. The lipid solution was then passed through a 0.20 μm Millipore (Billerica, MA) polycarbonate filter 21 times, the newly formed large unilamellar vesicle (LUV) suspension being collected in the syringe that did not contain the original suspension of MLVs to prevent the carryover of MLVs into the LUV solution. To obtain a sufficient quantity of LUVs, three independent 1 mL preparations were pooled together for the dialysis and subsequent potassium efflux experiments. The newly formed LUVs were dialyzed using Pierce (Rockford, IL) Slide-A-Lyzer MWCO 3,500 dialysis cassettes. The samples were dialyzed three times against 600 mL of Na buffer. The first two dialyses were two hours long, while the final dialysis was performed overnight.

Determination of Phosphorus Content

Determination of total phosphorus was adapted from the report of Chen and coworkers.[18] The LUV solution was diluted tenfold with Na buffer and three 10 μL samples of the diluted LUV suspension were added to three separate 7 mL vials. Subsequently, the solvent was removed with a stream of N_2. To each dried LUV film, and a fourth vial containing no lipids that was used as a blank, was added 450 μL of 8.9 M H_2SO_4. The four samples were incubated open to ambient atmosphere in a 225 °C aluminum heating block for 25 min and then removed to 23 °C and cooled for 5 minutes. After cooling, 150 μL of 30% w/v aqueous hydrogen peroxide was added to each sample, and the vials were returned to the 225 °C heating block for 30 minutes. The samples were then removed to 23 °C and cooled for 5 minutes before the addition of 3.9 mL water. Then 500 μL of 2.5% w/v ammonium molybdate was added to each vial and the resulting mixtures were then vortexed briefly and vigorously five times. Subsequently, 500 μL of 10% w/v ascorbic acid was added to each vial and the resulting mixtures were then vortexed briefly and vigorously five times. The vials were enclosed with a PTFE lined cap and

then placed in a 100 °C aluminum heating block for 7 minutes. The samples were removed to 23 °C and cooled for approximately 15 minutes prior to analysis by UV/Vis spectroscopy. Total phosphorus was determined by observing the absorbance at 820 nm and comparing this value to a standard curve obtained through this method and a standard phosphorus solution of known concentration.

Determination of Ergosterol Content

Ergosterol content was determined spectrophotometrically. The LUV solution was diluted tenfold with Na buffer, and 50 μL of the dilute LUV suspension was added to 450 μL 2:18:9 hexane:isopropanol:water (v/v/v). Three independent samples were prepared and then vortexed vigorously for approximately one minute. The solutions were then analyzed by UV/Vis spectroscopy and the concentration of ergosterol in solution was determined by the extinction coefficient of 10400 L mol^{-1} cm^{-1} at the UV_{max} of 282 nm and was compared to the concentration of phosphorus to determine the percent sterol content. The extinction coefficient was determined independently in the above ternary solvent system. LUVs prepared by this method contained between 7 and 14% ergosterol.

Efflux from LUVs

The LUV solutions were adjusted to 1 mM in phosphorus using Na buffer. 3 mL of the 1 mM LUV suspension was added to a 7 mL vial and the solution was gently stirred. The potassium ISE probe was inserted and data were collected for one minute prior to the addition of the compound. Then, 30 μL of a 0.1 mM, 1.0 mM, or 3.0 mM DMSO solution of the compound in question was added and data were collected for five minutes. Then to effect complete potassium release, 30 μL of a 10% v/v solution of triton X-100 was added and data were collected for an additional five minutes. The experiment was duplicated with similar results.

Data Analysis

The data from each run were analyzed in the same manner as the efflux data from *S. cerevisiae.*

Antifungal Assays

Growth Conditions for *S. cerevisiae*

S. cerevisiae was maintained with yeast peptone dextrose (YPD) growth media consisting of 10 g/L yeast extract, 20 g/L peptone, 20 g/L dextrose, and 20 g/L agar for solid media. The media was sterilized by autoclaving at 250 °F for 30 min. Dextrose was subsequently added as a sterile 40% w/v solution in water (dextrose solutions were filter sterilized). Solid media was prepared by pouring sterile media containing agar (20 g/L) onto Corning (Corning, NY) 100 x 20 mm polystyrene plates. Liquid cultures were incubated at 30 °C on a rotary shaker and solid cultures were maintained at 30 °C in an incubator.

Growth Conditions for *C. albicans*

C. albicans was cultured in a similar manner to *S. cerevisiae* except both liquid and solid cultures were incubated at 37 °C.

Broth Microdilution Minimum Inhibitory Concentration (MIC) Assay

The protocol for the broth microdilution assay was adapted from the Clinical and Laboratory Standards Institute document M27-A2.[22] 50 mL of YPD media was inoculated and incubated overnight at either 30 °C (*S. cerevisiae*) or 37 °C (*C. albicans*) in a shaker incubator. The cell suspension was then diluted with YPD to an OD_{600} of 0.10 (~5 x 10^5 cfu/mL) as measured by a Shimadzu (Kyoto, Japan) PharmaSpec UV-1700 UV/Vis spectrophotometer. The solution was diluted 10-fold with YPD, and 195 μL aliquots of the dilute cell suspension were added to sterile Falcon (Franklin Lakes, NJ) Microtest 96 well plates in triplicate. Compounds were prepared either as 400 μM (AmB, MeAmB) or 2 mM (AmdeB, MeAmdeB) stock solutions in DMSO and serially diluted to the following concentrations with DMSO: 1600, 1200, 800, 400, 320, 240, 200, 160, 120, 80, 40, 20, 10 and 5 μM. 5 μL aliquots of each solution were added to the 96 well plate in triplicate, with each column representing a different concentration of the test compound. The concentration of DMSO in each well was 2.5% and a control well to confirm viability using only 2.5% DMSO was also performed in triplicate. This 40-fold dilution gave the following final concentrations: 50, 40, 30, 20, 10, 8, 6, 4, 1, 0.5, 0.25 and 0.125 μM. The plates were covered and incubated at 30 °C (*S. cerevisiae*) or 37 °C (*C. albicans*) for 24 hours prior to analysis. The MIC was determined to be the concentration of compound that resulted in no visible growth of the yeast. The experiments were performed in duplicate and the reported MIC represents an average of two experiments.

Ergosterol Content Determination

Determination of Ergosterol Standard Curve

Ergosterol was prepared as a 0.1 mg/mL stock solution in $CHCl_3$ and serially diluted to the following concentrations with $CHCl_3$: 0.1, 0.08, 0.06, 0.03, 0.01 and 0.005 mg/mL. 10 µL aliquots of each solution were analyzed by analytical RP-HPLC (Waters Sunfire C_{18}, ODB 5 micron, 4.6 x 150 mm, 2 mL/min flow rate, MeCN:ethanol (200 proof) 80:20 isocratic over 10 minutes) in triplicate. Ergosterol was detected at 280 nm. Ergosterol concentration was plotted against the integration of the ergosterol peak (t_r = 5.1 min) the data was fitted with a linear least squares fit using Excel giving a standard curve.

Determination of Stigmasterol Standard Curve

Stigmasterol was prepared as a 4 mg/mL stock solution in toluene and serially diluted to the following concentrations with $CHCl_3$: 4, 2, 1, 0.5, 0.25 and 0.125 mg/mL. 10 µL aliquots of each solution were analyzed by analytical RP-HPLC (Waters Sunfire C_{18}, ODB 5 micron, 4.6 x 150 mm, 2 mL/min flow rate, MeCN:ethanol (200 proof) 80:20 isocratic over 10 minutes) in triplicate. Stigmasterol was detected at 210 nm. Stigmasterol concentration was plotted against the integration of the ergosterol peak (t_r = 7.8 min) the data was fitted with a linear least squares fit using Excel giving a standard curve.

Ergosterol Determination

Determination of total ergosterol was adapted from the report of Arnezeder and coworkers.[23] The starting yeast cultures were prepared identical to the yeast used in the MIC assays. 50 mL of YPD media was inoculated and incubated overnight at either 30 °C (*S. cerevisiae*) or 37 °C (*C. albicans*) in a shaker incubator. 15 mL of the overnight culture was centrifuged (300 g, 23 ^{o}C) for 5 minutes. The supernatant was decanted and the cells were resuspended in 15 mL of Na buffer (150 mM NaCl, 5 mM HEPES, pH 7.4) and centrifuged (300 g, 23 ^{o}C) for 5 minutes. This process was repeated two additional times and after the third wash, the cells were suspended in Na buffer to an OD_{600} of 1.3 as measured by a Shimadzu (Kyoto, Japan) PharmaSpec UV-1700 UV/Vis spectrophotometer. 40 mL of the OD_{600} = 1.3 yeast suspension were centrifuged (600 g, 23 ^{o}C) for 10 minutes. The supernatant was decanted and

the cells were resuspended in 50 mL sterile water and centrifuged (300 g, 23 ^{o}C) for 5 minutes. The supernatant was decanted and the resulting yeast pellet was suspended in 10 mL of 0.1 M aqueous HCl and transferred to 40 mL I-Chem vial. 0.9 mL of a 4 mg/mL standard solution of stigmasterol in toluene was added to the sample as an internal standard. The sample was incubated at 90 °C for 20 minutes and transferred to a 300 mL round bottom flask equipped with a stir bar. The I-Chem vial was washed with 50 mL of ethanol and 50 mL of 50% aqueous KOH and the washings were added to the 300 mL round bottom flask. The 300 mL round bottom flask was stirred at reflux for 30 minutes and then allowed to cool to room temperature. The solution was extracted three times with 30 mL of petroleum ether. The combined organic layers were dried over Na_2SO_4 and concentrated *in vacuo*. The resulting solid was dissolved in 3 mL of 3:1 isopropanol:acetone and filtered through a 0.22 μm low protein binding Durapore (PVDF) membrane. 10 μL aliquots of the filtered solution were analyzed by analytical RP-HPLC (Waters Sunfire C_{18}, ODB 5 micron, 4.6 x 150 mm, 2 mL/min flow rate, MeCN:ethanol (200 proof) 80:20 isocratic over 10 minutes) in triplicate. Ergosterol was detected at 280 nm and stigmasterol was detected at 210 nm. Ergosterol and stigmasterol concentrations were determined by comparing the integration of the ergosterol peak to the standard curves described above. The stigmasterol internal standard was used to adjust the ergosterol concentration for any loss of material during the extraction process. The experiment described above was repeated in triplicate for both *S. cerevisiae* and *C. albicans*.

Determination of Cell Concentration at OD_{600} = 1.3

10 μL of the OD_{600} = 1.3 yeast suspension described above was diluted tenfold with Na buffer. 10 μL of the diluted suspension was injected into the INCYTO Neubauer Improved Disposable Hemocytometer. Yeast cells were counted with an AMG EVOS fl Microscope. The cell concentration determination was repeated in triplicate.

Determination of Cell Concentration in the MIC Assay

The overnight cultures *S. cerevisiae* and *C. albicans* in YPD that were used in the ergosterol determination above were diluted with YPD to an OD_{600} of 0.10. This was done at the same time as the sterol determination experiment above to ensure that the sterol content directly related to the cell count. 10 μL of the suspension was injected into the INCYTO Neubauer

Improved Disposable Hemocytometer. Yeast cells were counted with an AMG EVOS fl Microscope. In the MIC assay, an OD_{600} = 0.10 yeast suspension was diluted 10-fold prior to running the assay so all cell counts were divided by 10 to get the cell concentration in the MIC assay. The cell concentration determination was repeated in triplicate.

3-6 References

1. Hoogevest, P. V.; de Kruijf, B. *Biochim. Biophys. Acta* **1978**, *511*, 397-407.
2. Szpilman,A. M.; Cereghetti, D. M.; Manthrope, j. M.; Wurtz, N. R.; Carreira, E. M. *Chem. Eur. J.* **2009**, *15*, 7117-7128.
3. Gray, K. C.; Palacios, D. S.; Dailey, I.; Endo, M. M.; Uno, B. E.; Wilcock, B. C.; Burke, M. D. *Proc. Natl. Acad. Sci. U. S. A.* **2012**, *109*, 2234-2239.
4. Gillis, E. P.; Burke, M. D. *J. Am. Chem. Soc.* **2007**, *129*, 6716-6717.
5. Gillis, E. P.; Burke, M. D. *Aldrichimica Acta* **2009**, *42*, 17-27.
6. Nicolaou, K. C.; Chakraborty, T. K.; Ogawa, Y.; Daines, R. A.; Simpkins, N. S.; Furst, G. T. *J. Am. Chem. Soc.* **1988**, *110*, 4660-4672.
7. Tsuchikawa, h.; Matsushita, N.; Matsumori, N.; Murata, M.; Oshi, T. Tetrahedron Lett. **2006**, *47*, 6187-6191.
8. Lee, S. J.; Anderson, T. M.; Burke, M. D. *Angew. Chem. Int. Ed.* **2010**, *49*, 8860-8863.
9. Bruggink, A.; Roos, E. C.; de Vroom, E. *Org. Process Rev. Dev.* **1998**, *2*, 128-133.
10. McVey, C. E.; Walsh, M. A.; Dodson, G. G.; Wilcocn, K. S.; Brannigan, J. A. *J. Mol. Biol.* **2001**, *313*, 139-150.
11. te Welscher, Y. M.; Jones, L.; van Leeuwen, M. R.; Dijkesterhuis, J.; de Kruijff, B.; Eitzen, G.; Breukink, E. *Antimicrob. Agents Chemother.* **2010**, *54*, 2618-2625.
12. Kato, M.; Wickner, W. *EMBO J.* **2001**, *20*, 4035-4040.
13. Heese-Peck, A.; Pichler, H.; Zanolari, B.; Watanabe, R.; Daum, G.; Riezman, H. *Mol. Biol. Cell* **2002**, *13*, 2664-2680.
14. Klose, C.; Ejsing, C. S.; Garcia-Saez, A. J.; Kaiser, H.; Sampaio, J. L.; Surma, M. A.; Shevchenko, A.; Schwille, P.; Simons, K. *J. Biol. Chem.* **2010**, *285*, 30224-30232.
15. Zhang, Y. Q. PLoS Pathog. **2010**, *6*, e1000939.
16. Pangborn, A.B.; Giardello, M.A.; Grubbs, R.H.; Rosen, R.K.; Timmers, F.J. *Organometallics* **1996**, *15*, 1518-1520.

17. Still, W. C.; Kahn, M.; Mitra, A. *J. Org. Chem.* **1978**, *43*, 2923-2925.
18. Chen, P. S.; Toribara, T. Y.; Warner, H. *Anal. Chem.* **1956**, *28*, 1756-1758.
19. Heerklotz, H.; Seelig, J. *Biochim. Biophys. Acta.* **2000**, *1508*, 69-85.
20. te Welscher, Y. M.; *et al*. *J. Biol. Chem.* **2008**, *283*, 6393-6401.
21. Hammond, S. A.; Lambert, P. A.; Kilger, B. N. *J. Gen. Microbiol.* **1974**, *81*, 325-330.
22. Clinical and Laboratory Standards Institute. Reference Method for Broth Dilution Antifungal Susceptibility Testing, M27-A2, Approved Standard 2nd Ed. Vol. 22, Number 15, **2002**.
23. Arnezeder, C. H.; Koliander, W.; Hampel, W. A. *Anal. Chim. Acta.* **1989**, *225*, 129-136.

Chapter 4

Electronic Tuning of Site-Selective Acylation on Amphotericin B

This chapter describes the investigation of site-selective acylation of hydroxyl groups on amphotericin B towards the goal of efficiently accessing derivatives. Several strategies were explored using both enzymatic and small molecule catalysts with a variety of acyl donors. Ultimately, the strategy of electronically tuning the acyl donor achieved high selectivity for the C2' hydroxyl. Selective acylation studies were performed by Brandon Wilcock. Production of intermediates was done by Brandon Wilcock, Brice Uno, Gretchen Bromann, Matt Clark, and Tom Anderson. Portions of this chapter were adapted from Wilcock, B. C.; Uno, B. E.; Bromann, G. L.; Clark, M. J.; Anderson, T. M.: Burke, M. D. *Nature Chemistry* **2012**, *4*, 996-1003.

4-1 Site-Selective Reactions for Efficient Access to Derivatives of Natural Products

Natural products and complex small molecules can have the capacity to perform a variety of useful functions, and many display important biological activity or medicinal properties. Structural derivatives of these compounds are useful tools for the study of their function and/or the development of therapeutics and pharmaceuticals. Often, access to derivatives of natural products and complex small molecules can be limited by time, labor, and cost intensive synthesis. Sometimes the natural product can be readily obtained from nature or through production by an organism. In these cases, site-selective functionalization is an attractive frontier synthesis strategy[1-7] that can have exceptional step efficiency compared to total synthesis for the generation of derivatives. However, this strategy can be challenging in complex small molecules that contain the same functional group at multiple sites. Thus, generalized approaches for maximizing site selectivity or enabling the development of reagents with the ability to override substrate bias to achieve site-divergent functionalizations would be highly useful in small molecule science.

Polyols are a common type of natural product where site-selective functionalization is especially sought after. For instance, sugars are commonly present in biomolecules and natural products and selective protection and derivatization of these sugar units is a major area of scientific research.[8] AmB is an excellent example of a polyol natural product that would greatly benefit from site-selective deoxygenation to efficiently access deoxyAmB derivatives to

elucidate the roles of the ten hydroxyl groups appended to this vital antifungal agent. Towards this end, site-selective acylation is a promising method for isolating single hydroxyl groups on polyol substrates.[1,9-19] Application of this method leads to the following strategy for the creation of deoxyAmB derivatives. First, site-selective acylation of a hydroxyl group followed by orthogonal protection of the remaining hydroxyls and subsequent deacylation isolates the hydroxyl. Second, the exposed hydroxyl is deoxygenated generating the desired derivative after global deprotection (Figure 4.1).

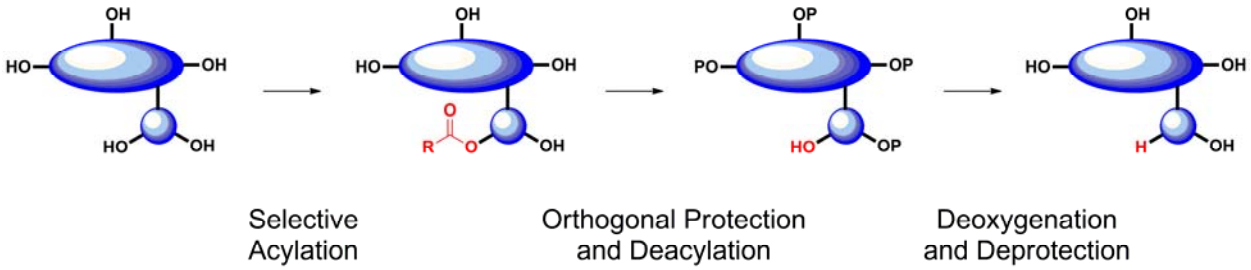

Figure 4.1. Strategy for generating deoxygenated amphotericin B derivatives using site selective acylation.

In order to achieve site-selective acylation on a polyol substrate under irreversible kinetic control, there must be a significant difference in the activation energies of the transition states for the rate-determining acyl transfer step. The transition state energies will be dependent upon the interactions between the acylating complex, generated from an acyl donor and a catalyst, and the polyol substrate. Thus, selective acylation can be achieved by finding a combination of acyl donor and catalyst that interacts with the polyol substrate in a fashion that results in a lower activation energy for the transition state of one of the hydroxyls in comparison to the other hydroxyls (Figure 4.2).

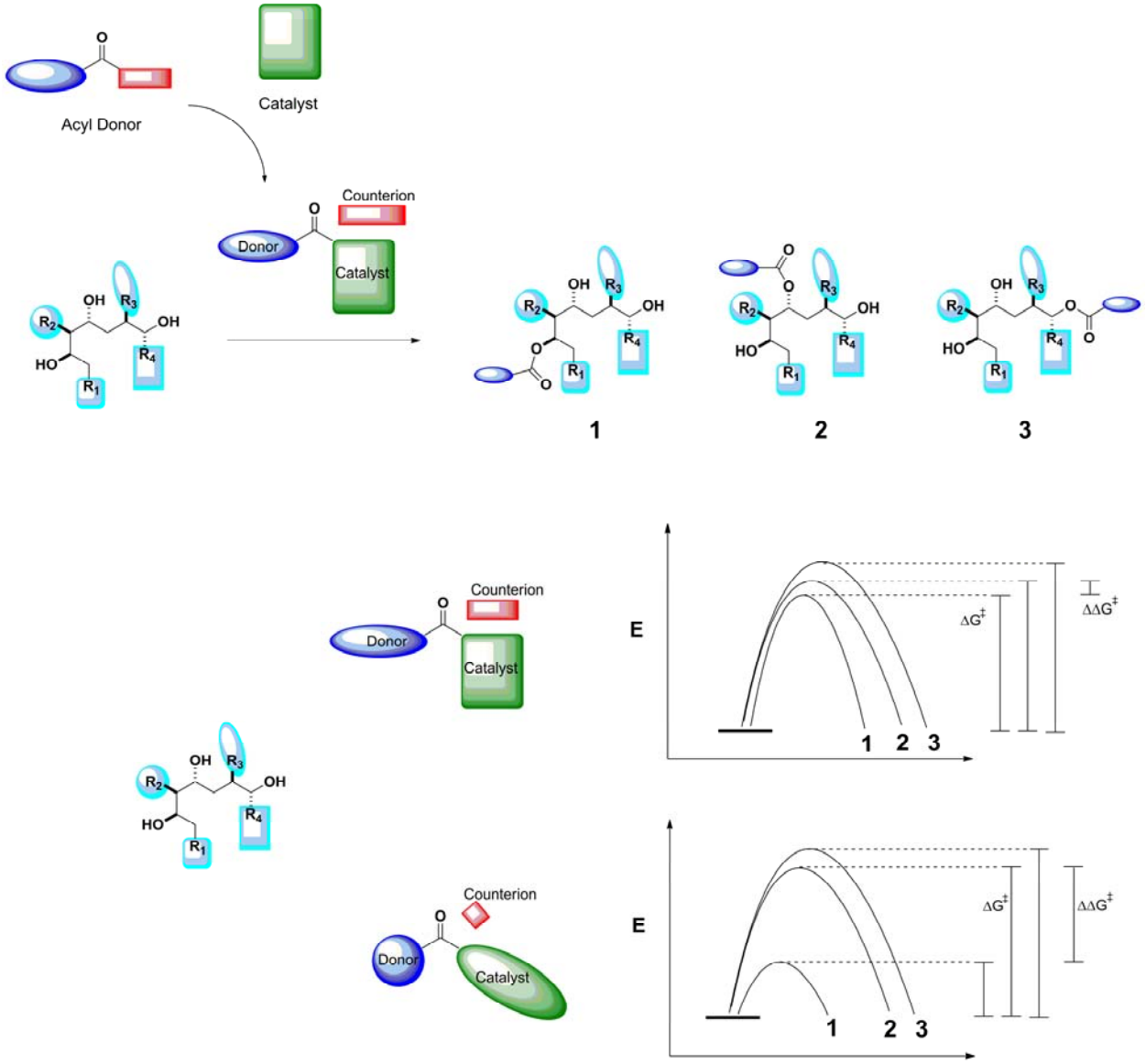

Figure 4.2. Basis for achieving site-selective acylation on a polyol substrate using a combination of acyl donor and catalyst to lower the activation energy of the transition state of one of the hydroxyls in comparison to the others.

Methods for achieving site-selective acylation have mostly focused on stereochemical modification of the acylation catalyst[1,9-17] and the use of enzymes.[18,19] The Miller group has had success employing this approach through the use of small peptide based catalyst libraries.[1,6,9-12] For example, erythromycin A is primarily acylated at the C4" position with *N*-methyl imidazole as the catalyst, but the C11 hydroxyl is the major site of acylation with a peptide catalyst (Figure 4.3 A).[1] In addition, enzymes have also been employed for selective acylation of natural products and sugars.[18,19] For instance, Gu and coworkers were able to selectively acylate rapamycin using a lipase from *Candida antartica B.* (Figure 4.3 B).[18] Other developments in this area include

chiral small molecule catalysts such as functionalized 4-*N*,*N*-dimethylaminopyridine (DMAP) derivatives.[13,14] For instance, Kawabata and coworkers were able to selectively acylate the C4 position of octyl β-D-glucopyranoside (Figure 4.3 C).[14] Another common approach is increasing the steric bulk of the acyl donor to gain bias towards the less sterically hindered site.[20,21] There are a couple of reports where the counterion of the acylating complex was able to significantly influence the site of acylation.[17,22]

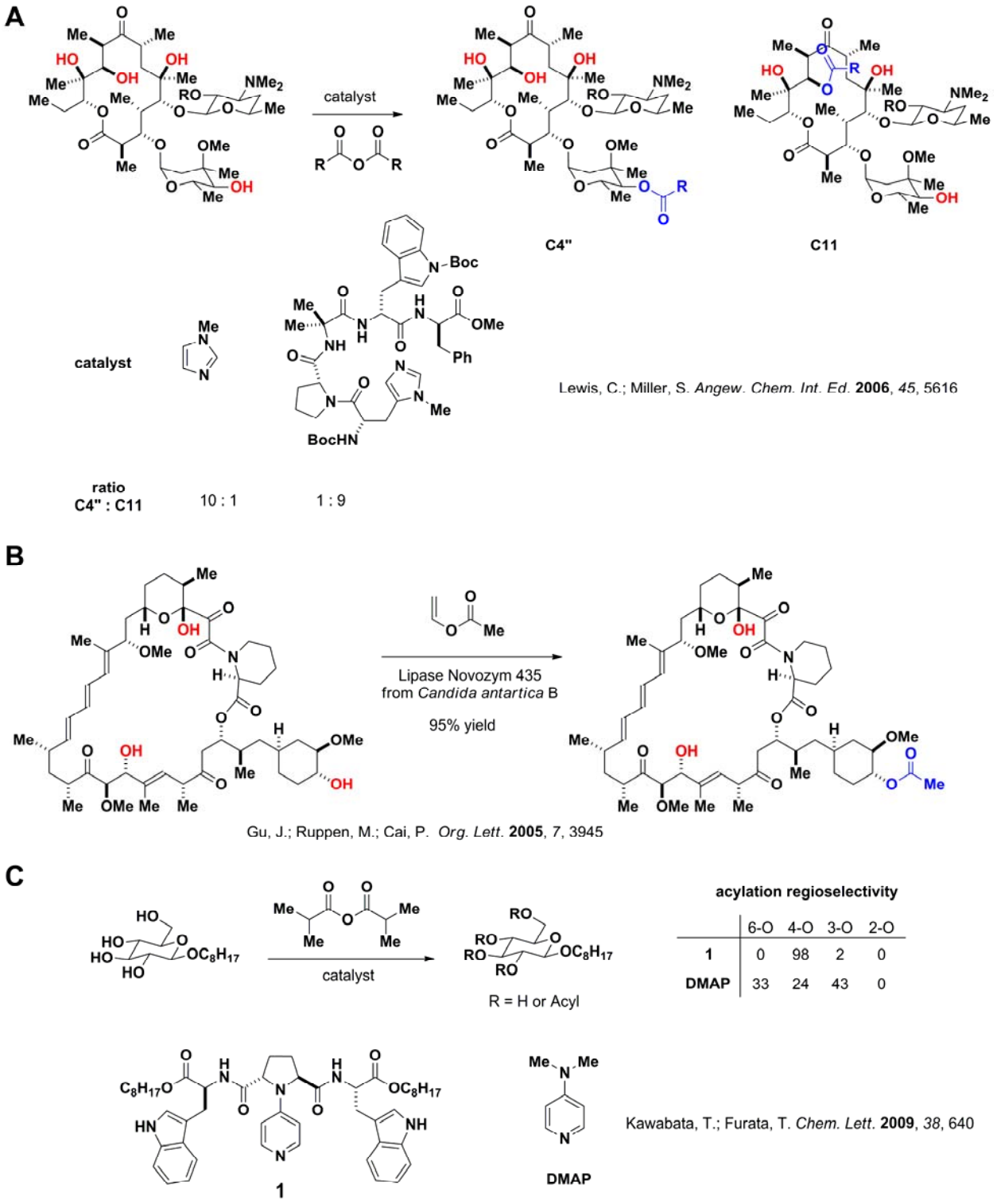

Figure 4.3. Examples of site-selective acylation. **A**. Peptide catalyzed acylation of erythromycin A by Lewis and Miller. **B**. Enzymatic acylation of rapamycin by Gu and coworkers. **C**. Selective acylation with functionalized DMAP by Kawabata and Furata.

4-2 Enzyme-Mediated Acylation of Amphotericin B Substrates

In order to generate a workable substrate for acylation, the more reactive carboxylic acid, amine, and hemiketal functionality present on AmB needed to be protected. These protections were also necessary to impart a reasonable level of solubility to perform the reactions, purification, and analysis. Substrate **4.1** was therefore synthesized according to Scheme 4.1.[23]

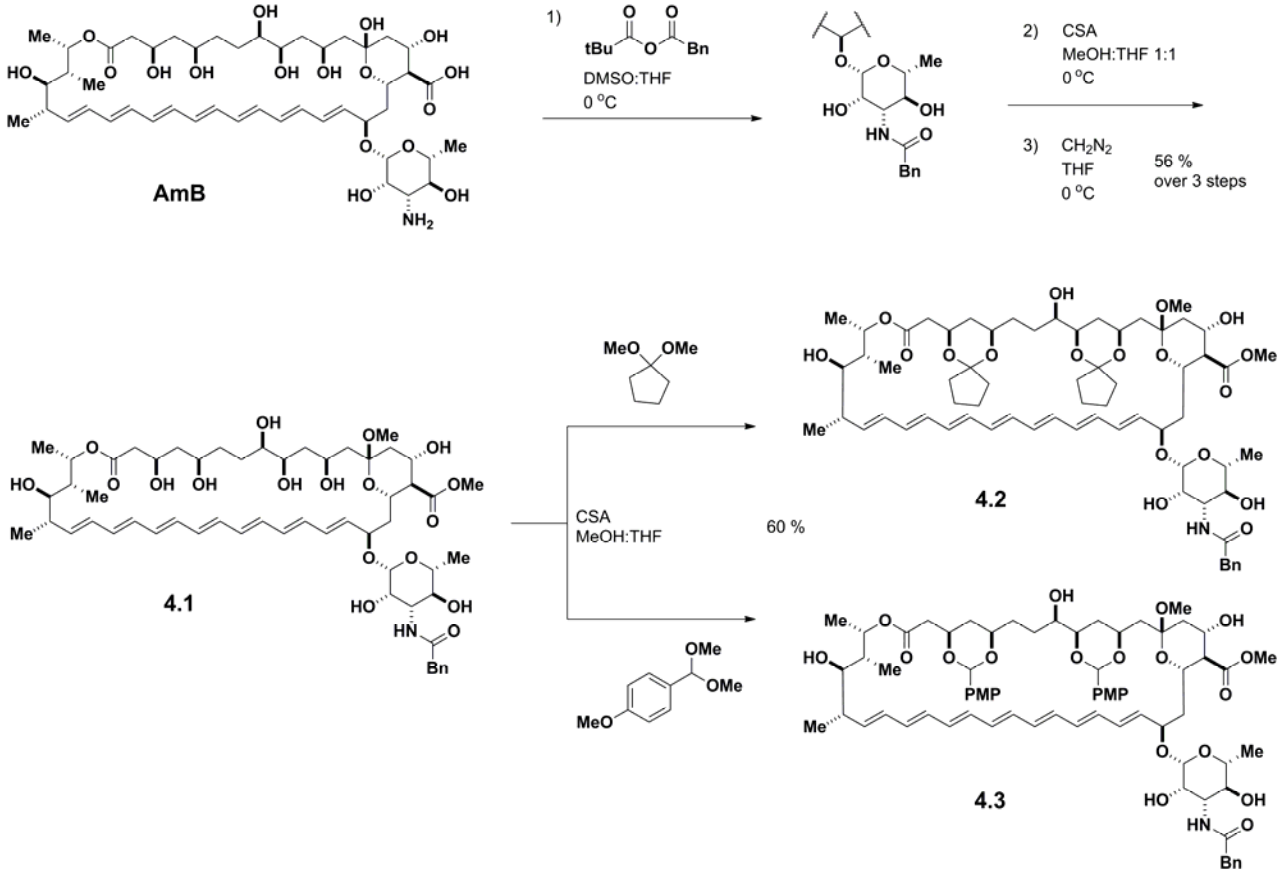

Scheme 4.1. Synthesis of AmB substrates for selective acylation experiments.

First, the amine was protected as the phenylacetyl amide. Next, the hemiketal was transformed to a methyl ketal, and then the carboxylic acid was methylated to generate a methyl ester. These series of protections gives a substrate containing nine free hydroxyls. Selectively acylating one out of nine hydroxyls is a significant synthetic challenge. I noticed, however, that this challenge could be significantly reduced if the desired target hydroxyl was not at C3, C5, C9, or C11. This is accomplished by installing 1,3 ketals or acetals on the C3/C5 and C9/C11 hydroxyl groups to give substrates **4.2** and **4.3**. This protection reduces the number of available

hydroxyl sites by four and also provides some steric discrimination against the adjacent C8 hydroxyl group thereby strategically targeting the hydroxyls at C35, C15, C4', and C2'.

I obtained a collection of 42 commercially available lipases and amidases and performed an initial screen of solvents utilizing the simple acyl donor vinyl acetate and **4.1**. Most of the enzymes failed to give any reactivity with AmB; however, a few enzymes did show reactivity in polar solvents such as DMF. The greater solubility of **4.1** in these more polar solvents significantly aided the reaction. Halogenated and protic solvents were not tolerated, and mixtures of DMF and nonpolar solvents had no observable affect on selectivity and reduced the rate of the

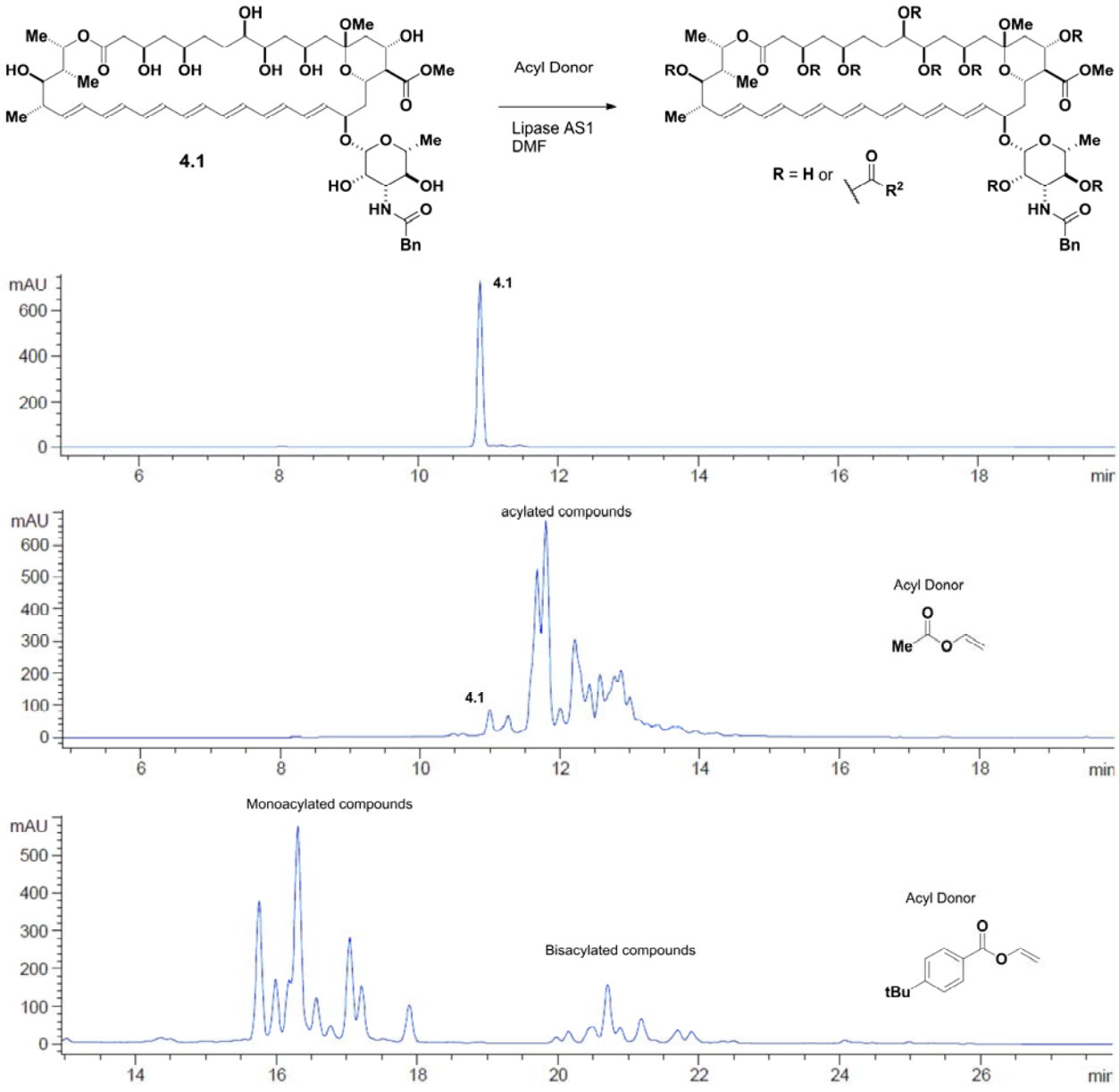

Figure 4.4. HPLC traces of lipase mediated acylation reactions on substrate **4.1**.

reaction. While some lipases accepted **4.1** as a substrate, very poor selectivity was observed by high-performance liquid chromatography (HPLC) and mass spectrometry (MS) analysis when simple acyl donors such as vinyl acetate were used (Figure 4.4). I observed unresolved mixtures of mono and polyacylated compounds. I therefore investigated a variety of acyl donors including substituted aromatic vinyl esters as well as straight chain and branched aliphatic vinyl esters. The selectivity increased for some donors, but useful levels of selectivity were still unobtainable with substrate **4.1** (Figure 4.4).

To address the selectivity issue, I screened the collection of lipases with substrate **4.2**. The increased steric demand of **4.2** greatly reduced reactions rates or resulted in complete inactivity with the enzymes that were active with **4.1**. However, I found that one lipase, AS1, was still significantly active with this substrate and benzoic vinyl ester. Aliphatic vinyl esters reacted at a much slower rate. The reaction with benzoic vinyl ester produced a major product and two minor products. After HPLC isolation of the products and 2-D nuclear magnetic resonance (NMR) analysis, I found the major product to be acylation at C2' and acylation at C4' and bisacylation (C2' and C4') were minor products (Figure 4.5).

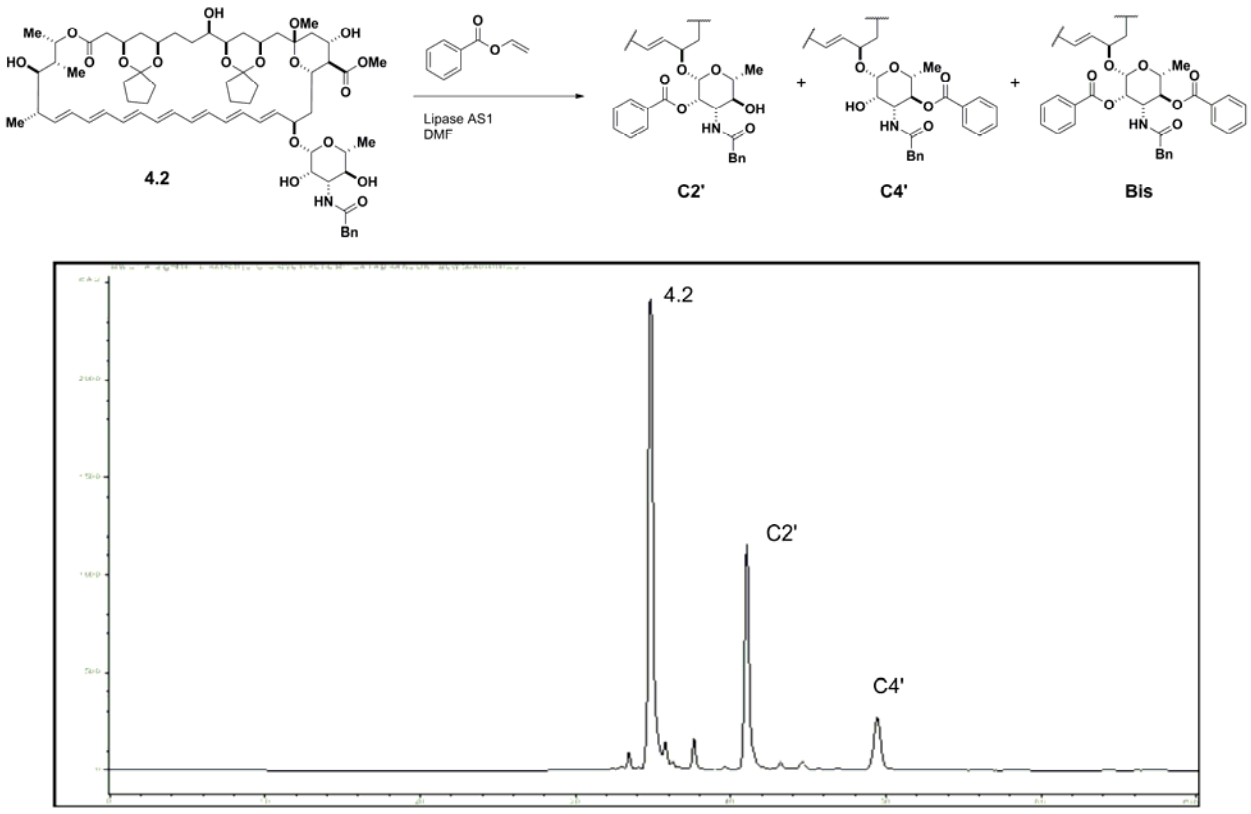

Figure 4.5. HPLC trace of the site-selective acylation of the C2' hydroxyl by lipase AS1.

I focused on substituted aromatic vinyl esters varying the position (para, ortho, and meta) as well as the steric bulk of the substitution (methyl, phenyl, tertbutyl). I found that in all cases acylation at the C2' hydroxyl was the major product; however, the reaction rate and ratio to the minor products varied (Table 4.1).

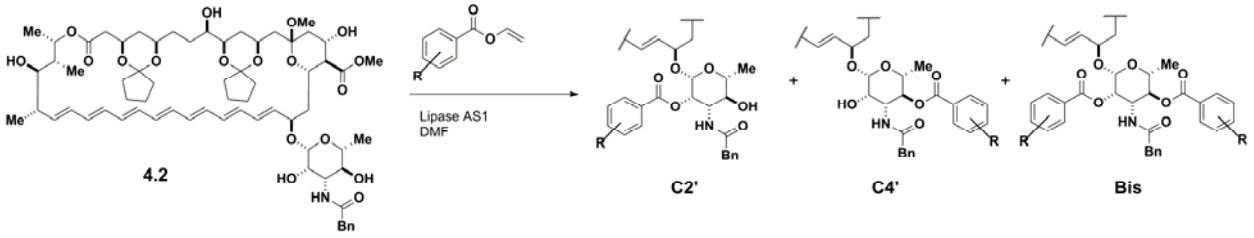

Acyl Donor R =	% Conversion to Products	Product Ratio 2' : 4' : Bis
H	50	6.7 : 1 : 1.5
2-Ph	8	6.9 : 1 : 0
3-Ph	75	8.0 : 1 : 4.5
4-Ph	32	10.9 : 1.7 : 1

Table 4.1. Site-selective acylation of substrate **4.2** by lipase AS1 and some selected vinyl esters.

I found *p*-tertbutylbenzoic vinyl ester gave an optimum balance of selectivity, 88% of the products were monoacylated at C2', and resolution for chromatographic purification (Scheme 4.2). The reaction was stopped at 50% conversion to prevent excessive generation of the bisacylated product via acylation of the product **4.4** at the C4' position. The starting material, **4.2**, was recovered and resubmitted.

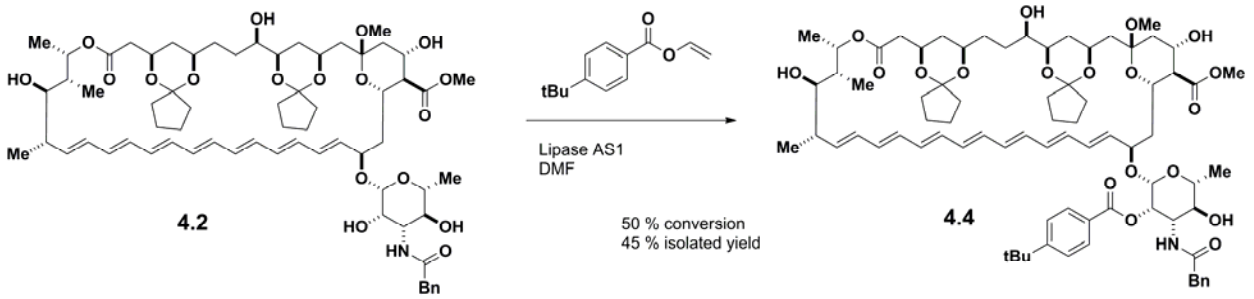

Scheme 4.2. Site-selective acylation of the C2' hydroxyl by lipase AS1.

Unfortunately, I found this reaction to be irreproducible between different batches of lipase powder. While the selectivity remained high when the lipase was active, many batches failed to react with **4.2** even though the lipase was active with smaller substrates. I suspected

small differences in the hydration state from the lyophilization process affected the flexibility of the lipase in the dry organic solvent used to run the reactions.[24] Increasing the temperature of the reaction to 70 °C increased reactivity in some batches. Relyophilization also activated some batches; however, I was unable to develop a reliable lyophilization process that would produce lipase powder with consistent activity. Thus, emphasis was placed on small-molecule catalyzed acylation to obtain a consistent and reliable acylation reaction.

4-3 DMAP Catalyzed Acylation on Amphotericin B Substrates

A common method to try to achieve site-selective acylation is modifying the catalyst's steric and stereochemical properties. Instead of employing this approach, I focused on changing the properties of the acyl donor; I could access a large variety of anhydrides and acid chlorides either commercially or synthetically significantly faster than modification of catalysts such as DMAP. I briefly investigated DMAP-catalyzed acylation on substrate **4.1**. I observed many

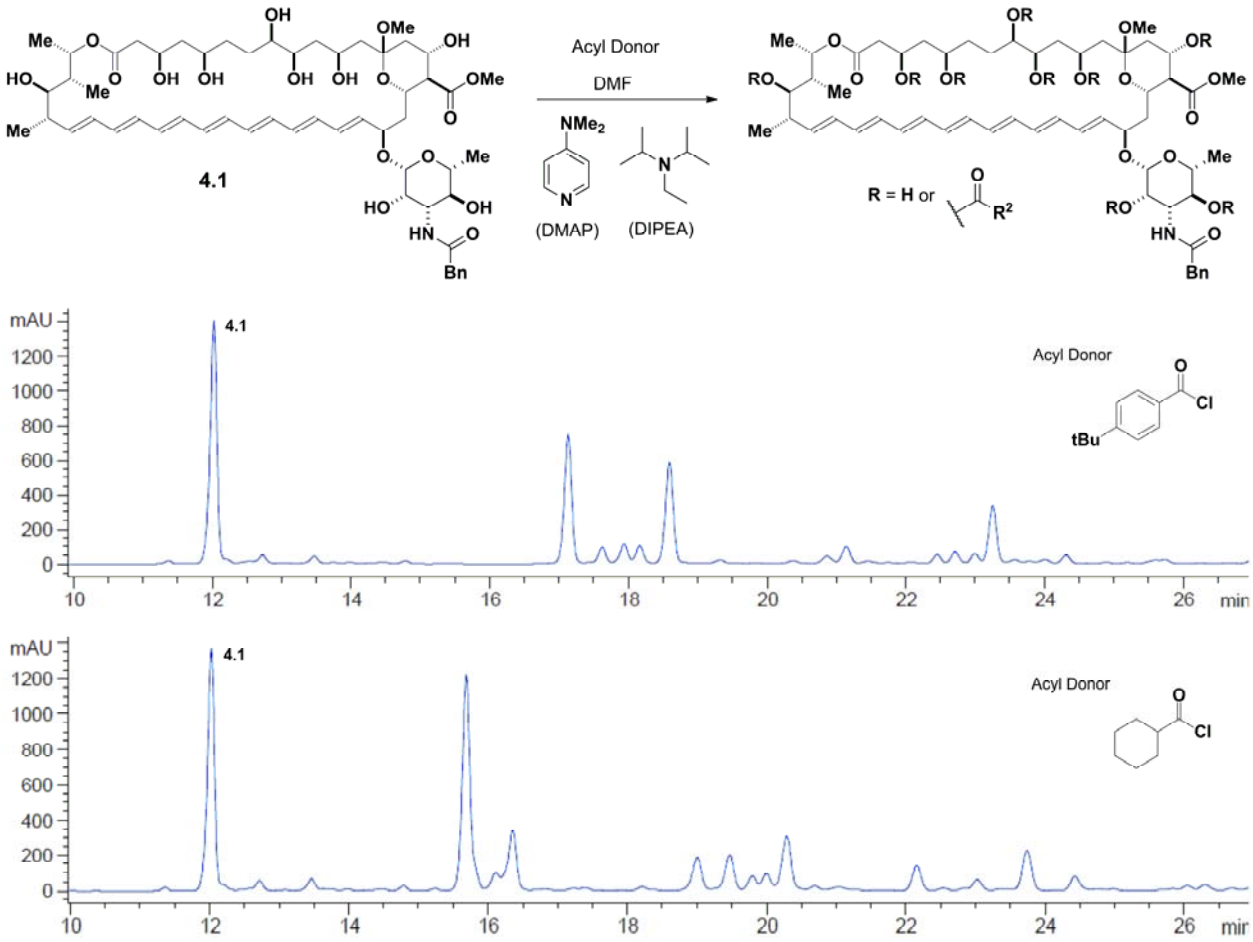

Figure 4.6. HPLC traces of acylation reactions with substrate **4.1** and DMAP.

mono and poly acylated products when these reactions were analyzed by HPLC and MS. Employing more sterically demanding acyl donors failed to produce a viable selective reaction (Figure 4.6). Therefore, I focused on site-selective acylation of substrate **4.3**. Specifically, I targeted the C2' hydroxyl on the mycosamine. The C2' hydroxyl is a high priority target since the mycosamine is essential for sterol binding and the antifungal activity of AmB (see Chapter 1), and it has been implicated in a possible hydrogen bond with the sterol (see Chapter 3).

I started with standard acylating conditions commonly found in the literature utilizing acetic anhydride and DMAP. HPLC and MS analysis of the reaction mixture showed a mixture of mono, bis, and tris acylated products (Figure 4.7, entry 1).[23] Characterization of preparative HPLC isolated peaks showed that monoacylated C2' product was only 2% of the total products. I systematically investigated increasing the steric bulk of the acyl donor by employing the anhydride series: propionic, isobutyric, and pivalic. I found the extremely sterically demanding pivalic anhydride to be unreactive under the reaction conditions. Propionic and isobutyric anhydride had little effect on the percentage of the products that was monoacylated at C2';

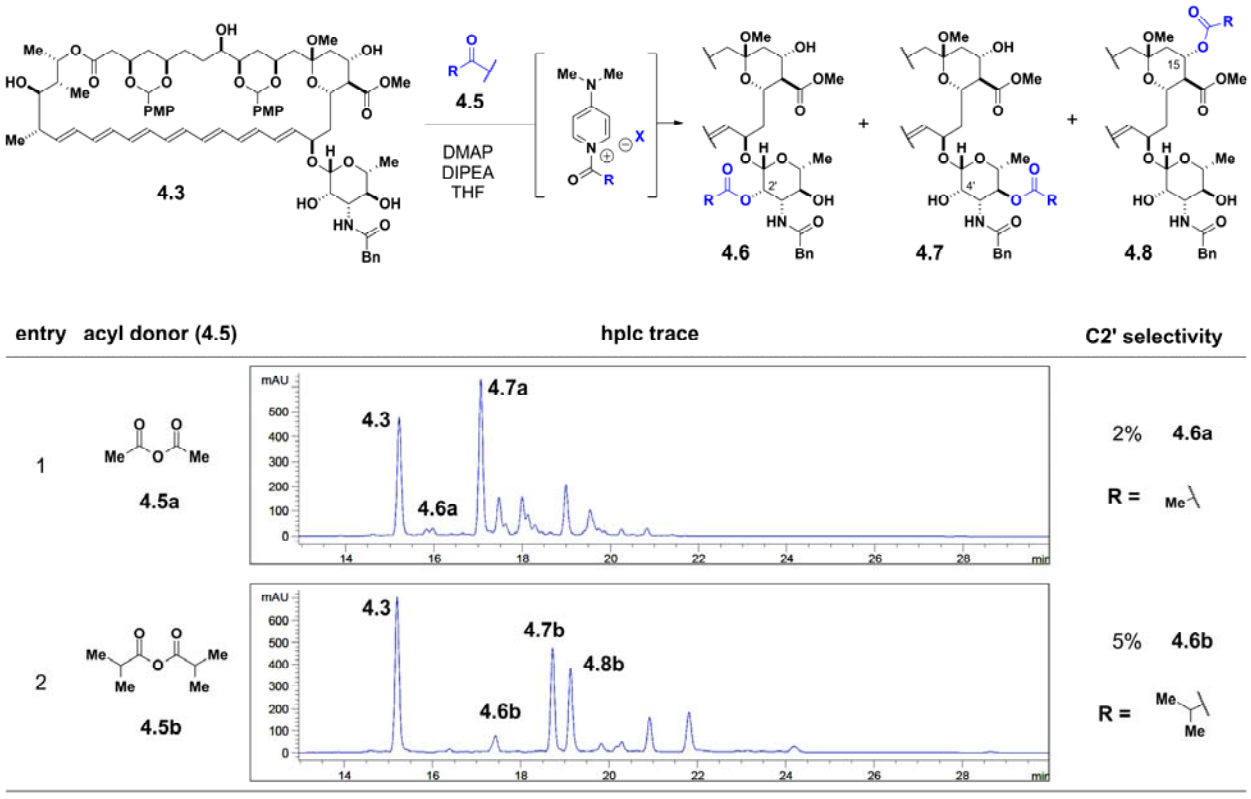

Figure 4.7. HPLC traces and C2' selectivity for acylation reactions. Increasing the steric bulk of the acyl donor had little effect on the C2' selectivity. C2' selectivity is defined as the percent of the products monoacylated at C2'. Figure adapted from ref. 23.

however, there was an impact on the ratio of C4' to C15 acylation. With acetic anhydride, C4' acylation is the major product, but with isobutyric anhydride, monoacylated C15 was produced in a nearly equal amount to C4' (Figure 4.7, entry 2).

There have been a few reports of site selectivity being influenced by switching the counterion of the acylating complex.[17,22] I explored this possibility by replacing the anhydride acyl donors, that produce a carboxylate counterion in the DMAP complex, with acyl chlorides which produce a chloride counterion. A significant increase in the amount of monoacylated C2' product was observed when the counterion was chloride. Acylation with acetyl chloride resulted in 26% selectivity compared to the 2% generated by utilizing the corresponding acetic anhydride (Figure 4.8, entry 1). I evaluated the same steric series used in the anhydride acyl donor studies and found that the C2' selectivity increased as the steric bulk of the acyl donor increased. While there was a significant increase in C2' selectivity, isobutyric chloride was only able to produce moderate selectivity of 48% (Figure 4.8, entry 2). This became problematic upon scale-up due to purification limitations separating out the other isomers found in significant quantities. The C2' selectivity needed to be increased to achieve a useful preparative process that could produce a large enough quantity of acylated C2' intermediate to make derivatives for biophysical evaluation.

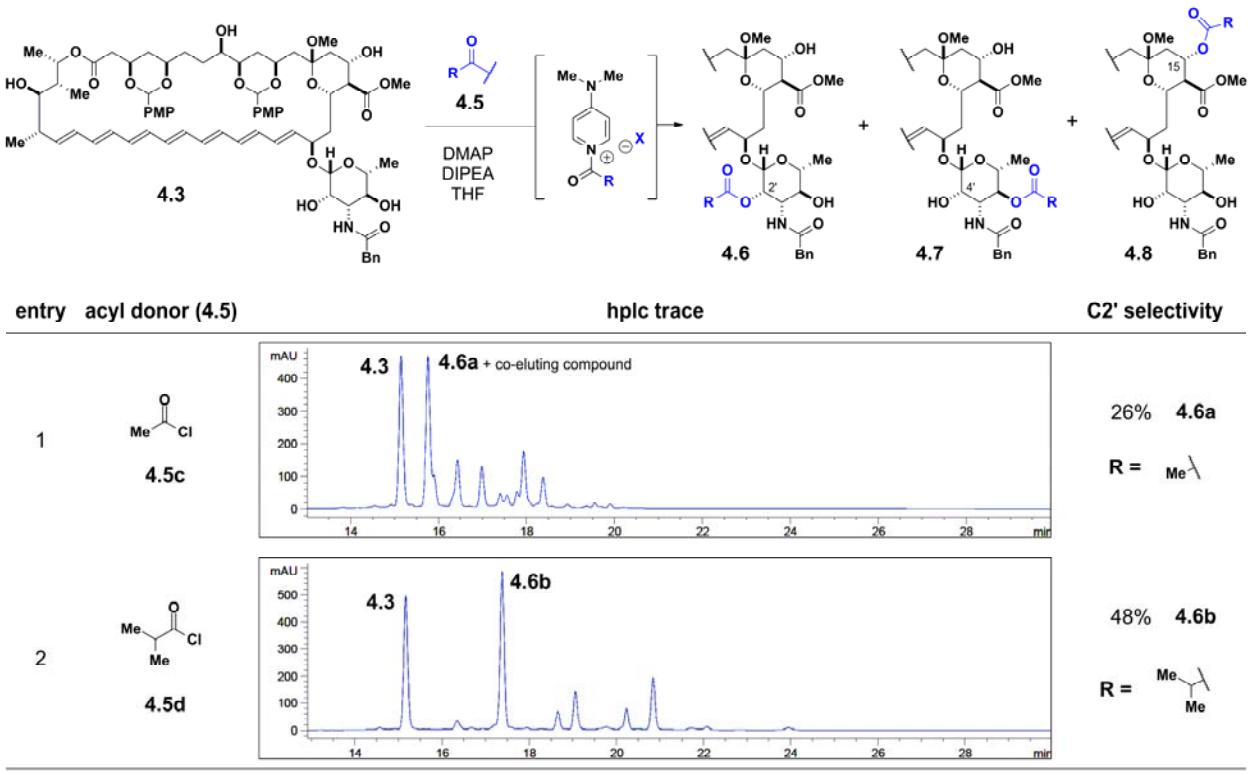

Figure 4.8. HPLC traces and C2' selectivity for acylation reactions. Acyl chloride donors produce higher C2' selectivity than anhydride donors (Figure 4.7) via a counterion effect. Selectivity is also enhanced by increased steric bulk with the acyl chloride donors. C2' selectivity is the percent of the products monoacylated at C2'. Figure adapted from ref. 23.

Inspiration was found in a strategy employed by Jacobsen and coworkers to improve the enantioselectivities of manganese-based epoxidations. Jacobsen found that utilizing more electron-rich salen ligands translated into higher enantioselectivities.[25] This phenomenon was linked to the Hammond postulate.[26] The electron-rich ligands engender milder manganese-based oxidants that react via a more product-like transition state. This results in higher enantioselectivity by presumably amplifying the enantiotopic face-discriminating interactions between the prochiral olefin and the chiral oxidant. These underlying principles should translate to site selectivity in acylation reactions. According to the Hammond postulate,[27] the transition state of the acylation reaction will become more product-like as the reaction becomes less exothermic. In a more product-like transition state, the site-discriminating interactions between the acylating complex and substrate will be magnified leading to increased site selectivity. Thus, using electron-rich acyl donors would create a milder reagent resulting in a less exothermic reaction with, presumably, greater site selectivity (Figure 4.9).

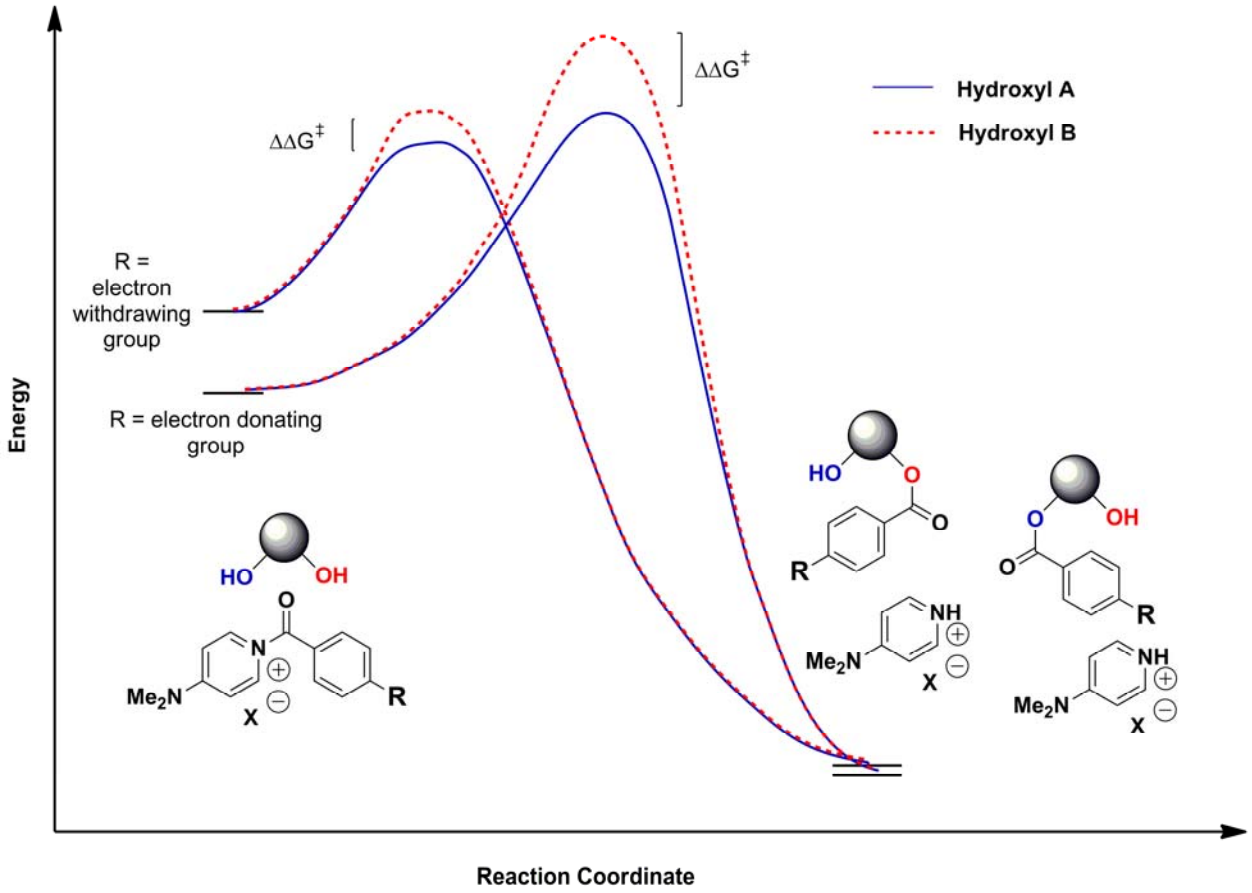

Figure 4.9. The Hammond postulate applied to site-selective acylation. More electron-rich acyl donors are predicted to react via a later, more product-like transition state magnifying the site-discriminating interactions between the substrate and the acylating reagent. The magnified interactions increase the difference between activation energies generating greater selectivity. Figure adapted from ref. 23.

To test this electronic tuning strategy hypothesis, I decided to use *para*-substituted benzoyl chlorides. Electron-poor donors gave low to moderate selectivities for C2' while high selectivities were observed with electron-rich donors. For example, employing *p*-nitrobenzoyl chloride resulted in 39% C2' selectivity in comparison to 72% with *p*-*N*,*N*-dimethylaminobenzoyl chloride (Figure 4.10).[23]

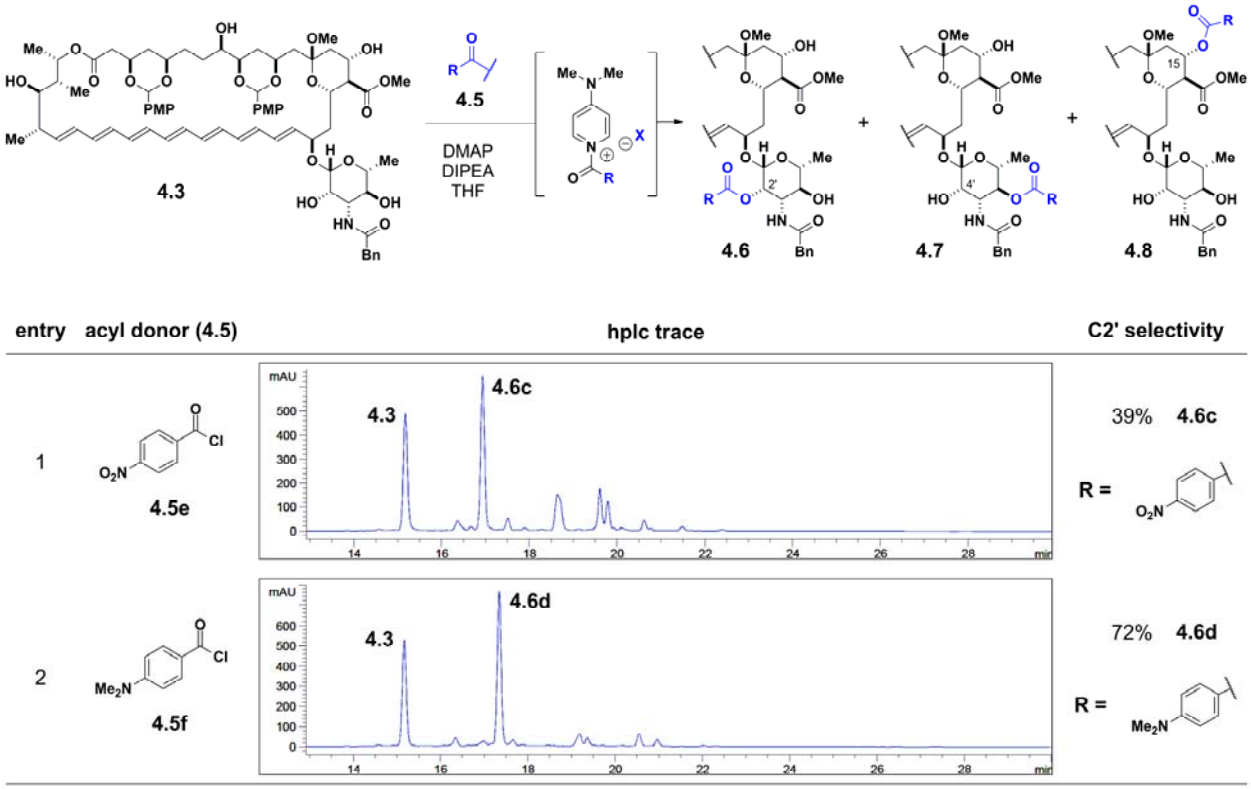

Figure 4.10. HPLC traces and C2' selectivity for acylation reactions. More electron-rich acyl donors produce higher C2' selectivity. C2' selectivity is defined as the percent of the products monoacylated at C2'. Figure adapted from ref. 23.

I performed a Hammett study[28] with five *para*-substituted benzoyl chlorides to see if the observed selectivities were consistent with the Hammond postulate.[23] I found as the electron-withdrawing capacity of the substituent increased, the site-selectivity decreased (Figure 4.11 A). A linear correlation was obtained when the log of the ratio of site isomers C2'/other was plotted against the σ_{para} values of the substituent of the corresponding acyl donors (Figure 4.11 B). If the observed selectivity trend was indeed the result of the Hammond postulate, there would also be a linear correlation with the rate of the reaction. I therefore determined the initial rates of these reactions and found that as the electron-donating capacity of the substituent increased, the rate decreased (Figure 4.11 A). A plot of the log of the initial rates against the σ_{para} values revealed a linear correlation (Figure 4.11 C). Combining these two experiments in a plot of selectivity against the initial rate also generated a linear correlation (Figure 4.11 D). This supports the Hammond postulate as the basis of the electronic tuning phenomenon.

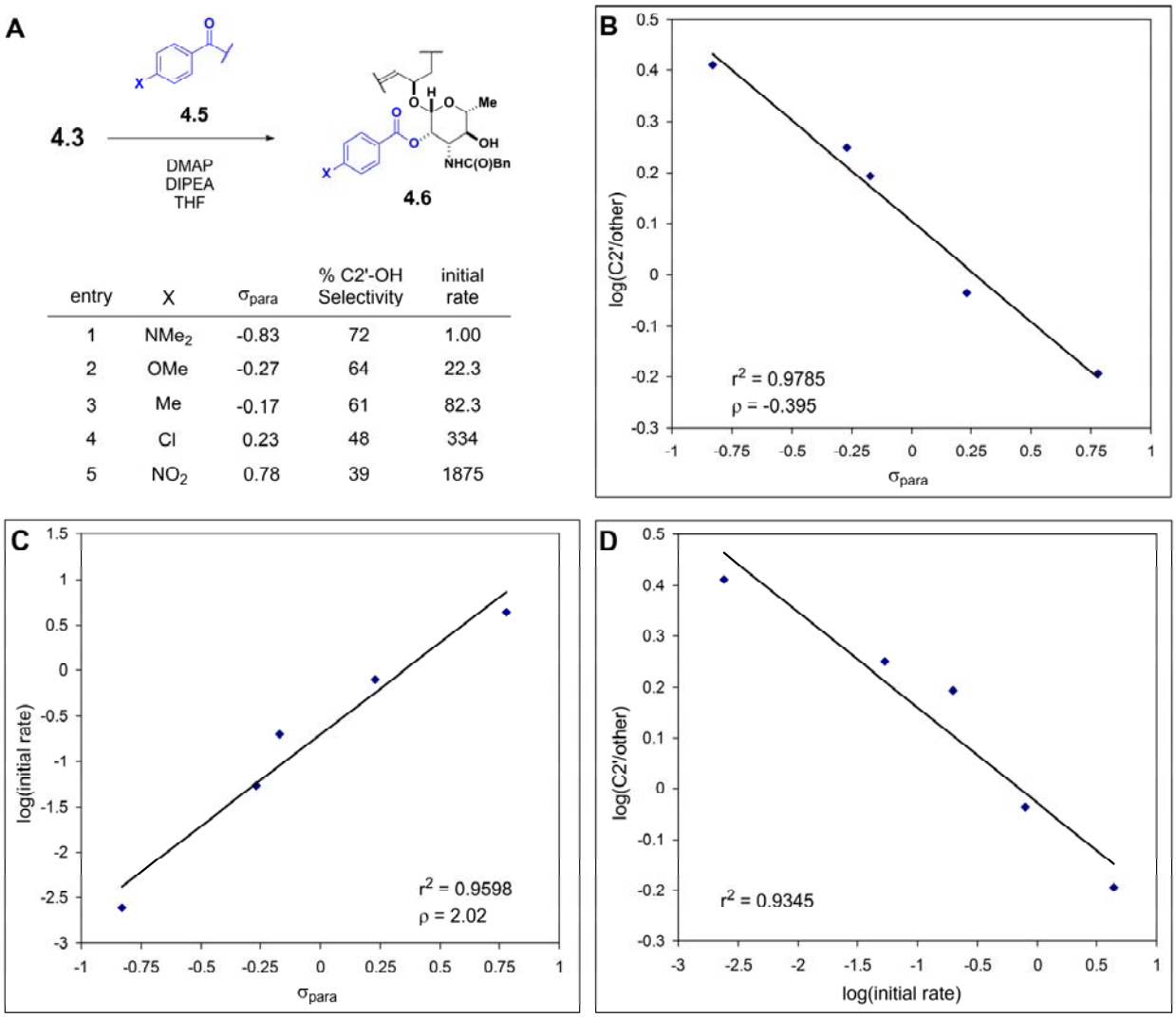

entry	X	σ_{para}	% C2'-OH Selectivity	initial rate
1	NMe_2	-0.83	72	1.00
2	OMe	-0.27	64	22.3
3	Me	-0.17	61	82.3
4	Cl	0.23	48	334
5	NO_2	0.78	39	1875

Figure 4.11. Hammett analysis of site-selective acylation reactions. **A**. Table of the σ_{para} value, C2' selectivity, and initial rate for the acyl donors. **B**. A Hammett plot of the log of the ratio of the C2' product to all other products vs. σ_{para}. **C**. Hammett plot of the log of the initial rate vs. σ_{para}. **D**. Plot of the C2' selectivity vs. the initial rate. Figure adapted from ref. 23.

Having achieved success with electronic tuning and the acylation of the C2' site, I wondered whether electronic tuning could also promote site divergency. When the counterion of the acylating complex is a carboxylate ion, the major products are C4'and C15 (Figure 4.7, entry 2). If symmetrical substituted-benzoic anhydrides were used, both the acyl donor and the counterion of the acylating complex would be electronically tuned. This could create competing or synergistic effects making predictions about the outcome difficult. I tested the electron-poor *p*-nitrobenzoic anhydride and the electron-rich *p*-tertbutylbenzoic anhydride and found that site divergency could be achieved.[23] In the case of the electron-poor *p*-nitrobenzoic anhydride,

acylation at C15 was favored over C4' with a selectivity ratio of 3:1 C15:C4' (Figure 4.12, entry 1). In contrast, the electron-rich *p*-tertbutylbenzoic anhydride favored acylation at C4' over C15 with a selectivity ratio of 2:1 C4':C15 (Figure 4.12, entry 2).

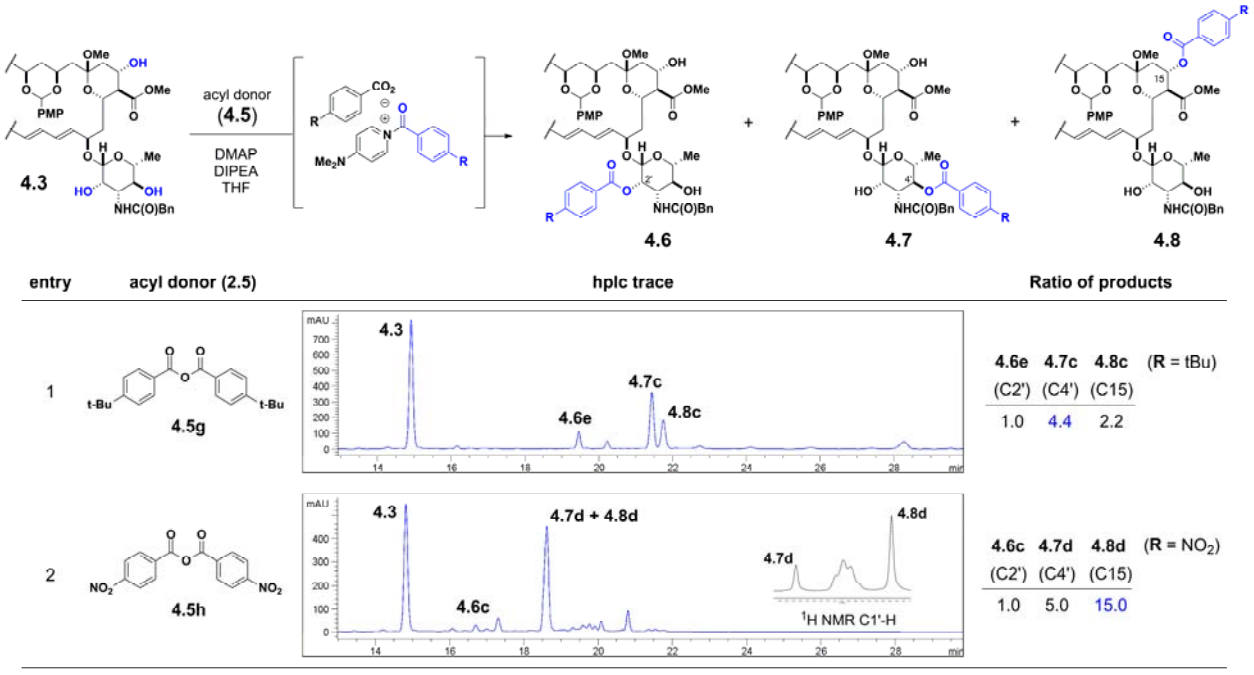

Figure 4.12. HPLC traces and product ratios for acylation reactions. Electronic tuning of symmetrical anhydrides results in site-divergent acylations. Figure adapted from ref. 23.

I also investigated how the position of the substituent on the aromatic ring influenced the selectivity of the selective acylation. Specifically, I employed para, ortho, and meta phenyl-substituted benzoyl chlorides and found that the reaction remained C2' selective. However, I did observe a significant decrease in selectivity as the phenyl group approached the carbonyl, C2' selectivity: para>meta>ortho (Figure 4.13).

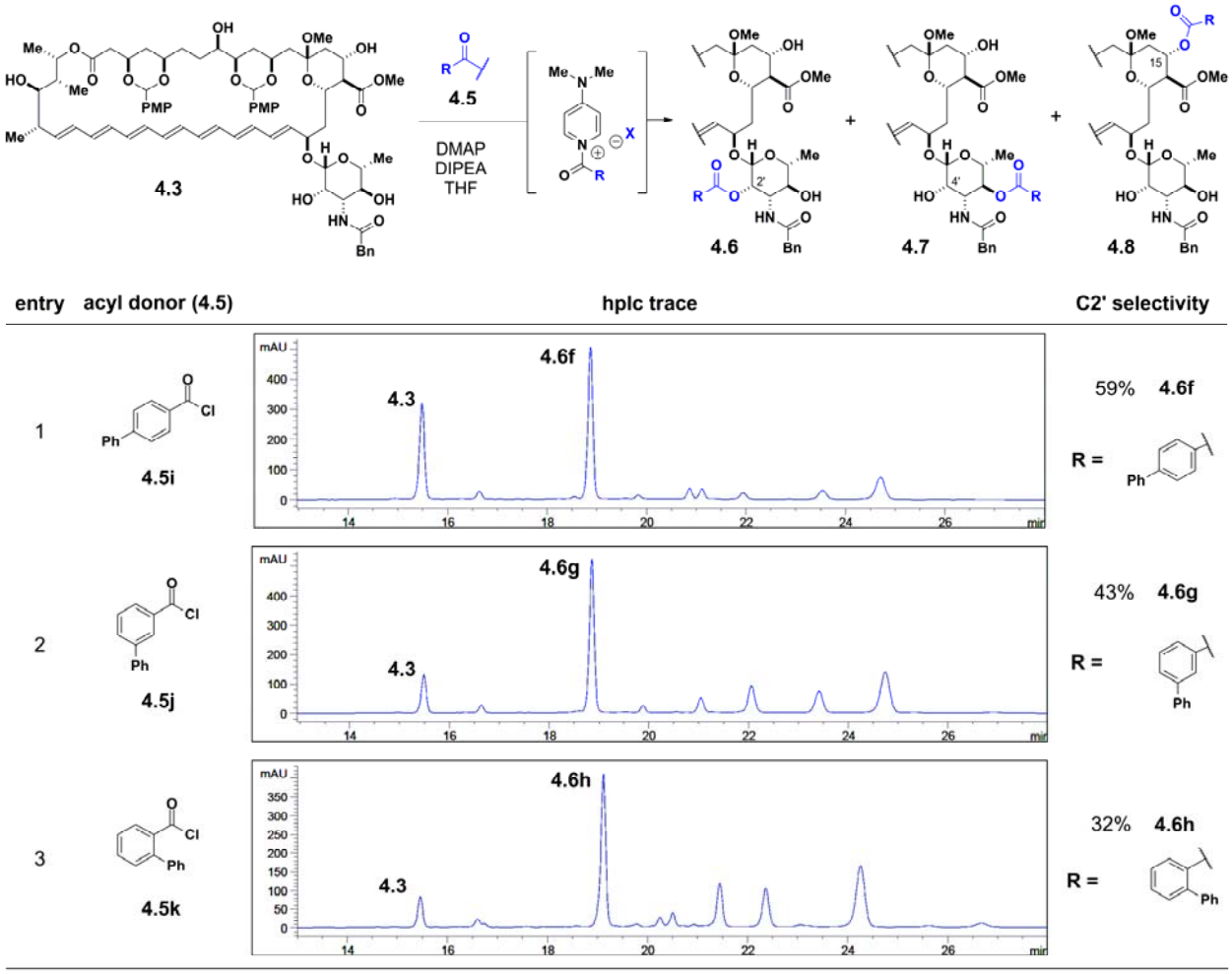

Figure 4.13. HPLC traces and C2' selectivity for acylation reactions. The C2' selectivity as a function of the position of the sterically bulky phenyl substituent on the benzoyl chloride.

Additional screening of electron-rich acyl chloride donors lead to the selection of *p*-tertbutylbenzoyl chloride as the acyl donor for the large scale production of an acylated C2' intermediate. The *p*-tertbutylbenzoyl chloride acyl donor provided an optimized combination of C2' site selectivity (66%), conversion (68%), and ease of purification by standard silica gel chromatography resulting in 45% isolated yield (Scheme 4.3).[23] It is noteworthy to mention that this result is comparable to the lipase mediated acylation (Scheme 4.2) showing that small molecules can sometimes have the potential to perform higher order functions displayed by proteins.

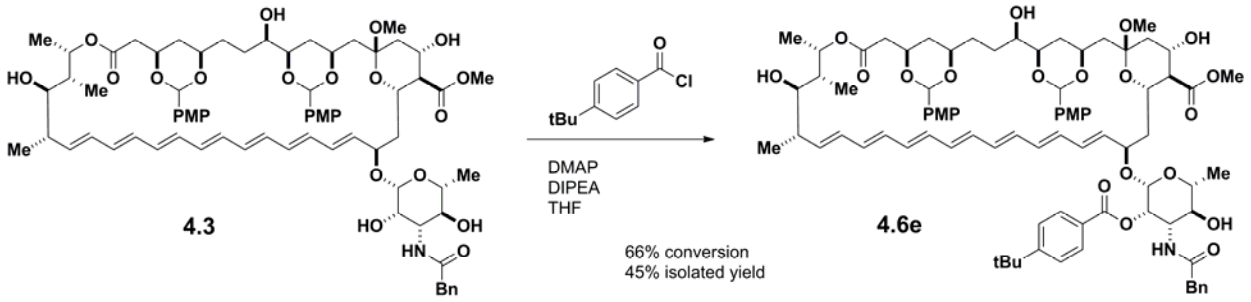

Scheme 4.3. DMAP-mediated site-selective acylation of the C2' hydroxyl group. Figure adapted from ref. 23.

4-4 Summary

Electronic tuning of the acyl donor has proven to be an effective means for increasing the selectivity of acylation reactions on amphotericin. It is important to note that the reactions performed utilized only achiral reagents. This suggests that physical or mechanistic features other than stereochemistry can impact site-divergent functionalization in ways that exceed current understanding and utilization. In addition, since electronic tuning operates by magnifying the interactions between reagent and substrate, electronic tuning can be utilized to enhance selectivity for a particular reagent-substrate pair even if the site-discriminating interactions are unknown. Importantly, electronic tuning is a complementary method to the stereochemical approach. There are many chiral small-molecule catalysts employed for acyl transfer. Electronic tuning can be combined with stereochemical approaches with catalysts and donors. Thus electronic tuning has the potential to have a significant impact on site-selective acylations and the development of site-divergent acylations of complex small molecules and natural products.

4-5 Experimental

The experimental section is adapted from ref. 23.

General Methods

Materials

Amphotericin B was a gift from the Bristol-Myers Squibb Company. All other commercially available reagents were obtained from Sigma-Aldrich, TCI America, Fischer Scientific, Combi-Blocks Inc., and Oakwood Products. Chemicals were used without further purification unless otherwise specified. Camphorsulfonic acid was purified before use by recrystallization with ethyl

acetate. Triethyl amine, diisopropylethyl amine, pyridine, and 2,6-lutidine were freshly distilled over calcium hydride under nitrogen atmosphere. All solvents were obtained from a solvent purification system utilizing packed columns as described by Pangborn and coworkers.[29]

Reactions

All reactions were performed under argon atmosphere in low light conditions with flame dried glassware unless otherwise indicated. All compounds were stored in the dark under argon atmosphere. Thin layer chromatography or reverse phase HPLC was used to monitor reaction progress. Thin layer chromatography was performed on silica gel 60 F_{254} plates from Merck with the indicated solvent. Visualization of the compounds was accomplished with a UV lamp (λ_{254}) and ceric ammonium molybdate (CAM) stain. Analytical HPLC was done on an Agilent 1100 Series HPLC with a C_{18} 5 μm, 4.6 x 150 mm, Symmetry® column from Waters Corp at a flow rate of 1 mL/min with the indicated solvent and gradient. The detection wavelength was set to 383 nm.

Purification and Analysis

Merck silica gel 60 230-400 mesh and SiliCycle reverse phase C18 (17%) 40-63 μm 60 angstrom silica gel was used for flash chromatography with the indicated solvent. HPLC reverse phase purification was done on a waters C18 5 μm, 30 x 150 mm Sunfire column at a flow rate of 25 mL/min with the indicated solvent and gradient. The detection wavelength was set to 383 nm. ^{1}H NMR spectra were taken at 23 °C on a Varian Unity Inova Narrow Bore spectrometer at a ^{1}H frequency of 500 MHz with a Varian 5 mm $^{1}H\{^{13}C/^{15}N\}$pulsed-field gradient Z probe. Chemical shifts (δ) are reported in parts per million (ppm) downfield from tetramethylsilane and referenced internally to the residual protium in the NMR solvent (CHD_2OD, δ = 3.30, center line; $CD_3C(O)CHD_2$, δ = 2.04, center line; $CD_3S(O)CHD_2$, δ = 2.50, center line; CCl_3H, δ = 7.26, center line). Data is reported as follows: chemical shift, multiplicity (s = singlet, d = doublet, t = triplet, m = multiplet, b = broad, app = apparent), coupling constant (*J*) in Hertz (Hz) and integration. ^{13}C spectra were obtained at 23 °C with a Varian Unity Inova spectrometer at a ^{13}C frequency of 125 MHz with a 5 mm Nalorac gradient $\{^{13}C/^{15}N\}^{1}H$ quad probe. Chemical shifts (δ) are reported downfield of tetramethylsilane and are referenced to the carbon resonances in the NMR solvent (CD_3OD, δ = 49.0, center line; $CD_3C(O)CD_3$, δ = 29.8, center line; $CD_3S(O)CD_3$,

δ = 39.5, center line; $CDCl_3$, δ = 77.0, center line). ESI high resolution mass spectra (HRMS), ESI low resolution mass spectra (LRMS) and matrix-assisted laser desorption/ionization (MALDI) spectra were obtained at the University of Illinois mass spectrometry facility.

Synthesis of AmB derivatives

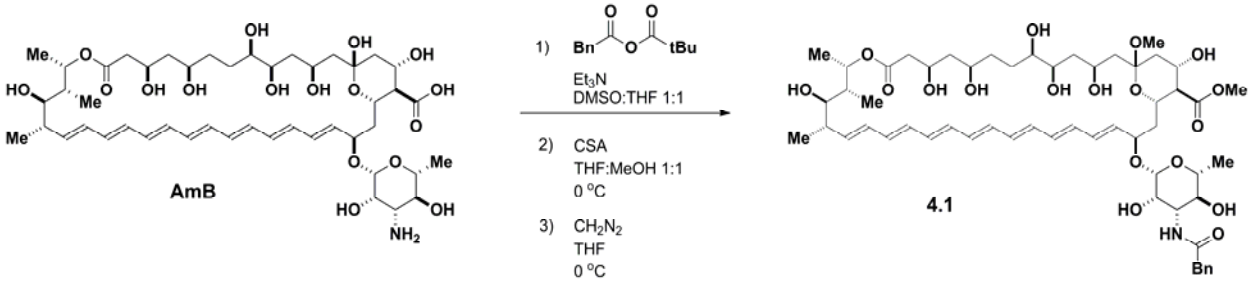

N-phenylacetyl, methyl ketal, methyl ester 4.1

Phenyl acetic acid (662 mg, 1.62 mmol, 3 eq) was dissolved in THF (30 mL). Trimethyl acetyl chloride (400 μL, 3.25 mmol, 2 eq) was added followed by triethyl amine (900 μL, 6.46 mmol, 4 eq). The reaction was allowed to stir for 8 hours at room temperature. The reaction was placed in an ice bath, and DMSO (30 mL) was added over 2 minutes as it cooled. Once the reaction reached 0 °C, AmB (1.5 g, 1.62 mmol, 1 eq) was added. The yellow-tan suspension slowly became soluble over 90 minutes stirring at 0 °C. The reaction was poured slowly into rapidly stirring diethyl ether (1.8 L) at 0 °C. After 15 minutes of stirring, the resulting yellow precipitate was vacuum filtered with a Buchner funnel equipped with Whatman 50 filter paper and washed 3 times with diethyl ether (200 mL). The yellow powder was dried under vacuum for 8 hours.

The powder was then suspended in THF:MeOH 1:1 (60 mL) and cooled to 0 °C. Camphorsulfonic acid (94 mg, 405 μmol, 0.25 eq) was added, and the yellow-tan suspension slowly became soluble over 45 minutes of stirring at 0 °C. The reaction was quenched by triethyl amine (57 μL, 405 μmol, 0.25 eq) at 0 °C. The reaction solution was concentrated by approximately 2/5 by rotary evaporation and poured into diethyl ether:hexane 1:1 (1.2 L) while stirring rapidly. After stirring 15 minutes, the yellow precipitate was collected in a Buchner funnel equipped with Whatman 50 filter paper by vacuum filtration. The precipitate was washed 3 times with diethyl ether (200 mL). The powder was dried under vacuum for 8 hours.

The powder was suspended in THF (60 mL) and cooled to 0 °C. Freshly distilled diazomethane (8.10 mmol, 5 eq) was added dropwise to the suspension over 20 minutes at 0 °C. The reaction was allowed to stir for 30 additional minutes at 0 °C. After quenching with acetic acid (8.10 mmol, 5 eq) at 0 °C, the solution was then concentrated under reduced pressure and purified by flash chromatography (SiO_2; DCM:MeOH 9:1) to give **4.1** as a yellow solid (971 mg, 907 μmol, 56 %).

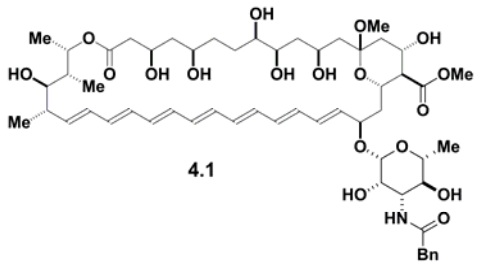

TLC (DCM:MeOH 9:1)

R_f = 0.2, stained by CAM

HPLC

tR = 18.1 min; flow rate = 1mL/min, gradient = 5 → 95 % MeCN in water over 30 min.

^{1}HNMR (500 MHz, pyridine *d-5*:CD_3OD 10:1)

δ 9.01 (d, *J* = 8.5 Hz, 1H), 7.53 (m, 2H), 7.25 (m, 3H), 6.58-6.32 (m, 12H), 6.23 (m, 1H), 5.69 (m, 2H), 4.95 (m, 1H), 4.90 (s, 1H), 4.83 (m, 1H), 4.67 (m, 2H), 4.46 (m, 2H), 4.38 (app d, *J* = 3 Hz, 1H), 4.17 (m, 1H), 4.01 (m, 2H), 3.86 (m, 2H), 3.74 (m, 5H), 3.56 (m, 1H), 3.26 (s, 3H), 2.94 (m, 1H), 2.84 (t, *J* = 10.5 Hz, 1H), 2.69 (m, 2H), 2.54 (m, 1H), 2.31-1.81 (m, 13 H), 1.72 (m, 1H), 1.57 (d, *J* = 6 Hz, 3H), 1.44 (d, *J* = 6 Hz, 3H), 1.32 (d, *J* = 6.5 Hz, 3H), 1.24 (d, *J* = 7 Hz, 3H)

^{13}CNMR (125 MHz, pyridine *d-5*:CD_3OD 10:1)

δ 174.4, 174.2, 172.3, 171.9, 137.9, 137.5, 134.8, 134.7, 134.3, 134.2, 133.8, 133.7, 133.6, 133.5, 133.1, 132.9, 132.4, 130.5, 130.1, 129.1, 127.3, 102.3, 99.4, 78.2, 75.8, 75.7, 75.4,

75.0, 72.1, 71.4, 71.0, 68.5, 67.8, 67.7, 67.1, 57.8, 56.8, 52.2, 45.2, 44.1, 43.8, 43.6, 42.1, 36.6, 31.0, 19.2, 18.9, 18.0, 12.8.

HRMS (ESI)

Calculated for $C_{57}H_{83}NO_{18}$ $(M + Na)^+$: 1092.5508

Found: 1092.5515

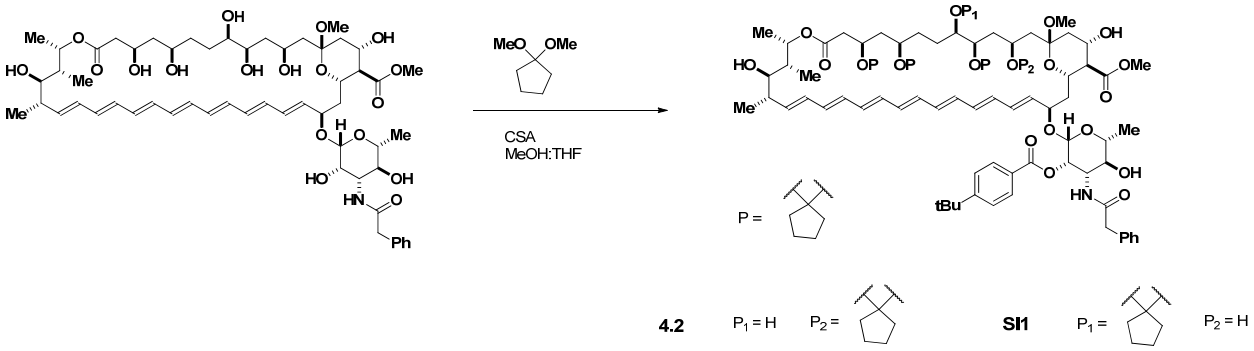

Cyclopentylidene ketals 4.2 and SI1

To a suspension of **4.1** (1.54 g, 1.44 mmol, 1 eq) in methanol (24 mL) was added 1,1-dimethoxy cyclopentane (7.2 mL) followed by camphorsulfonic acid (84 mg, 360 μmol, 0.25 eq). The solution was stirred for 1 hour. The reaction was quenched with saturated sodium bicarbonate (900 mL) and extracted 3 times with ethyl acetate (900 mL). The organic layers were washed with water (900 mL) and then with saturated sodium chloride (900 mL). The organic layers were combined and dried over magnesium sulfate and concentrated *in vacuo* after filtration. The reaction resulted in **4.2** and **SI1** as a 1:1 mixture. Flash chromatography (SiO_2; DCM:MeOH 97:3→19:1) purification yielded a yellow-orange solid (1.04 g, 864 mmol, 60 %). The two isomers were separated by preparative HPLC (C18 SiO_2, water:MeCN, 95:5 → 5:95 over 30 minutes) for acylation experiments

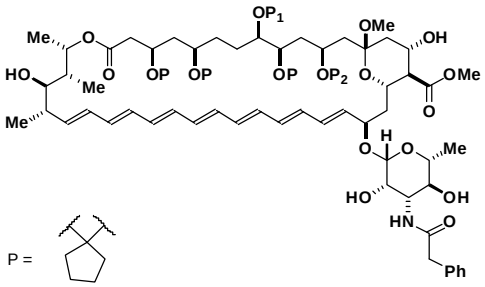

4.2 P_1 = H P_2 = 

SI1 P_1 =  P_2 = H

TLC (DCM:MeOH 9:1)

R_f = 0.38, stained by CAM

HPLC

4.2 tR = 27.1 min; **SI1** tR = 27.9 min; flow rate = 1mL/min, gradient = 30 → 95% MeCN in water over 30 min.

^{1}HNMR (500 MHz, acetone *d-6*)

δ 7.35 (m, 4H), 7.29 (m, 4H), 7.24-7.18 (m, 4H), 6.40-6.18 (m, 24H), 5.90 (m, 2H), 5.56 (m, 2H), 5.24 (m, 1H), 5.18 (m, 1H), 4.65 (app t, *J* = 5 Hz, 2H), 4.58 (bs, 2H), 4.20 (m, 2H), 4.17-4.06 (m, 4H), 4.01 (m, 2H), 3.94 (m, 3H), 3.87 (m, 3H), 3.65-3.60 (m, 11H), 3.49 (m, 2H), 3.37-3.27 (m, 4H), 3.09 (s, 3H), 3.03 (s, 3H), 2.42-2.11 (m, 12H), 2.00-1.74 (m, 22H) 1.71-1.51 (m, 27H), 1.43-1.25 (m, 9H), 1.20 (m, 6H), 1.18 (m, 6H), 1.10 (d, *J* = 7 Hz, 6H), 1.01 (d, *J* = 7 Hz, 6H)

^{13}CNMR (125 MHz, acetone *d-6*)

δ 173.6, 173.5, 172.7, 169.8, 169.7, 137.4, 137.0, 136.7 136.1, 134.4, 134.3, 134.1, 133.9, 133.7, 133.6, 133.4, 133.3, 133.1, 132.8, 132.5, 132.3, 132.1, 130.0, 129.5, 129.1, 129.0, 127.2, 118.6, 110.6, 101.8, 101.0, 98.2, 81.6, 79.9, 78.0, 75.6, 74.6, 74.4, 73.4, 72.9, 70.8, 70.5, 70.4, 69.9, 69.8, 67.7, 67.4, 67.0, 66.9, 66.2, 57.5, 57.4, 56.4, 54.8, 51.9, 48.5, 48.4,

43.4, 43.3, 42.8, 42.0, 41.7, 41.5, 40.9, 40.8, 40.7, 38.1, 38.0, 37.8, 37.7, 37.2, 36.9, 33.9, 33.8, 33.3, 31.7, 31.6, 24.9, 24.8, 24.0, 23.9, 18.7, 18.6, 18.0, 17.6, 17.4, 11.8, 11.7.

HRMS (ESI)

Calculated for $C_{67}H_{95}NO_{18}$ $(M + Na)^+$: 1224.6447

Found: 1224.6410

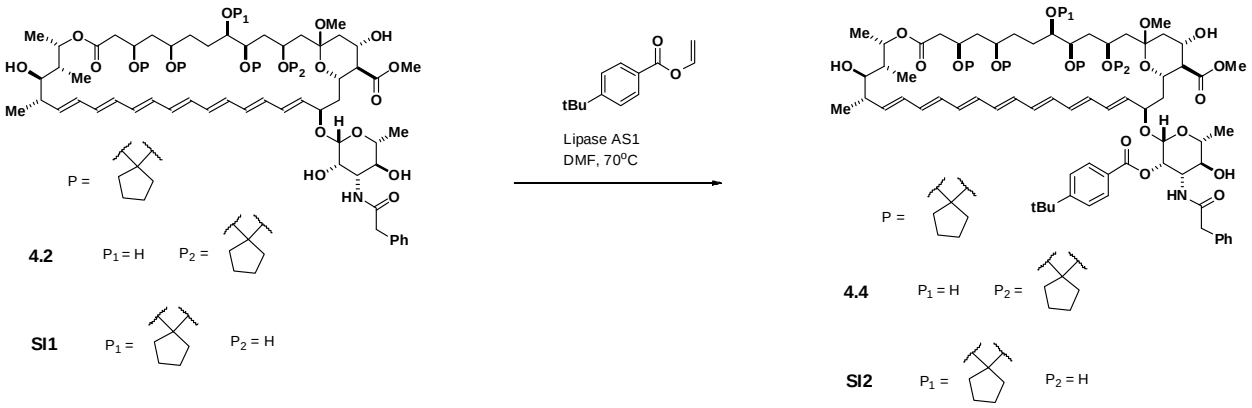

4-*t*-Butyl benzoate ester 6

To a non-flame dried flask was added **4.2** (600 mg, 499 μmol, 1 eq) and lipase AS1 powder (150 mg, 0.25 mass eq). DMF (25 mL), exposed to the air for 5 minutes to provide residual water, was added followed by 4-*t*-butyl benzoate vinyl ester (306 μL, 1.50 mmol, 3 eq). The reaction was placed under argon and heated to 70 °C over 15 minutes. The reaction was stirred at 70 °C for 24 hours where the yellow solution turned dark brown. The reaction was vacuum filtered by Buchner funnel equipped with Whatman 50 filter paper. The enzyme powder was washed with ethylacetate:acetone 1:2 (100 mL). The combined filtrates were concentrated *in vacuo* followed by purification by flash chromatography (SiO_2; DCM:MeOH 49:1→19:1) to remove the vinyl ester and other acylated compounds. The resulting mixture of starting material and product, a yellow-orange powder, was subjected to reverse phase chromatography (C_{18}; water:acetonitrile 3:2 → 1:19) resulting in **4.4** and **SI2** (270 mg, 225 μmol, 45 %).

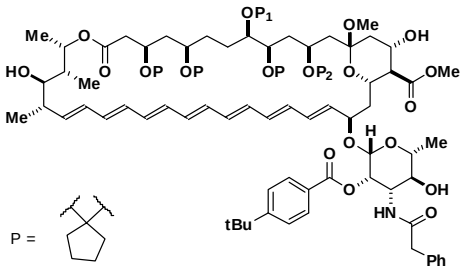

4.4 P_1 = H P_2 = 

SI2 P_1 =  P_2 = H

TLC (DCM:MeOH 9:1)

R_f = 0.33, stained by CAM

HPLC

4.4 tR = 34.3 min; **SI2** tR = 35.0 min; flow rate = 1ml/min, gradient = 5 → 50 % MeCN in water over 10 min followed by 50 → 95 % MeCN in water over 25 min.

^{1}HNMR (500 MHz, acetone *d-6*)

δ 8.00 (m, 4H), 7.60 (m, 4H), 7.41 (m, 2H), 7.23-7.11 (m, 10H), 6.36-6.11 (m, 22H), 6.05 (m, 2H), 5.93-5.76 (m, 2H), 5.68 (m, 2H), 3.56 (m, 2H), 5.14 (m, 1H), 5.06 (m, 1H), 4.87 (s, 2H), 4.65 (bs, 2H), 4.25-4.01 (m, 8H), 4.00-3.76 (m, 8H), 3.68-3.37 (m, 14H), 3.25 (m, 2H), 2.86 (s, 3H), 2.81 (s, 3H), 2.41-2.32 (m, 5H), 2.27-2.19 (m, 2H), 2.17-2.11 (m, 5H), 1.99-1.49 (m, 40H), 1.44-1.21 (m, 42H), 1.18 (m, 6H), 1.10 (m, 6H) 1.00 (m, 6H)

^{13}CNMR (125 MHz, acetone *d-6*)

δ 173.2, 171.6, 169.8, 169.7, 165.8, 157.1, 137.5, 136.8, 134.2, 134.1, 134.0, 133.8, 133.8, 133.7, 133.6, 133.5, 133.1, 132.8, 132.5, 132.4, 131.8, 131.6, 131.3, 131.1, 130.5, 129.9, 128.8, 127.8, 127.7, 127.0, 126.0, 118.5, 110.6, 110.5, 101.5, 100.7, 96.5, 81.6, 79.9, 77.7, 75.5, 74.5, 743.4, 73.3, 73.2, 72.1, 70.8, 69.8, 67.5, 67.3, 66.9, 66.5, 66.3, 57.9, 57.8, 54.6, 51.8, 48.3, 48.2, 43.6, 43.2, 43.1, 42.8, 42.6, 41.9, 41.6, 41.5, 40.8, 40.7, 38.0, 37.9, 37.8, 37.6, 36.9, 36.8, 35.5, 33.9, 33.8, 33.2, 31.6, 31.3, 31.2, 28.5, 28.2, 24.9, 24.8, 24.7, 23.9, 22.9, 22.8, 18.3, 18.0, 17.8, 11.8, 11.7

HRMS (ESI)

Calculated for $C_{78}H_{107}NO_{19}$ $(M + Na)^+$:	1384.7335
Found:	1384.7300

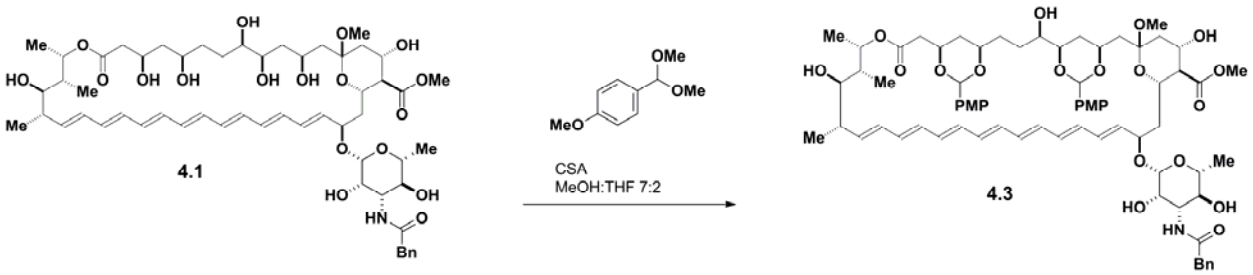

***p*-methoxybenzylidene acetal 4.3**

To a suspension of **4.1** (1.50 g, 1.40 mmol, 1 eq) in MeOH:THF 2:1 (17 mL) was added anisaldehyde dimethyl acetal (2 mL) followed by camphorsulfonic acid (81 mg, 0.35 mmol, 0.25 eq). The solution was stirred for 20 min. The reaction was quenched with triethylamine dropwise until the dark tan solution underwent a color change to light tan. The reaction was poured into saturated sodium bicarbonate and extracted 3 times with ethyl acetate. The organic layers were washed with water followed by a wash with saturated sodium chloride. The organic layers were combined and dried over sodium sulfate, filtered, and concentrated under reduced pressure. Flash chromatography (SiO_2; EtOAc:Hexane:MeOH 77:20:3) purification yielded **4.3** as a yellow-orange solid (1.10 g, 0.84 mmol, 60 %).

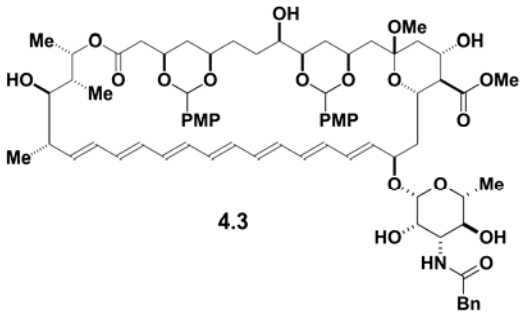

TLC (EtOAc:Hexane:MeOH 77:20:3)

R_f = 0.25, stained by CAM

HPLC

tR = 15.4 min; flow rate = 1mL/min, gradient = 5% MeCN in water for 2 min then 5 → 54% MeCN in water over 3 min then 54 → 95% MeCN in water over 13 min.

^{1}HNMR (500 MHz, $CD_3C(O)CD_3$)

δ 7.42 (m, 2H), 7.35 (m, 4H), 7.29 (m, 2H), 7.21 (m, 2H), 6.86 (m, 4H), 6.43-6.20 (m, 12H), 5.88 (m, 1H), 5.58 (m, 1H), 5.51 (s, 1H), 5.46 (s, 1H), 5.26 (m, 1H), 4.64 (m, 1H), 4.58 (app s, 1H), 4.20-4.10 (m, 2H), 4.02 (m, 1H), 3.95-3.86 (m, 3H), 3.78 (m, 6H), 3.75 (m, 2H), 3.66 (s, 3H), 3.63 (m, 1H), 3.45 (m, 2H), 3.36 (m, 1H), 3.30 (m, 2H), 3.05 (s, 3H), 2.57 (m, 1H), 2.40 (m, 1H), 2.31-2.24 (m, 3H), 1.96 (m, 1H), 1.89-1.45 (m, 9H), 1.37 (m, 2H), 1.22 (m, 4H), 1.19 (d, *J* = 6 Hz, 3H), 1.17 (m, 1H), 1.11 (d, *J* = 6.5 Hz, 3H), 1.01 (d, *J* = 7.5 Hz, 3H)

^{13}CNMR (125 MHz, $CD_3C(O)CD_3$)

δ 173.6, 172.7, 169.7, 160.6, 160.5, 137.5, 136.9, 136.2, 134.1, 134.0, 133.9, 133.7, 133.6, 133.5, 132.9, 132.6, 132.5, 132.2, 129.9, 129.8, 128.9, 128.3, 128.2, 127.2, 120.9, 117.6, 113.8, 101.0, 100.7, 100.6, 98.1, 81.1, 77.9, 76.2, 74.7, 74.4, 73.2, 73.1, 72.9, 72.8, 70.7, 70.5, 67.2, 66.9, 57.3, 56.4, 55.4, 51.8, 48.6, 43.4, 43.3, 42.6, 41.8, 41.5, 37.8, 36.8, 33.8, 33.2, 28.7, 18.7, 18.0, 17.4, 11.8.

HRMS (ESI)

Calculated for $C_{73}H_{95}NO_{20}$ $(M + Na)^+$:	1328.6369
Found:	1328.6388

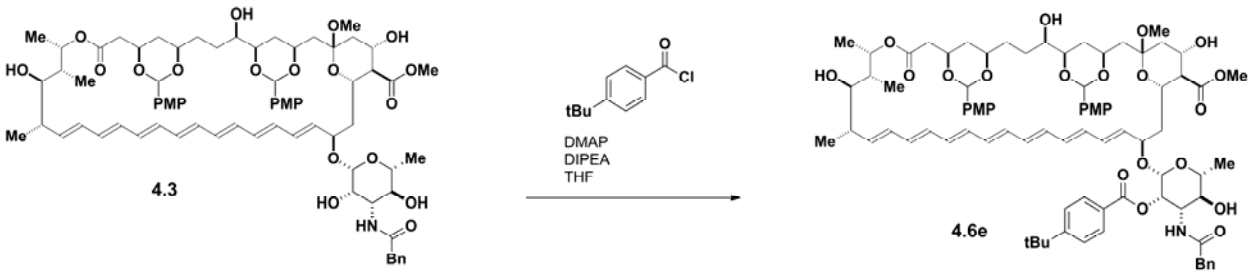

C2'-*p*-tertbutylbenzoic ester 4.6e

THF (160 mL) was added to a flask containing **4.3** (6.16 g, 4.72 mmol, 1 eq). DMAP (922 mg) was added to a separate flask and dissolved in THF (100 mL). 4-tertbutylbenzoyl chloride (1.29 mL, 6.60 mmol, 1.4 eq) was added dropwise to the DMAP solution creating a white suspension. DIPEA (1.31 mL, 7.54 mmol, 1.6 eq) was added to the solution of **4.3**. A portion of the white suspension was then transferred dropwise to the solution of **4.3** and DIPEA (over approximately 1 hr) until the majority of **4.3** had been consumed as evidenced by TLC. The reaction was pored into EtOAc and washed with water followed by saturated sodium bicarbonate. Two more washes with water were performed followed by a wash with saturated sodium chloride. The organic layer was then dried over sodium sulfate and filtered. The solvent was removed under reduced pressure and column chromatography (SiO_2; EtOAc:Hexane:MeOH 60:37:3) purification yielded **4.6e** as a yellow-orange solid (3.11 g, 2.12 mmol, 45 %) as well as unreacted **4.3**.

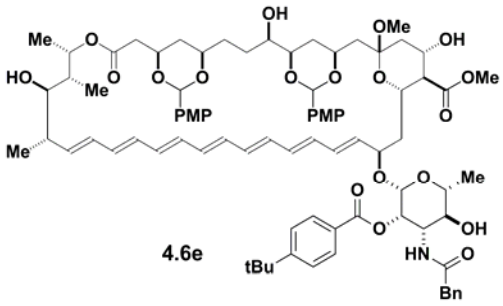

TLC (EtOAc:Hexane:MeOH 60:37:3)

R_f = 0.22, stained by CAM

HPLC

tR = 19.4 min; flow rate = 1mL/min, gradient = 5% MeCN in water for 2 min then 5 → 54% MeCN in water over 3 min then 54 → 95% MeCN in water over 13 min.

^{1}HNMR (500 MHz, $CD_3C(O)CD_3$)

δ 7.99 (d, *J* = 8.5 Hz, 2H), 7.59 (d, *J* = 8.5 Hz, 2H), 7.39 (m, 3H), 7.34 (m, 2H), 7.23 (m, 2H), 7.17 (m, 2H), 7.12 (m, 1H), 6.85 (m, 4H), 6.39-6.13 (m, 10H), 6.07 (m, 1H), 5.92 (m, 1H), 5.76 (m, 1H), 5.68 (m, 1H), 5.56 (m, 1H), 5.48 (s, 1H), 5.43 (s, 1H), 5.14 (m, 1H), 4.88 (app s, 1H), 4.65 (m, 1H), 4.24 (m, 1H), 4.15 (m, 2H), 3.97 (m, 1H), 3.91-3.82 (m, 2H), 3.77 (s, 6H), 3.68 (m, 5H), 3.51 (m, 2H), 3.47 (m, 1H), 3.40 (m, 2H), 2.84 (s, 3H), 2.54 (m, 1H), 2.41 (m, 1H), 2.27 (m, 1H), 2.13 (m, 1H), 1.95 (m, 1H), 1.86 (m, 1H), 1.78-1.42 (m, 10H), 1.40-1.31 (m, 13H), 1.30-1.19 (m, 2H), 1.18 (d, *J* = 6.5 Hz, 3H), 1.11 (d, *J* = 6.5 Hz, 3H), 1.01 (d, *J* = 7.0 Hz, 3H)

^{13}CNMR (125 MHz, $CD_3C(O)CD_3$)

δ 172.7, 171.1, 169.2, 165.3, 160.1, 160.0, 156.7, 137.1, 136.4, 136.3, 133.6, 133.5, 133.4, 133.3, 133.2, 133.1, 132.5, 132.1, 132.0, 131.2, 131.1, 130.0, 129.4, 128.3, 127.7, 126.5, 125.6, 120.7, 113.3, 100.5, 96.1, 80.5, 77.2, 75.7, 74.1, 73.1, 72.6, 72.4, 71.7, 70.6, 66.4, 66.2, 57.2, 54.8, 54.1, 51.3, 47.9, 43.0, 42.7, 41.9, 40.9, 37.2, 36.3, 35.1, 33.4, 32.6, 30.8, 17.8, 17.4, 11.3.

HRMS (ESI)

Calculated for $C_{84}H_{107}NO_{21}$ $(M + Na)^+$: 1488.7233

Found: 1488.7212

DMAP-mediated Acylation Studies

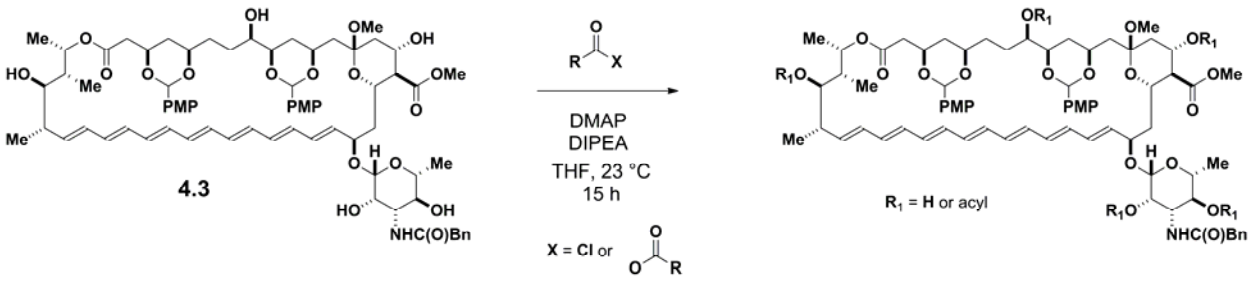

General Procedure for Acylation Reactions

4.3 (5 mg, 3.83 μmol, 1 eq) was added to a vial and dissolved in THF (450 μL). DIPEA (0.8 μL, 4.60 μmol, 1.2 eq) and DMAP (0.515 mg, 4.21 μmol, 1.1 eq) were added to the solution. The acyl chloride or anhydride (1 eq) in THF (50 μL) was added to the reaction. The reaction was allowed to stir at room temperature for 15 hrs. The reaction was filtered and analyzed by reversed-phase HPLC (C18, MeCN/H_2O).

HPLC gradient

flow rate = 1mL/min, gradient = 5% MeCN in water for 2 min then 5 → 54% MeCN in water over 3 min then 54 → 95% MeCN in water over 13 min., hold 95% MeCN in water for 7 min. followed by gradient to 5% water, 75% MeCN, 20% THF over 3 min. then increasing to 5% water, 95% THF in one minute and holding 95% THF in water for 3 min.

Determination of Selectivity

The conversion and ratio of products were determined by integration of the HPLC trace to get the area under the peaks. The identification of major peaks is covered in section IV. Conversion was calculated as the sum of the product peak areas over the total area. % C2' selectivity was calculated as the area for the C2' mono-acylated product over the total product area. The ratio of site isomers used in the Hammett analysis is the C2' mono-acylated product over the sum of the other product areas.

Major Product Characterization

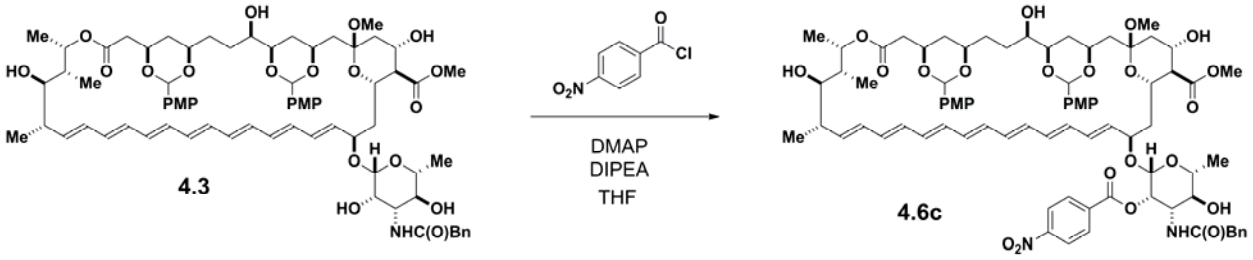

C2'-*p*-nitrobenzoic ester 4.6c

HPLC

tR = 17.0 min

^{1}HNMR (500 MHz, $CD_3C(O)CD_3$)

δ 8.40 (d, *J* = 8.5 Hz, 2H), 8.29 (d, *J* = 8.5 Hz, 2H), 7.44 (m, 1H), 7.39 (d, *J* = 9.0 Hz, 2H) 7.34 (d, *J* = 8.5 Hz, 2H), 7.21 (m, 2H), 7.16 (m, 2H), 7.11 (m, 1H), 6.85 (m, 4H), 6.39-6.12 (m, 10H), 6.01 (m, 2H), 5.79 (m, 1H), 5.65 (m, 1H), 5.61 (m, 1H), 5.48 (s, 1H), 5.43 (s, 1H), 5.18 (m, 1H), 4.92 (app s, 1H), 4.65 (m, 1H), 4.27 (m, 1H), 4.14 (m, 2H), 3.98 (m, 1H), 3.88 (m, 2H), 3.77 (m, 6H), 3.69 (m, 5H), 3.65-3.38 (m, 5H), 2.86 (s, 3H), 2.55 (m, 1H), 2.40 (m, 1H), 2.28 (m, 2H), 2.17 (m, 1H), 1.94 (m, 1H), 1.85 (m, 1H), 1.80-1.40 (m, 10H), 1.34 (d, *J* = 5.0 Hz, 3H), 1.27 (m, 2H), 1.18 (d, *J* = 6.5 Hz, 3H), 1.11 (d, *J* = 6.5 Hz, 3H), 1.00 (d, *J* = 7.0 Hz, 3H)

HRMS (ESI)

Calculated for $C_{80}H_{98}N_2O_{23}$ $(M + Na)^+$: 1477.6458

Found: 1477.6404

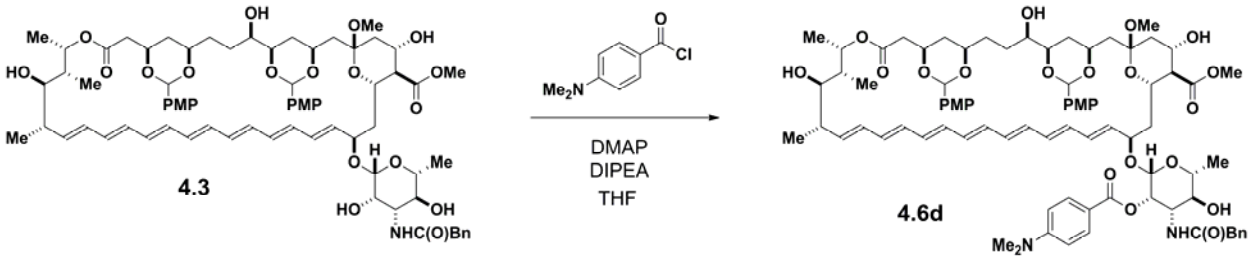

C2'-*p*-dimethylaminobenzoic ester 4.6d

HPLC

tR = 17.3 min

^{1}HNMR (500 MHz, $CD_3C(O)CD_3$)

δ 7.89 (d, *J* = 9.0 Hz, 2H), 7.36 (m, 6H), 7.18 (m, 4H), 6.82 (m, 6H), 6.40-6.04 (m, 11H), 5.82 (m, 1H), 5.73 (m, 2H), 5.52 (m, 1H), 5.48 (s, 1H), 5.43 (s, 1H), 5.11 (m, 1H), 4.84 (app s, 1H), 4.65 (m, 1H), 4.16 (m, 3H), 3.87 (m, 3H), 3.77 (s, 6H), 3.68 (m, 5H), 3.51-3.38 (m, 5H), 3.09 (s, 6H), 2.85 (s, 3H), 2.53 (m, 1H), 2.40 (m, 1H), 2.27 (m, 2H), 2.14 (m, 1H), 1.93 (m, 1H), 1.87 (m, 1H), 1.78-1.40 (m, 10H), 1.32 (d, *J* = 5.5 Hz, 3H), 1.26 (m, 2H), 1.18 (d, *J* = 6.5 Hz, 3H), 1.10 (d, *J* = 6.5 Hz, 3H), 1.01 (d, *J* = 7.0 Hz, 3H)

HRMS (ESI)

Calculated for $C_{82}H_{104}N_2O_{21}$ $(M + Na)^+$: 1475.7029

Found: 1475.6982

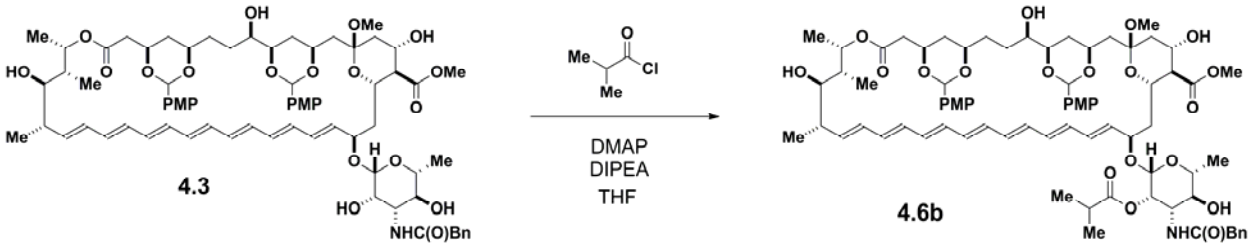

C2'-isobutyric ester 4.6b

HPLC

tR = 17.3 min

^{1}HNMR (500 MHz, $CD_3C(O)CD_3$)

δ 7.45 (app d, *J* = 8.5 Hz, 2H), 7.37 (app d, *J* = 8.5 Hz, 2H), 7.29 (m, 3H), 7.24 (m, 1H), 7.09 (app d, *J* = 7.5 Hz, 1H), 6.90 (app d, *J* = 7.5 Hz, 4H), 6.46-6.21 (m, 12H), 5.90 (m, 1H), 5.66 (m, 1H), 5.54 (s, 1H), 5.48 (s, 1H), 5.36 (m, 1H), 5.24 (m, 1H), 4.77 (app s, 1H), 4.65 (m, 1H), 4.19 (m, 2H), 4.11 (m, 1H), 3.96 (m, 3H), 3.81 (s, 6H), 3.74 (m, 5H), 3.52-3.36 (m, 5H), 3.05 (s, 3H), 2.60 (m, 2H), 2.43 (m, 1H), 2.32 (m, 2H), 2.23 (m, 1H), 1.99-1.86 (m, 2H), 1.79-1.66 (m, 4H), 1.61-1.48 (m, 4H), 1.36 (m, 2H), 1.30 (d, *J* = 6.0 Hz, 3H), 1.21 (m, 5H), 1.18-1.13 (m, 9H), 1.04 (d, *J* = 7.0 Hz, 3H)

HRMS (ESI)

Calculated for $C_{77}H_{101}NO_{21}$ $(M + Na)^+$: 1398.6764

Found: 1398.6758

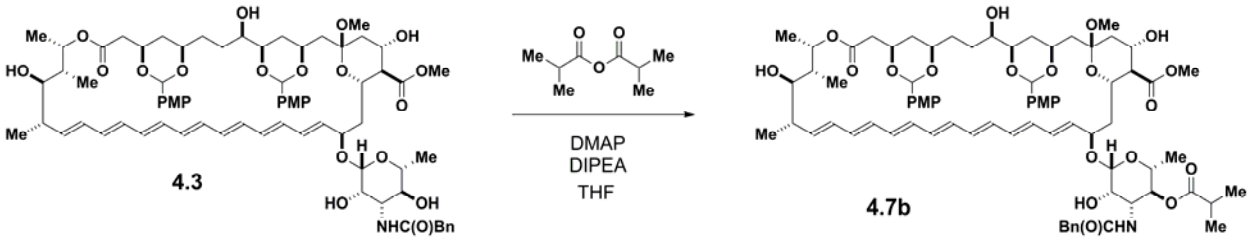

C4'-isobutyric ester 4.7b

HPLC

tR = 18.7 min

^{1}HNMR (500 MHz, $CD_3C(O)CD_3$)

δ 7.41 (app d, *J* = 8.5 Hz, 2H), 7.35-7.26 (m, 5H), 7.21 (m, 1H), 6.87 (m, 5H), 6.42-6.18 (m, 12H), 5.88 (m, 1H), 5.57 (m, 1H), 5.51 (s, 1H), 5.45 (s, 1H), 5.25 (m, 1H), 4.79 (t, *J*=10.0, 1H), 4.65 (m, 2H), 4.21-4.10 (m, 3H), 4.01-3.91 (m, 3H), 3.77 (s, 6H), 3.71 (m, 3H), 3.65 (s, 3H), 3.54 (m, 2H), 3.44-3.35 (m, 2H), 3.05 (s, 3H), 2.56 (m, 1H), 2.41-2.22 (m, 5H), 1.99-1.45 (m, 10H), 1.31 (m, 2H), 1.18 (m,4H), 1.10 (m, 7H), 1.02-0.98 (m, 9H)

HRMS (ESI)

Calculated for $C_{77}H_{101}NO_{21}$ $(M + Na)^+$: 1398.6764

Found: 1398.6740

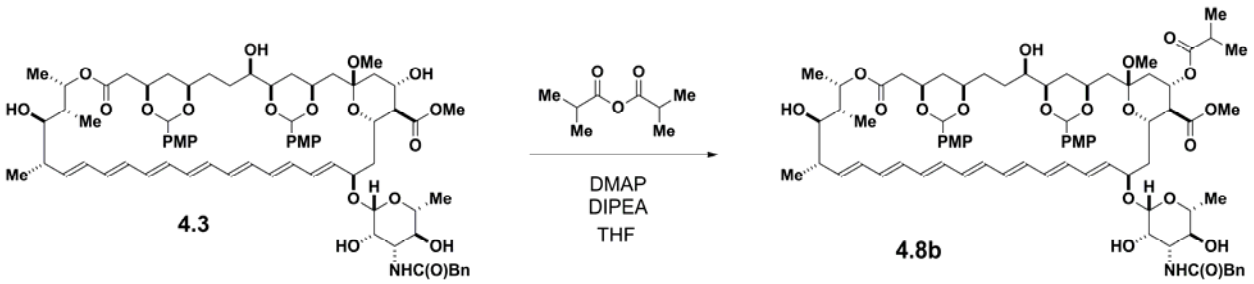

C15-isobutyric ester 4.8b

HPLC

tR = 19.1 min

^{1}HNMR (500 MHz, $CD_3C(O)CD_3$)

δ 7.38-7.18 (m, 9H), 6.85 (m, 4H), 6.43-6.18 (m, 12H), 5.88 (m, 1H), 5.58 (m, 1H), 5.51 (s, 1H), 5.45 (s, 1H), 5.29 (m, 2H), 4.67 (m, 1H), 4.59 (app s, 1H), 4.18 (m, 1H), 4.04 (m, 1H), 3.93 (m, 2H), 3.86 (m, 1H), 3.77 (m, 6H), 3.71 (m, 2H), 3.64 (m, 4H), 3.50 (m, 1H), 3.45 (m, 1H), 3.34 (m, 1H), 3.29 (m, 2H), 3.09 (s, 3H), 2.61-2.28 (m, 5H), 2.00 (m, 1H), 1.93-1.25 (m, 12H), 1.19 (m, 6H), 1.12 (m,5H), 1.05 (m, 6H), 1.01 (d, *J* = 7.0 Hz, 3H)

HRMS (ESI)

Calculated for $C_{77}H_{101}NO_{21}$ $(M + Na)^+$: 1398.6764

Found: 1398.6755

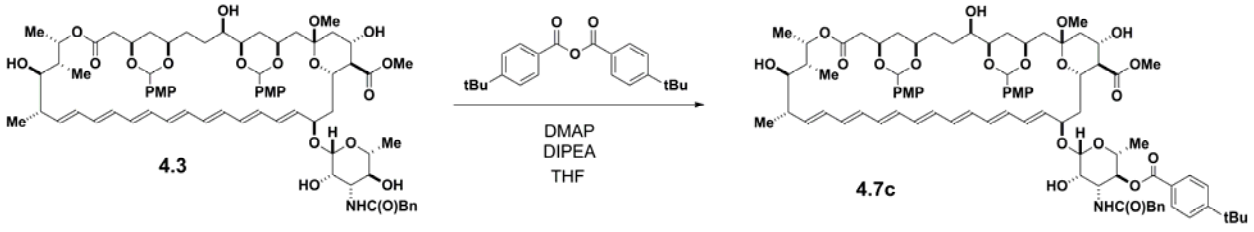

C4'-*p*-tertbutylbenzoic ester 4.7c

HPLC

tR = 21.4 min

^{1}HNMR (500 MHz, $CD_3C(O)CD_3$)

δ 7.84 (d, *J* = 8.0 Hz, 2H), 7.49 (d, *J* = 8.5 Hz, 2H), 7.42 (d, *J* = 8.5 Hz, 2H), 7.35 (d, *J* = 8.5 Hz, 2H), 7.04 (m, 6H), 6.86 (m, 4H), 6.43-6.19 (m, 12H), 5.90 (m, 1H), 5.57 (m, 1H), 5.52 (s, 1H), 5.46 (s, 1H), 5.26 (m, 1H), 5.06 (t, *J* = 10 Hz, 1H) 4.76 (app s, 1H), 4.69 (m, 1H), 4.40 (m, 1H), 4.16 (m, 2H), 4.04 (m, 1H), 3.95 (m, 2H), 3.85 (m, 1H), 3.79 (s, 6H), 3.72 (m, 3H), 3.69 (s, 3H), 3.52-3.34 (m, 3H), 3.08 (s, 3H), 2.59 (m, 1H), 2.40 (m, 1H), 2.29 (m, 3H), 2.00 (m, 1H), 1.92-1.83 (m, 3H), 1.77-1.62 (m, 3H), 1.58-1.46 (m, 4H), 1.36 (s, 9H), 1.33(m, 1H), 1.20-1.16 (m, 8H), 1.11 (d, *J* = 6.0 Hz, 3H), 1.01 (d, *J* = 7.0 Hz, 3H)

HRMS (ESI)

Calculated for $C_{84}H_{107}NO_{21}$ $(M + Na)^+$: 1488.7233

Found: 1488.7230

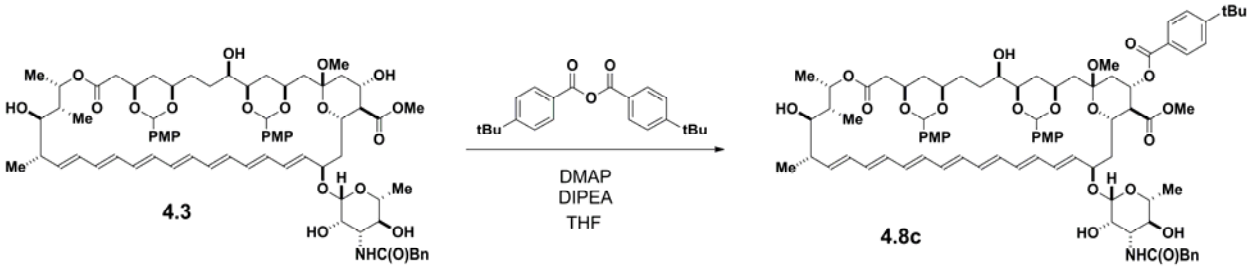

C15-*p*-tertbutylbenzoic ester 4.8c

HPLC

tR = 21.7 min

^{1}HNMR (500 MHz, $CD_3C(O)CD_3$)

δ 7.91 (d, *J* = 8.5 Hz, 2H), 7.56 (d, *J* = 8.5 Hz, 2H), 7.32 (m, 8H), 7.19 (m, 2H), 6.86 (d, *J* = 8.5 Hz, 2H), 6.65 (d, *J* = 8.5 Hz, 2H), 6.41-6.18 (m, 12H), 5.91 (m, 1H), 5.55 (m, 2H), 5.50 (s, 1H), 5.45 (s, 1H), 5.27 (m, 1H), 4.69 (m, 1H), 4.62 (app s, 1H), 4.17 (m, 1H), 4.12 (m, 1H), 3.95 (m, 2H), 3.87 (m, 1H), 3.80 (m, 1H), 3.78 (s, 3H), 3.71 (m, 2H), 3.64 (m, 6H),

3.52-3.43 (m, 2H), 3.35-3.28 (m, 3H), 3.14 (s, 3H), 2.71 (m, 2H), 2.58 (m, 1H), 2.39 (m, 1H), 2.30 (m, 1H), 1.97-1.84 (m, 3H), 1.74-1.38 (m, 9H), 1.34 (s, 9H), 1.22-1.16 (m, 8H), 1.10 (d, J = 6.5 Hz, 3H), 1.01 (d, J = 7.0 Hz, 3H)

HRMS (ESI)

Calculated for $C_{84}H_{107}NO_{21}$ $(M + Na)^+$: 1488.7233

Found: 1488.7214

Determination of the Site of Acylation

The major products of the acylation reaction were purified by HPLC. Mass spectrometry was utilized to determine if the products were mono- or bis-acylated. ^{1}H and gradient COSY NMR analysis was performed on the starting material (**4.3**) and the products, and the proton signals were assigned. Upon acylation, the signal of the proton on the carbon bearing the acylated hydroxyl was found to move significantly downfield (approximately 1.5 ppm).

Determination of the Initial Rates

Acylation reactions were set up according to the general procedure described in section III. Aliquots were taken and quenched in a solution of piperidine in DMF over the course of the reaction. The aliquots were filtered and analyzed by HPLC as described in the general procedure. The conversion was determined and plotted against time. The initial rate was then determined from the slope of a linear line fitted to the earliest time points.

Control Experiments

Determining the reversibility of acylation.

Acylation reactions were setup according to the general procedure described in section III. The mono-acylated products of the acylation reactions were purified by preparative HPLC. Each product was then resubmitted to acylating conditions:

Acylated product (1 eq) was added to a vial and dissolved in THF (450 μL). DIPEA (0.8 μL, 4.60 μmol, 1.2 eq) and DMAP (0.515 mg, 4.21 μmol, 1.1 eq) were added to the solution. The

solution was allowed to stir at room temperature for 15 hrs. The reaction was then analyzed by reversed-phase HPLC (C18, MeCN/H_2O).

In all cases there was no acyl transfer to other hydroxyl groups confirming the reaction is irreversible.

Assessing the Extent of Background Acylation.

Acylation reactions for the para-substituted benzoyl chloride reagents were setup according to the general procedure described in section III excluding the DMAP reagent:

4.3 (5 mg, 3.83 μmol, 1 eq) was added to a vial and dissolved in THF (450 μL). DIPEA (0.8 μL, 4.60 μmol, 1.2 eq) was added to the solution. The acyl chloride (1 eq) in THF (50 μL) was added to the reaction. The reaction was allowed to stir at room temperature for 15 hrs. The reaction was quenched in a solution of piperidine in DMF and filtered. The reactions were then analyzed by reversed-phase HPLC (C18, MeCN/H_2O).

In all cases the conversion was less than 10%. This shows the reaction rate for the DMAP catalyzed acylation is sufficiently faster than the uncatalyzed reaction. The small differences in the rates of background acylation do not account for the 33% difference in C2' selectivity between the nitro and dimethylamino substituted donors. To further suppress any background acylation, all acylation reactions were run with 1.1 eq of DMAP. The equilibrium between free DMAP/acyl chloride and Acyl-DMAP ion/chloride ion is known to favor the ion complex,[2] and salt formation is immediately observed after addition of the acyl chloride to DMAP.

Using a full equivalent of DMAP ensures that the vast majority of the acyl chloride is associated with DMAP during the reaction thus further reducing the rate of background acylation to a negligible amount.

(2) Lutz, V.; Glatthaar, J.; Wurtele, C.; Seratin, M.; Hausmann, H. *Chem. Eur. J.* **2009**, *15*, 8548-8557.

4-6 References

1. Lewis, C. A.; Miller, S. J. *Angew. Chem. Int. Ed.* **2006**, *45*, 5616-5619.
2. Chen, M. S.; White, M. C. *Science* **2007**, *318*, 783-787.
3. Wender, P. A.; Hilinski, M. K.; Mayweg, A. V. W. *Org. Lett.* **2005**, *7*, 79–82.
4. Peddibhotla, S.; Dang, Y.; Liu, J. O.; Romo, D. *J. Am. Chem. Soc.* **2007**, *129*, 12222-12231.

5. Snyder, S. A.; Gollner, A.; Chiriac, M. I. *Nature* **2011**, *474*, 461-466.
6. Pathak, T. P.; Miller, S. J. *J. Am. Chem. Soc.* **2012**, *134*, 6120-6123.
7. Afagh, N. A.; Yudin, A. K. *Angew. Chem. Int. Ed.* **2010**, *49*, 262-310.
8. Robertson, J.; Stafford, P. M. *Carbohydrates* **2003**, 9-68.
9. Griswold, K. S.; Miller, S. J. *Tetrahedron* **2003**, *59*, 8869-8875.
10. Sanchez-Rosello, M.; Puchlopek, A. L.; Morgan, A. J.; Miller, S. J. *J. Org. Chem.* **2008**, *73*, 1774-1782.
11. Lewis, C. A.; Merkel, J.; Miller, S. J. *Bioorg. Med. Chem. Lett.* **2008**, *18*, 6007-6011.
12. Lewis, C. A.; Longcore, K. E.; Miller, S. J.; Wender, P. A. *J. Nat. Prod.* **2009**, *72*, 1864-1869.
13. Kurahashi, T.; Mizutani, T.; Yoshida, J. *Tetrahedron* **2002**, *58*, 8669-8677.
14. Kawabata, T.; Furuta, T. *Chem. Lett.* **2009**, *38*, 640-647.
15. Kurahashi, T.; Mizutani, T.; Yoshida, J. *J. Chem. Soc., Perkin Trans 1* **1999**, 465-473.
16. Luning, U. *et al*. *Eur. J. Org. Chem.* **1998**, 1077-1084.
17. Katting, E.; Albert, M. *Org. Lett.* **2004**, *6*, 945-948.
18. Gu, J.; Ruppen, M. E.; Cai, P. *Org. Lett.* **2005**, *7*, 3945-3948.
19. Park, H. G.; Do, J. H.; Chang, H. N. *Biotechnol. Bioprocess Eng.* **2003**, *8*, 1-8.
20. Jiang, L.; Chan, T. *J. Org. Chem.* **1998**, *63*, 6035-6038.
21. Nicolaou, K. C.; Webber, S. E. *Synthesis* **1986**, 453.
22. Philippe, M. *et al*. *Chem. Pharm. Bull.* **1990**, *38*, 1672-1674.
23. Wilcock, B. C.; Uno, B. E.; Bromann, G. L.; Clark, M. J.; Anderson, T. M.: Burke, M. D. *Nature Chemistry* **2012**, *4*, 996-1003.
24. Ru, M. T.; Dordick, J. S.; Reimer, J. A.; Clark, D. S. *Biotechnol. Bioeng.* **1999**, *63*, 223-241.
25. Jacobsen, E. N.; Zhang, W.; Guler, M. L. *J. Am. Chem. Soc.* **1991**, *113*, 6703-6704.
26. Palucki, M. *et al*. *J. Am. Chem. Soc.* **1998**, *120*, 948-954.
27. Hammond, G. S. *J. Am. Chem. Soc.* **1955**, *77*, 334-338.
28. Hammett, L. P. *Chem. Rev.* **1935**, *17*, 125-136.
29. Pangborn, A.B.; Giardello, M.A.; Grubbs, R.H.; Rosen, R.K.; Timmers, F.J. *Organometallics* **1996**, *15*, 1518-1520.

Chapter 5

Semisynthesis of C2'-deoxyAmphotericin B

This chapter details the development of a degradative synthetic route to C2'-deoxyAmB including the isolation and deoxygenation of the C2' hydroxyl and protecting group scheme optimization. Additionally, the development of a hybrid based synthetic route is described. The deoxygenation and deprotection studies were performed by Brandon Wilcock. Large scale production of intermediates was done by Brandon Wilcock, Brice Uno, Gretchen Bromann, Matt Clark, and Tom Anderson. Brice Uno prepared the C2'-epi-AmB, AmB-ergosterol conjugate, amine protecting groups, and the sugar donor for the hybrid route. Portions of this chapter were adapted from Wilcock, B. C.; Uno, B. E.; Bromann, G. L.; Clark, M. J.; Anderson, T. M.: Burke, M. D. *Nature Chemistry* **2012**, *4*, 996-1003.

5-1 Importance and Predicted Roles of the C2' Hydroxyl

Having established mycosamine-mediated ergosterol binding as the primary mechanism of the antifungal activity of AmB (Chapter 3), further research involving the mycosamine subunit is needed to acquire a better understanding of the mechanism on a molecular level. The mycosamine has three protic functional groups that could play essential roles in the sterol binding process. This is critical as the high toxicity of AmB is proposed to arise from the difference in the main sterol in the membrane, cholesterol in human cells versus ergosterol in yeast. Figuring out important interactions in the binding of ergosterol and cholesterol by AmB could lead to the design of AmB derivatives with improved therapeutic indexes. Thus, AmB derivatives that lack one of the protic groups on the mycosamine, the C2' hydroxyl, the C3' amine, or the C4' hydroxyl group are useful probes.

Recent reports in the literature have made the C2' hydroxyl an interesting target for deoxygenation. Computer molecular modeling studies have predicted a hydrogen bonding interaction between the C2' hydroxyl and the 3-β hydroxyl of the sterol.[1-3] In addition to our studies showing the mycosamine is essential for sterol binding, Murata reports restricting the mycosamine orientation with a tether from the C3' amine to the C41 acid has an effect on the selectivity for sterol-containing membranes over sterol-free membranes.[4]

Carreira has reported the synthesis of an AmB derivative with the C2' hydroxyl in the equatorial position instead of the native axial position and the C41 acid protected as the methyl ester (C2'-epi-AmE).[5] No loss of activity was observed with this derivative compared to the corresponding amphotericin B methyl ester; however, methylation of the C2'-epi hydroxyl drastically reduced the antifungal activity. No sterol binding studies were performed, and the conclusions that can be drawn from these derivatives are limited. The effects of having the acid protected as the methyl ester are unknown. If there is a hydrogen bond between the C2' hydroxyl and the 3-β hydroxyl of the sterol, the C2'-epi hydroxyl might still be able to interact via rotation of the mycosamine unit. While methylation reduces the ability to hydrogen bond, it does not completely eliminate the ability. Also, methylation introduces steric effects that could be behind the loss of activity. Thus, sterol binding experiments with a C2'-deoxyAmB derivative are needed to further elucidate the role of the C2' hydroxyl.

To efficiently generate the C2'-deoxyAmB derivative, a top-down degradative synthesis would be more efficient, step and material wise, than a hybrid or total synthesis route. Utilizing the selective acylation chemistry I have developed (see Chapter 4), the C2' hydroxyl group can be successfully isolated. Deoxygenation of the C2' hydroxyl on the sensitive AmB framework is a very challenging problem. Many of the reagents usually employed in common deoxygenation reactions are incompatible with one or more of the functional groups on AmB. For instance, the polyene motif is highly sensitive to radical conditions in Barton-McCombie[6] type deoxygenations. AmB also contains functional groups sensitive to some metal reagents and strong hydride reducing agents.

5-2 Isolation and Deoxygenation of the C2' Hydroxyl

In order to deoxygenate the C2' hydroxyl, it must be isolated and unprotected. To accomplish this, I selectively installed a temporary acyl protecting group on the C2' hydroxyl generating intermediate **4.4** (see Chapter 4). Orthogonal protection of the remaining hydroxyl groups was readily achieved with tertbutyldimethylsilyl (TBS) groups (Scheme 5.1). Next, the C2' ester was cleaved with either sodium methoxide or potassium cyanide in methanol. The C2' hydroxyl was now isolated and exposed for further functionalization such as deoxygenation.

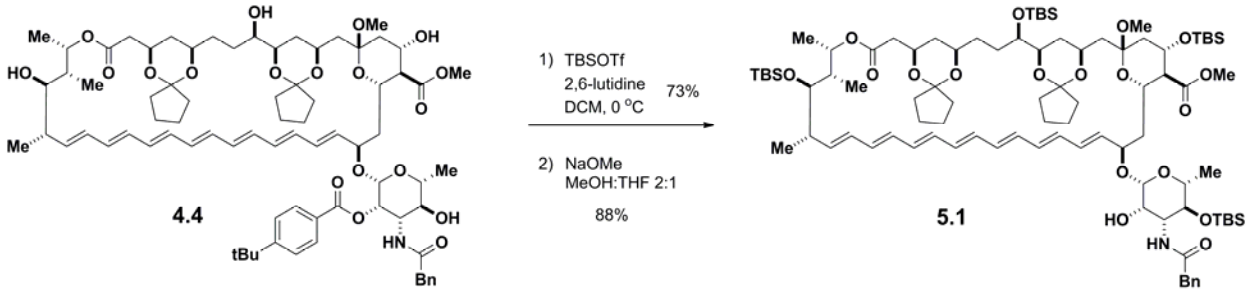

Scheme 5.1. Isolation of the C2' hydroxyl group.

I first attempted activation of the hydroxyl through mesylation followed by direct displacement by hydride sources, but I found this sequence unproductive due difficulty installing the mesyl group as well as inactivity with mild hydride reagents and elimination side products in the subsequent reduction reaction. Stronger aluminum based hydride reagents caused decomposition. I therefore decided to explore if there was a window of reactivity with radical based conditions where deoxygenation at C2' might be faster than destruction of the polyene unit of AmB. Model studies showed that a significant amount of AmB could survive under some mild radical deoxygenation conditions utilized on a model sugar substrate. However, attempts to install thiocarbonyl functionality on the C2' hydroxyl to attempt a Barton-McCombie deoxygenation[6] failed. The major product isolated was a bicycle generated by attack from the C3' nitrogen to form thiocarbamate (Scheme 5.2).

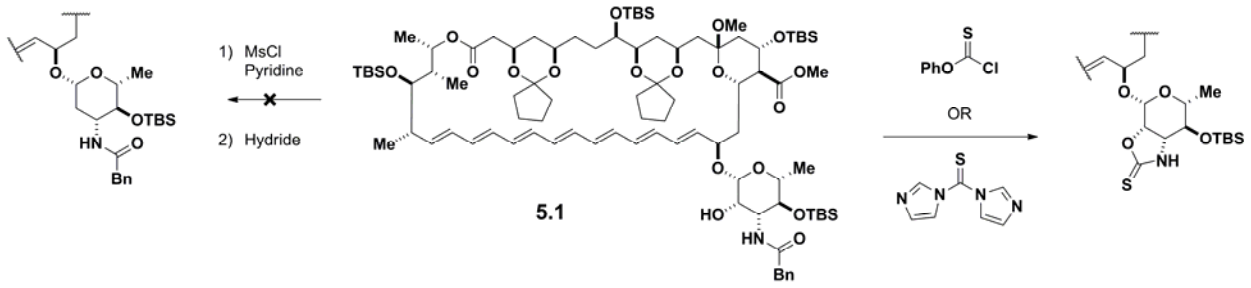

Scheme 5.2. Initial attempts at deoxygenation of the C2' hydroxyl group.

To avoid this problem, I pursued the possibility of transforming the C2' hydroxyl group into an iodide which could undergo radical deoxygenation or reductive displacement with a hydride. I found the standard conditions of iodine and triphenylphosphine unreactive at low temperatures. Upon heating these conditions resulted in decomposition. However, I found a report of an alcohol to iodide transformation for sugars using the alternative reagent triiodoimidazole.[7] I was able to employ this alternative method on AmB successfully generating the C2' iodide in 80% yield (Scheme 5.3). With this new substrate **5.2**, I attempted radical based

conditions using tributyltin hydride and various initiators such as azobisisobutyronitrile (AIBN) and peroxides. I found the rate of deiodination to be uncompetitive with the decomposition of the polyene on AmB.

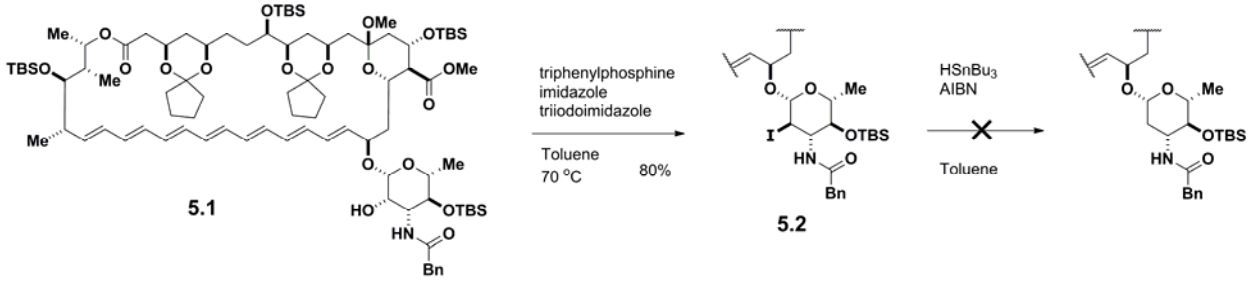

Scheme 5.3. Formation of the C2' iodide and radical deoxygenation attempt.

In light of the radical sensitivity of AmB, I turned to hydride reagents to reduce the iodide at C2'. The AmB framework is sensitive to strong hydride reagents such as lithium aluminum hydride commonly used to reduce halides. AmB, however, is compatible with milder hydrides such as sodium borohydride. The reduction of secondary iodides with sodium borohydride can be problematic and usually requires harsh conditions; high temperature and polar aprotic solvents are often needed to affect this transformation.[8] If the iodide is sterically hindered, the problem of elimination instead of substitution can be significant. I observed no reductive deiodination with sodium borohydride in DMPU up to 65 °C, and at higher temperatures significant decomposition and elimination occurred (Scheme 5.4).

I explored the possibility of activating the iodide through the addition of a halophilic salt in a similar fashion to the way that a Lewis acid may activate a carbonyl towards nucleophilic attack by associating with the oxygen. I tried several silver and mercury salts and discovered that addition of silver acetate facilitated the deiodination to give a useful 61% yield (Scheme 5.4). Having developed a working deoxygenation, synthetic efforts were directed at the protecting group strategy in order to generate the final C2'-deoxyAmB compound.

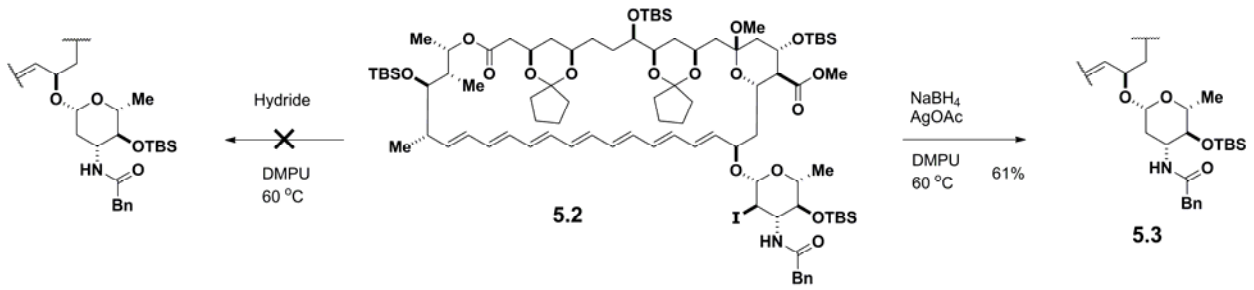

Scheme 5.4. Silver assisted reductive deiodination at C2'.

5-3 Deprotection and the Protecting Group Strategy

Having achieved site-selective acylation and deoxygenation of the C2' hydroxyl group, all that remained was global deprotection to generate C2'-deoxyAmB. Model studies I conducted on AmB and previous synthetic work on AmB from Nicolaou,[9,10] and Murata,[11] suggested that the robust protecting groups (phenylacetyl amide for the amine, methyl ester for the acid, TBS ethers and cyclopentylidene ketals for the hydroxyls, and methyl ketal for the hemiketal) could be deprotected in synthetically useful yields. Thus, I used these groups in the development of the selective acylation and deoxygenation chemistry previously described in Chapters 4 and 5. Unfortunately, I found that the protected C2'-deoxyAmB substrate is far more sensitive to the deprotection conditions than protected AmB; this was especially true for the acidic reaction steps. As a result, I encountered large amount of side products and decomposition resulting in low yields (Scheme 5.5).

I began by investigating several sources of fluoride for the silyl ether removal. Conditions utilizing Tetra-*n*-butylammonium fluoride (TBAF) resulted in incomplete conversions and tris(dimethylamino)sulfonium difluorotrimethylsilicate (TASF) caused complete decomposition. HF-pyridine was more successful at removing the TBS groups; however, the TBS group at C35 required heating to remove resulting in less than 10% yield.

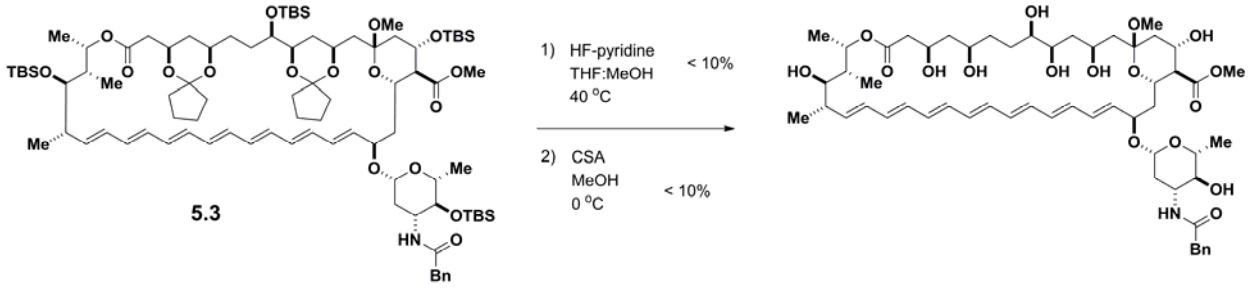

Scheme 5.5. Attempted deprotections on C2'-deoxyAmB intermediate **5.3**.

I also observed greater sensitivity to acidic conditions used to remove the cyclopentylidene ketals on the polyol motif of the protected C2'-deoxyAmB substrate. I screened various types of acids, temperatures, concentrations, and solvents to find the mildest conditions that would remove the cyclopentylidene ketal groups. I determined that the most compatible acid was camphorsulfonic acid (CSA). Dry HCl, generated from the addition of acetyl chloride to MeOH, was also tolerated, but other inorganic acids performed poorly. Significant side products and decomposition limited the yield to less than 10% in all cases. Thus, I decided to replace the

TBS and cyclopentylidene groups with more labile groups. I determined that triethylsilyl (TES) groups were not stable enough to survive the deacylation step in the route. However, diethylisopropylsilyl (DEIPS) groups were stable enough if sodium methoxide was replaced with potassium cyanide in the C2' ester deacylation step. The cyclopentylidene ketals were replaced with *p*-methoxybenzylidene acetals. I found that the *p*-methoxybenzylidene acetals were able to be deprotected with less acid and in less time resulting in decreased decomposition and higher yields.

With these optimized protecting groups in place, I was able to follow the synthetic route in Scheme 5.6 utilizing the selective acylation and reductive deiodination chemistry previously described to arrive at the C2'-deoxyAmB intermediate **5.6**.[12] Optimization of the protecting groups and attempts at producing C2'-deoxyAmB were greatly facilitated by the production of intermediates on large scale in collaboration with my colleagues Gretchen Broman, Brice Uno, Matt Clark, and Thomas Anderson.

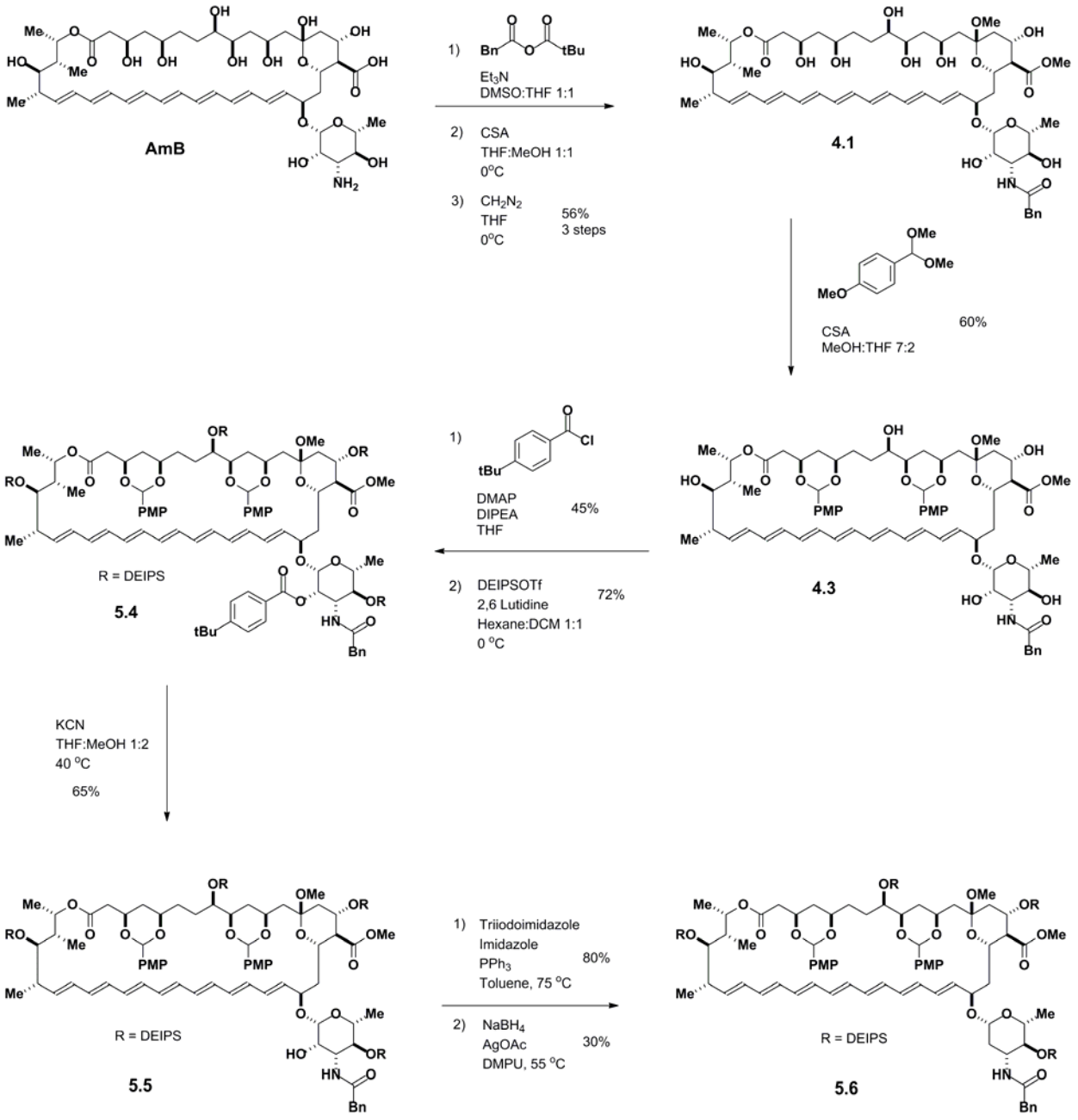

Scheme 5.6. Synthesis of C2'-deoxyAmB intermediate **5.6** utilizing optimized protecting groups. Scheme adapted from ref. 12.

The yields for the C2' ester cleavage and C2' iodide reduction steps were lower, but the rest of the chemistry translated well from the previous protecting group scheme route with comparable yields. The versatility of intermediate **5.5**, containing the free hydroxyl at C2', was further investigated by colleague Brice Uno. He found that a variety of other C2' derivatives could be generated besides the methylene.[12] For instance, the C2' hydroxyl was able to be inverted via standard Mitsunobu[13] conditions. Also, a molecule of ergosterol was successfully

tethered to the C2' hydroxyl,[12] making an AmB small-molecule conjugate reminiscent of the proposed AmB-ergosterol complex (Scheme 5.7).[14]

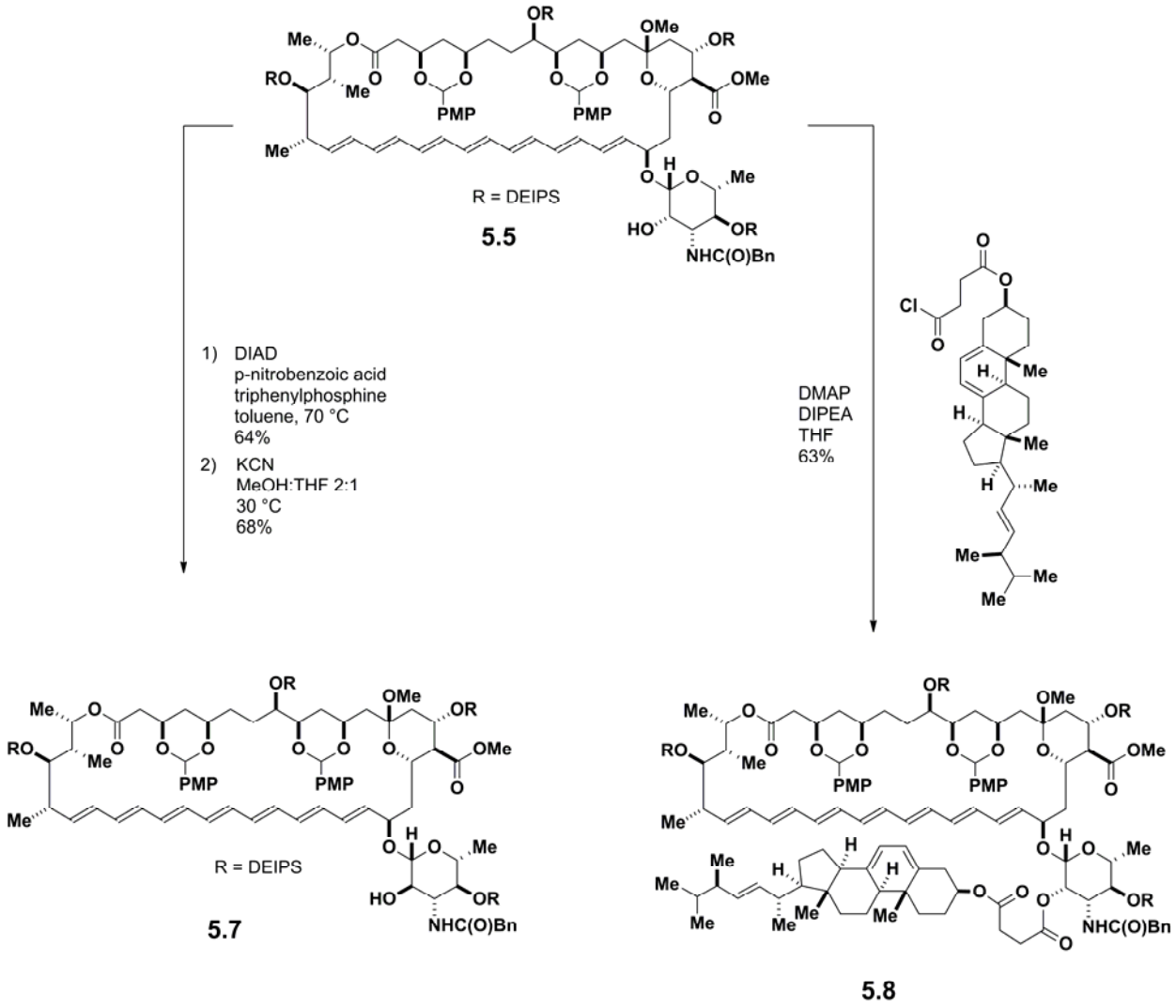

Scheme 5.7. Functionalization of the free C2' hydroxyl group. Scheme adapted from ref. 12.

With C2'-deoxyAmB intermediate **5.6** in hand, I began global deprotection to see if the more liable DEIPS and *p*-methoxybenzylidene acetals utilized in this route could be removed in synthetically useful yields (Scheme 5.8). After extensive optimization, I was able to improve the yield for the HF-pyridine deprotection of the silyl groups to 38%. As with the cyclopentylidene ketals, I screened a variety of acids, solvent mixtures, and concentrations to find conditions to remove the *p*-methoxybenzylidene acetals and/or methyl ketal. While the *p*-methoxybenzylidene acetals were removed under more mild conditions with methanol and CSA, I found the methyl

ketal deprotection to the hemiketal required forcing conditions with aqueous acid that resulted in less than 10% yield as before.

I therefore hypothesized if cleaving the methyl ester first might impact the reactivity of the C13 methyl ketal center. This became problematic due to some base sensitivity of the *p*-methoxybenzylidene acetal at C3/C5. Strong bases will cause elimination at C2-C3 expelling the *p*-methoxybenzylidene acetal. However, I was able to find a window of reactivity with potassium hydroxide that gave a moderate yield for the methyl ester deprotection. Fortunately, the methyl ketal exchange to the hemi ketal was more facile with the free acid at C41. After optimization, I was able to remove both *p*-methoxybenzylidene acetals and the methyl ketal in one step thereby removing an acidic deprotection step. I determined it was critical to keep the amount of water co-solvent to a minimum, and acetonitrile was essential to accelerate the reaction rate. While the yields for the removal of the silyl ethers, methyl ketal, and *p*-methoxybenzylidene acetals were improved, they were still low. The final step of removing the phenylacetyl group on the C3' amine with PGA proceeded with very low conversion and produced an unresolved and inseparable mixture of products. MS analysis of the mixture showed a mass peak consistent with

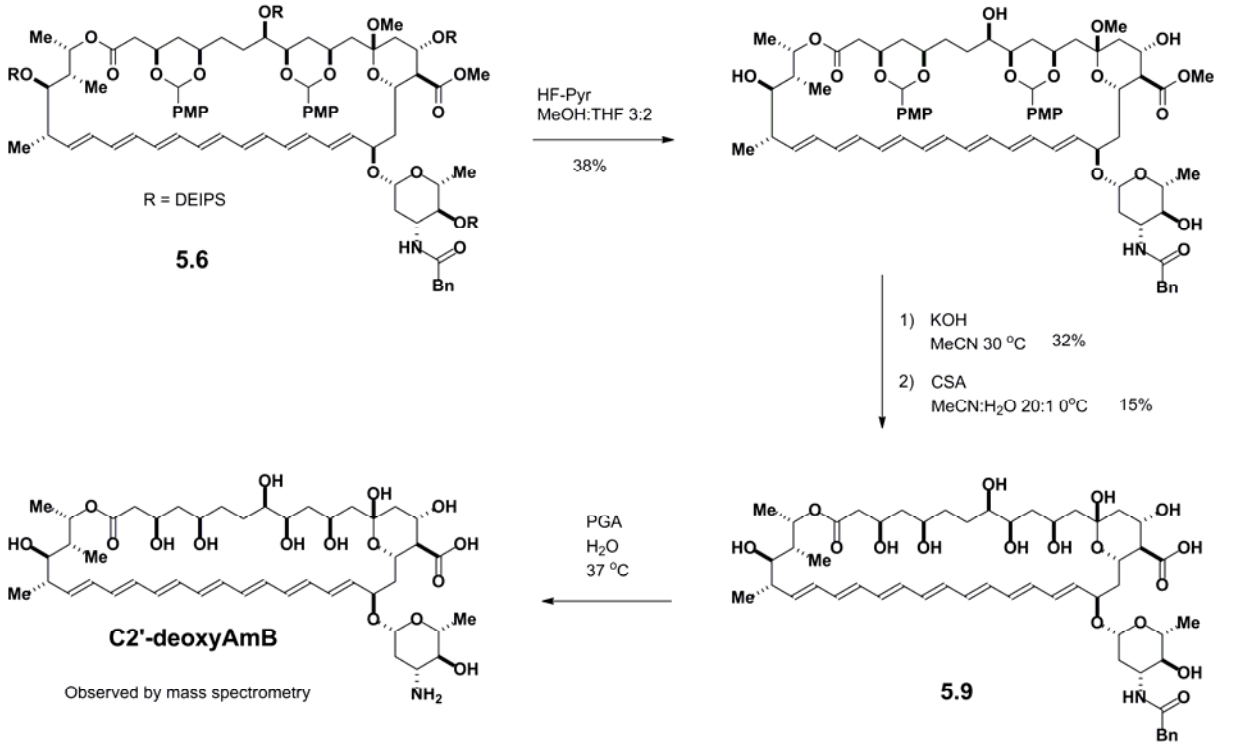

Scheme 5.8. Global deprotection of C2'-deoxyAmB intermediate **5.6**.

the desired C2-deoxyAmB product; however, even after attempts at optimization, I was unable to isolate any product from the decomposition mixture (Scheme 5.8).

An alternative C3' amine protecting group was needed if the route was going to be synthetically viable. The selective acylation chemistry readily transferred to AmB substrates containing alternative amine protecting groups such as Fluorenylmethyloxycarbonyl (Fmoc), allyloxycarbonyl (alloc), and various other amides and carbamates. Fmoc was unstable to the deacylation conditions, and the C2' acyl group transferred to the neighboring C3' amine. Alloc was a suitable substitution except for the reductive deiodination step which failed. The reduction of the iodide was highly dependent upon the identity of the protecting group on the C3' amine. Alloc was exchanged for various other protecting groups, many synthesized by colleague Brice Uno, shown in Scheme 5.9.

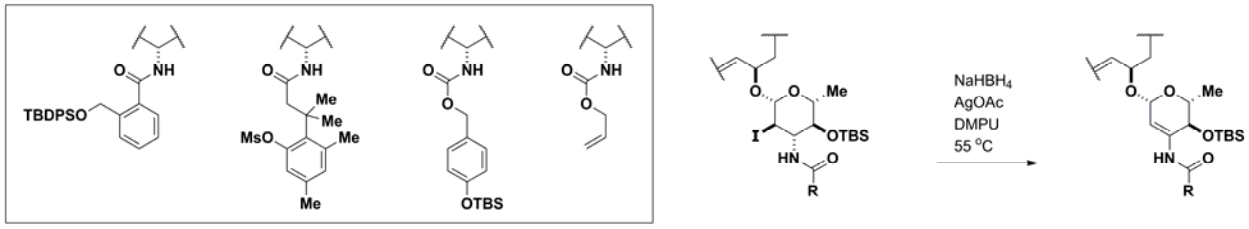

Scheme 5.9. Examples of alternative C3' amine protecting groups investigated for the reductive deiodination at C2'. Reactions with these groups resulted in large amounts of the competitive elimination reaction product, decomposition, or inactivity.

I found that they caused the elimination side product to become dominate or inactivity under the reaction conditions. Interestingly enough, elimination was also a common product when alloc was removed from the C2'-iodoAmB derivative with palladium or nickel conditions. Attempts at selectively reducing the elimination products with borohydride based hydride reagents were unsuccessful. In light of the low yielding deprotection steps and the need to develop a new method for deoxygenation of the C2' hydroxyl, an alternative route to C2'-deoxyAmB was considered.

5-4 The Hybrid Route to C2'-deoxyAmB

A hybrid approach to C2'-deoxyAmB and other AmB derivatives that are functional-group deficient on the mycosamine can be summed up as follows: global protection and removal of the mycosamine, synthesis of the functional-group deficient sugar, and glycosidation followed by deprotection (Figure 5.1).

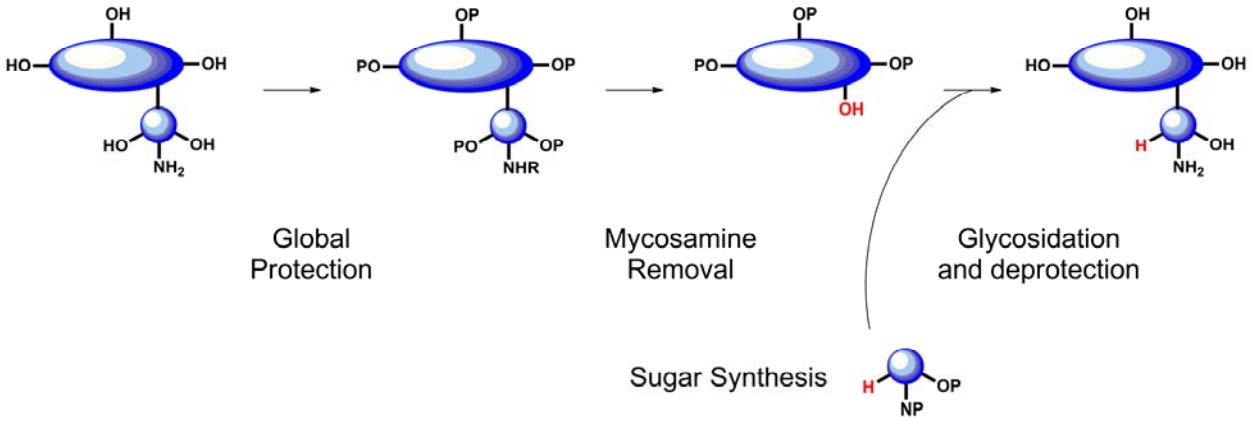

Figure 5.1. Hybrid strategy to access mycosamine derivatives of amphotericin B.

Even though the synthetic route requires the synthesis of the sugar donor, it does a have the significant advantage of less demanding chemistry being performed on the AmB framework. This is extremely beneficial for the protecting group strategy and overall yield. I was able to eliminate the acetals on the polyol by globally silylating with the easily removed TES groups. In addition, the methyl ester was replaced with a triisopropylsilyl (TIPS) ester which is deprotected in good yield in the same step as the TES ethers thus saving a step.

The protected amphoteronolide substrate was generated according to Scheme 5.10. Fmoc protection of the amine followed by hemiketal protection as the methyl ketal and global silylation of the hydroxyl groups lead to intermediate 5.10.[15] Protection of the acid as the TIPS ester, oxidative cleavage of the mycosamine, and reduction of the conjugated ketone completes the synthesis of the protected amphoteronolide acceptor.

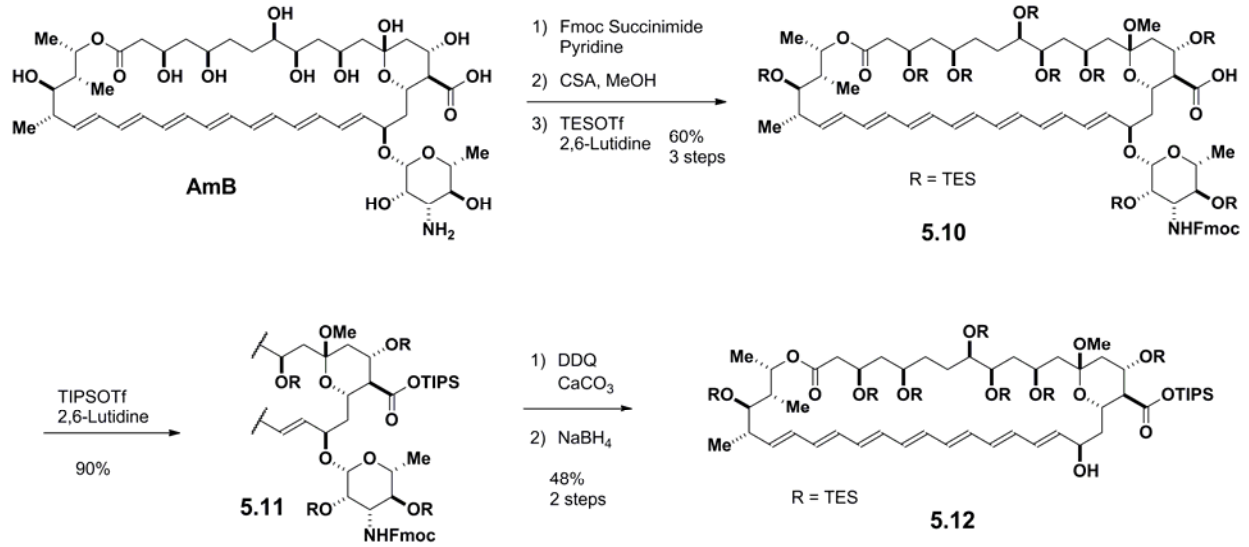

Scheme 5.10. Synthesis of protected amphoteronolide B.

Synthesis of the C2'-deoxysugar donor was done by colleague Brice Uno. Sugar intermediate **5.13** (Scheme 5.11) is known in the literature reached in 6 steps from 2-furyl methyl ketone.[5,16,17] The hydroxyl of **5.13** was protected as the TBS ether,[19] and then the epoxide was opened with lithium triethylborohydride. The resulting hydroxyl was mesylated to create intermediate **5.14**. Subsequent nucleophilic displacement of the mesylated hydroxyl by sodium azide completes the installation of all the functional groups. Removal of the para-methoxybenzyl (PMB) group on the hydroxyl at C1' generates the deoxysugar donor **5.15** (Scheme 5.10). With the acosamine sugar donor and protected amphoteronolide acceptor synthesized, focus turned to achieving glycosidation.

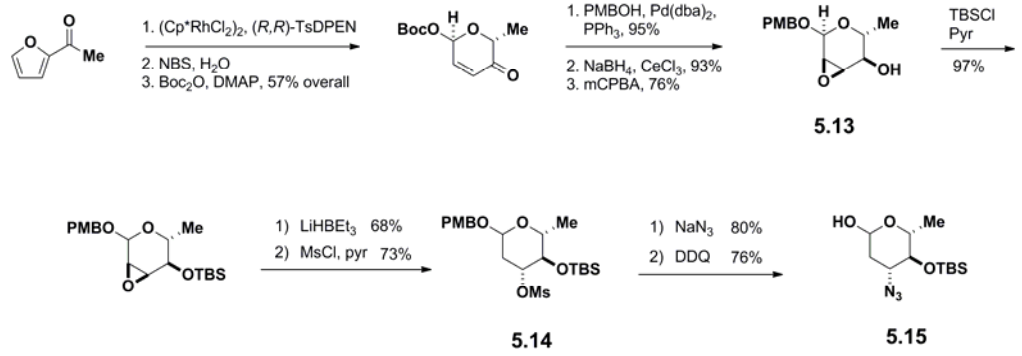

Scheme 5.11. Synthesis of the C2-deoxysugar donor. Synthesis of the intermediate **5.13** has been previously reported in refs. 5, 16, and 17.

The mycosamine on AmB is attached via a β-1,2-cis linkage. This can be a difficult linkage to form as the alpha linkage is favored with direct attack onto the oxocarbenium sugar intermediate due to the anomeric effect and steric hindrance from the axial substituent at the C2 position (Figure 5.2A). Normally glycosidations to obtain these types of linkages are done with participating groups located at the C2 position of the sugar donor. For instance, Nicolaou[18] and Carreira[19] have attached sugars to protected amphoteronolide B substrates using anchimeric assistance from the neighboring equatorial group at the C2 position followed by inversion at the C2 position (Figure 5.2B). In the case of a C2-deoxysugar this method is not an option to achieve β selective glycosidation.

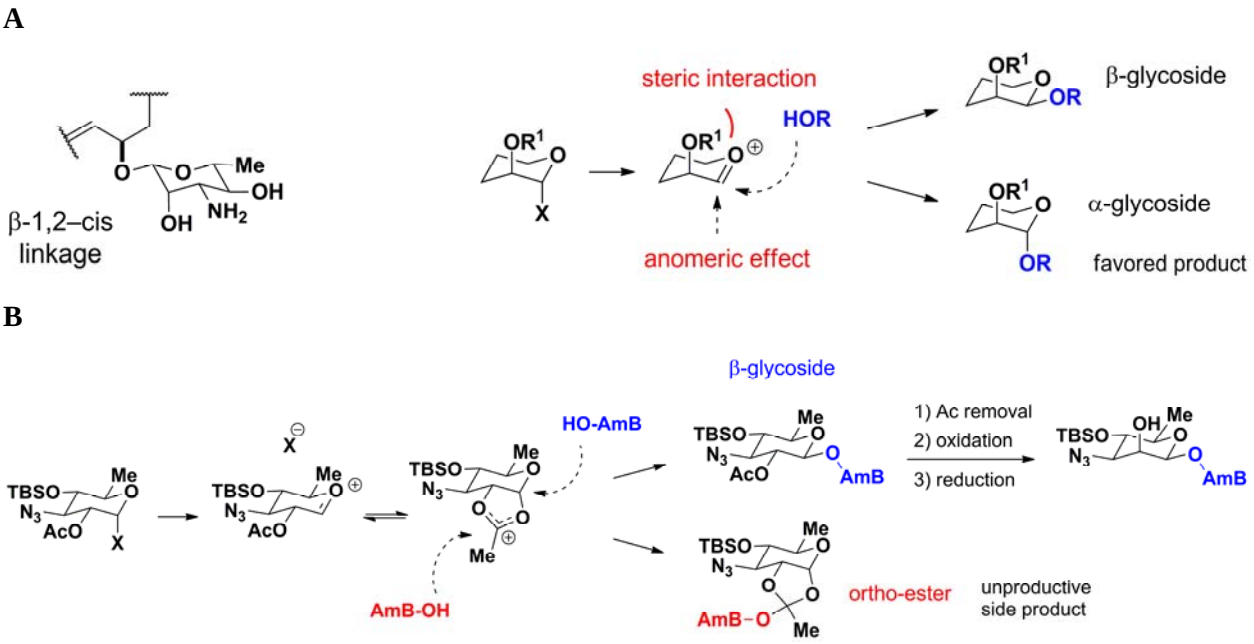

Figure 5.2. Glycosidation linkage of AmB. **A**. Factors disfavoring the formation of the β-1,2-cis linkage on AmB via direct glycosidation. **B**. Anchimeric assistance traditionally used to achieve β selective glycosidation of the protected AmB aglycone.

Methods to achieve β-selective direct glycosidation of C2-deoxysugars are rare.[20-23] Selectivity is often highly influenced by the stereochemistry and protecting groups of the substituents on the sugar. There are many options for anomeric activating groups and reagents for direct glycosidation. I investigated preparing the trichloroacetimidate donor and found this donor to be unstable, and it gave poor results under a variety of glycosidation conditions. I found that conditions involving oxidative reagents such as I_2 or *N*-iodosuccinimide also did poorly causing decomposition as well as reoxidation of the C19 hydroxyl on AmB. Thus, I turned to using a one pot procedure where a more stable donor could be generated and attached under buffered conditions with diphenyl sulfoxide, triflic anhydride, and 2,6-lutidine.[24,25] Both the donor and the protected amphoteronolide substrate were stable and glycosidation proceeded in an efficient fashion under these conditions (Scheme 5.12). Due to the lack of an participating group at the C2 position of the sugar, the ratio of α to β linkage varied in the range of 2:1 to 1:1 α:β.

The isomers were inseparable at this stage, but after removal of the silyl groups with HF-pyridine, the two isomers could be purified by preparative HPLC. I found the C2'-deoxyAmB intermediates containing the azide protecting group were sensitive to base if water was present. In addition, having a free amine at C3' greatly accelerated the rate of methyl ketal conversion to the hemiketal under aqueous CSA conditions in comparison to the C3' azide intermediate. This

acceleration provided a significant increase in the yield and cleanliness of the reaction; thus, it was critical that the azide was deprotected before the methyl ketal. Mild deprotection of the azide was achieved with trimethylphosphine and water in good yield, and subsequent methyl ketal exchange to the hemi ketal generated C2'-deoxyAmB (Scheme 5.12).

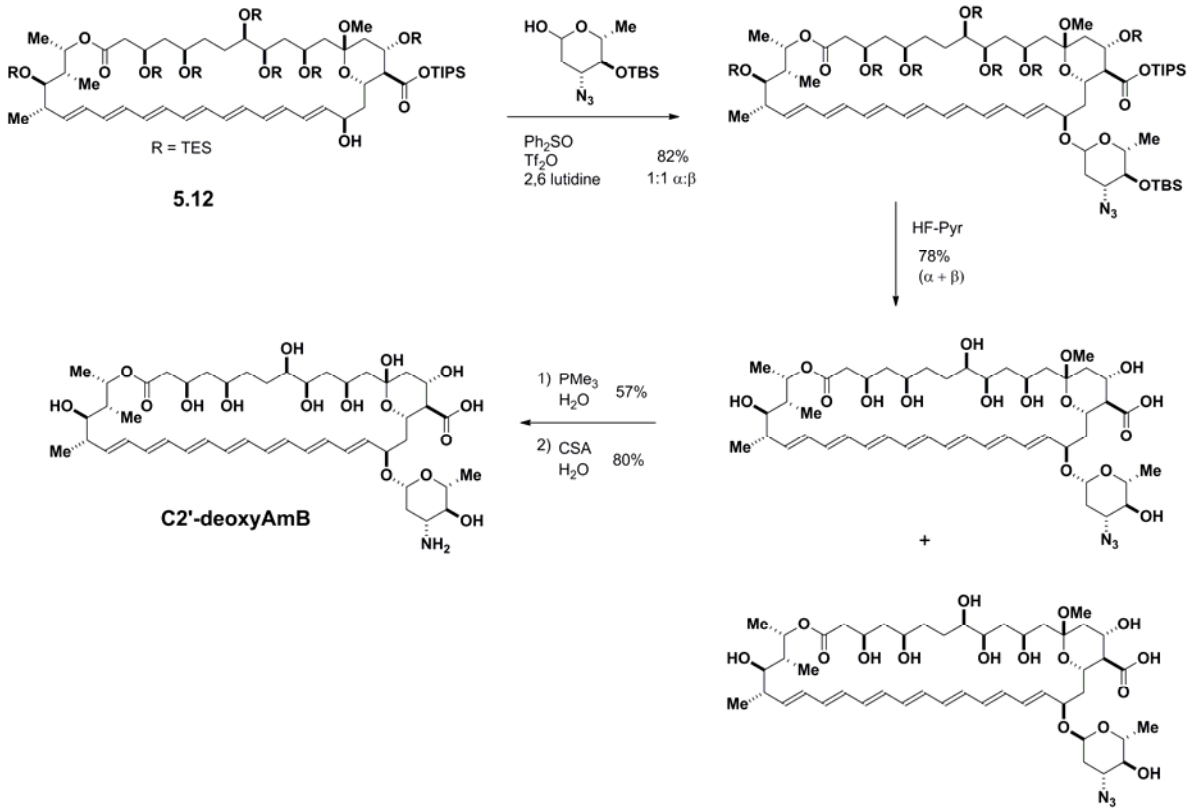

Scheme 5.12. Glycosidation and global deprotection of protected amphoteronolide B to generate C2'-deoxyAmB.

5-5 Summary

With the completion of the hybrid route, C2'-deoxyAmB can now be generated in large quantities for biophysical experiments. Evaluation of this derivative with the same biophysical studies that have proven successful with the derivatives discussed in Chapters 2 and 3 will further elucidate the sterol-AmB interaction by determining the role the C2' hydroxyl plays. The hybrid strategy can also be adapted to create a synthetic route to C4'-deoxyAmB and C3'-deaminoAmB. Since the primary antifungal mechanism of AmB is ergosterol binding (Chapter 3), and it is likely that cholesterol binding underlies human toxicity, a better understanding of the sterol binding events enabled by all of these functional-group deficient derivatives will provide insight in the development of AmB derivatives with improved therapeutic index.

5-6 Experimental

Portions of the experimental section are adapted from ref. 12.

General Methods

Materials

Amphotericin B was a gift from the Bristol-Myers Squibb Company. All other commercially available reagents were obtained from Sigma-Aldrich, TCI America, Fischer Scientific, Combi-Blocks Inc., and Oakwood Products. Chemicals were used without further purification unless otherwise specified. Camphorsulfonic acid was purified before use by recrystallization with ethyl acetate. Triethyl amine, diisopropylethyl amine, pyridine, and 2,6-lutidine were freshly distilled over calcium hydride under nitrogen atmosphere. All solvents were obtained from a solvent purification system utilizing packed columns as described by Pangborn and coworkers.[26]

Reactions

All reactions were performed under argon atmosphere in low light conditions with flame dried glassware unless otherwise indicated. All compounds were stored in the dark under argon atmosphere. Thin layer chromatography or reverse phase HPLC was used to monitor reaction progress. Thin layer chromatography was performed on silica gel 60 F_{254} plates from Merck with the indicated solvent. Visualization of the compounds was accomplished with a UV lamp (λ_{254}) and ceric ammonium molybdate (CAM) stain. Analytical HPLC was done on an Agilent 1100 Series HPLC with a C_{18} 5 μm, 4.6 x 150 mm, Symmetry® column from Waters Corp at a flow rate of 1 mL/min with the indicated solvent and gradient. The detection wavelength was set to 383 nm.

Purification and Analysis

Merck silica gel 60 230-400 mesh and SiliCycle reverse phase C18 (17%) 40-63 μm 60 angstrom silica gel was used for flash chromatography with the indicated solvent. HPLC reverse phase purification was done on a waters C18 5 μm, 30 x 150 mm Sunfire column at a flow rate of 25 mL/min with the indicated solvent and gradient. The detection wavelength was set to 383 nm. ^{1}H NMR spectra were taken at 23 °C on a Varian Unity Inova Narrow Bore spectrometer at

a ^{1}H frequency of 500 MHz with a Varian 5 mm $^{1}H\{^{13}C/^{15}N\}$pulsed-field gradient Z probe. Chemical shifts (δ) are reported in parts per million (ppm) downfield from tetramethylsilane and referenced internally to the residual protium in the NMR solvent (CHD_2OD, δ = 3.30, center line; $CD_3C(O)CHD_2$, δ = 2.04, center line; $CD_3S(O)CHD_2$, δ = 2.50, center line; CCl_3H, δ = 7.26, center line). Data is reported as follows: chemical shift, multiplicity (s = singlet, d = doublet, t = triplet, dd = doublet of doublets, td = triplet of doublets, m = multiplet, b = broad, app = apparent), coupling constant (*J*) in Hertz (Hz) and integration. ^{13}C spectra were obtained at 23 °C with a Varian Unity Inova spectrometer at a ^{13}C frequency of 125 MHz with a 5 mm Nalorac gradient $\{^{13}C/^{15}N\}^{1}H$ quad probe. Chemical shifts (δ) are reported downfield of tetramethylsilane and are referenced to the carbon resonances in the NMR solvent (CD_3OD, δ = 49.0, center line; $CD_3C(O)CD_3$, δ = 29.8, center line; $CD_3S(O)CD_3$, δ = 39.5, center line; $CDCl_3$, δ = 77.0, center line). ESI high resolution mass spectra (HRMS), ESI low resolution mass spectra (LRMS) and matrix-assisted laser desorption/ionization (MALDI) spectra were obtained at the University of Illinois mass spectrometry facility.

Synthesis of Compounds

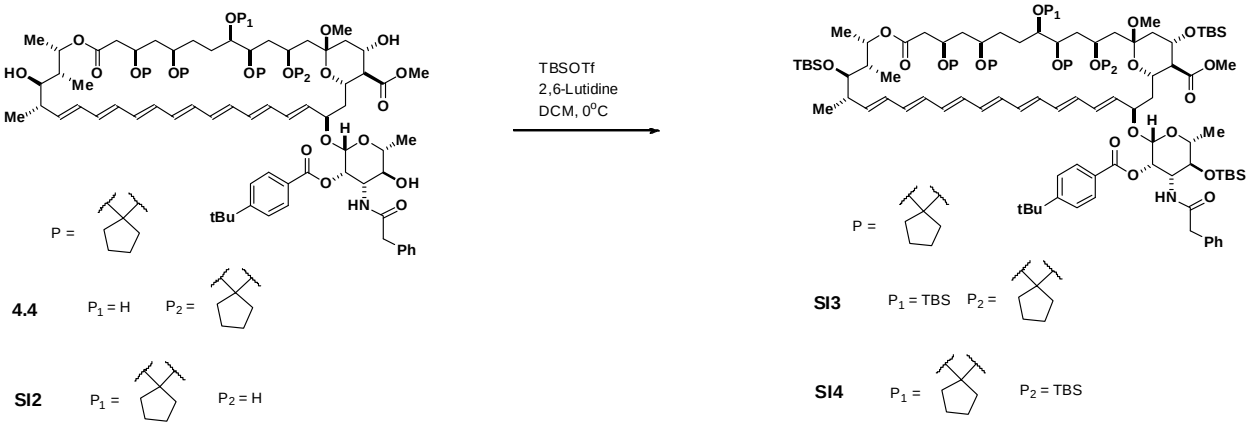

TBS Ether SI3 and SI4

Prior to the reaction, **4.4**/**SI2** (300 mg, 220 μmol, 1 eq) was azeotropically dried with acetonitrile followed by DCM and placed under vacuum for 8 hours. The orange powder was

dissolved in DCM (7.3 mL), and 2,6-lutidine (282 μL, 2.42 mmol, 11 eq) was added. The solution was cooled to 0 °C, and then TBS triflate (455 μL, 1.98 mmol, 9 eq) was added dropwise over 10 minutes. The reaction was allowed to stir at 0 °C for 90 minutes where the solution turned from orange to blackish color. The reaction was diluted with diethyl ether (500 mL) at 0 °C followed by quenching with saturated sodium bicarbonate (500 mL). The ether extract was washed twice with cupric sulfate (400 mL), water (400 mL), and saturated sodium chloride (400 mL). Each of the washes was back extracted with diethyl ether (300 mL). The combined ether layers were then dried over magnesium sulfate, filtered, and concentrated *in vacuo.* Flash chromatography (SiO_2; hexane:ethyl acetate 19:1 → 4:1) purification yielded a yellow-orange solid (294 mg, 162 μmol, 73 %).

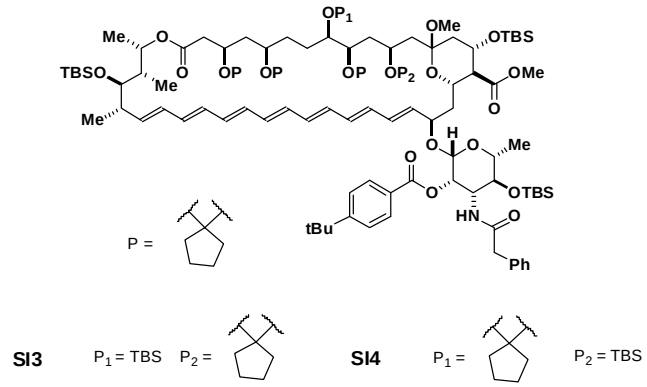

TLC (hexane:ethyl acetate 4:1)

R_f = 0.38, stained by CAM

^{1}HNMR (500 MHz, acetone *d-6*)

δ 8.03 (m, 4H), 7.64 (m, 4H), 7.32-7.13 (m, 12H), 6.35-6.15 (m, 22H), 6.02 (m, 2H), 5.88 (m, 2H), 5.50 (m, 2H), 4.92 (m, 2H), 4.75 (m, 2H), 4.65 (m, 2H), 4.35 (m, 3H), 4.25 (m, 2H), 4.03 (m, 3H), 3.88-3.66 (m, 15H), 3.58-3.40 (m, 9H), 2.84 (s, 3H), 2.73 (s, 3H), 2.43 (m, 3H), 2.37-2.19 (m, 3H), 2.15 (m, 6H), 1.96-1.48 (m, 42H), 1.47-0.96 (m, 58H), 0.95-0.80 (m, 72H), 0.11-(-0.01) (m, 48H)

^{13}CNMR (125 MHz, acetone *d-6*)

δ 173.1, 170.9, 169.9, 169.8, 166.0, 157.3, 138.1, 136.7, 135.0, 134.8, 134.7, 134.4, 134.4, 134.1, 133.9, 133.7, 133.5, 133.2, 132.5, 132.3, 132.1, 131.9, 127.2, 127.1, 126.1, 118.5, 110.6, 110.5, 101.1, 100.6, 96.4, 96.2, 80.7, 77.7, 75.1, 74.7, 73.7, 73.0, 72.7, 69.8, 68.7, 67.4, 66.8, 66.6, 66.4, 66.2, 58.1, 54.2, 51.8, 48.5, 48.3, 43.8, 43.5, 43.0, 41.3, 41.0, 40.7, 38.3, 38.1, 37.6, 36.7, 35.7, 33.8, 33.7, 32.0, 31.6, 31.4, 26.5, 26.3, 26.2, 26.0, 25.9, 25.3, 24.9, 24.3, 23.9, 23.3, 22.8, 19.2, 18.9, 18.6, 18.4, 18.3, 18.2, -3.2, -3.3, -3.5, -3.6, -4.0, -4.1, -4.3, -4.9.

HRMS (ESI)

Calculated for $C_{102}H_{163}NO_{19}Si_4$ $(M + Na)^+$: 1841.0794

Found: 1841.0776

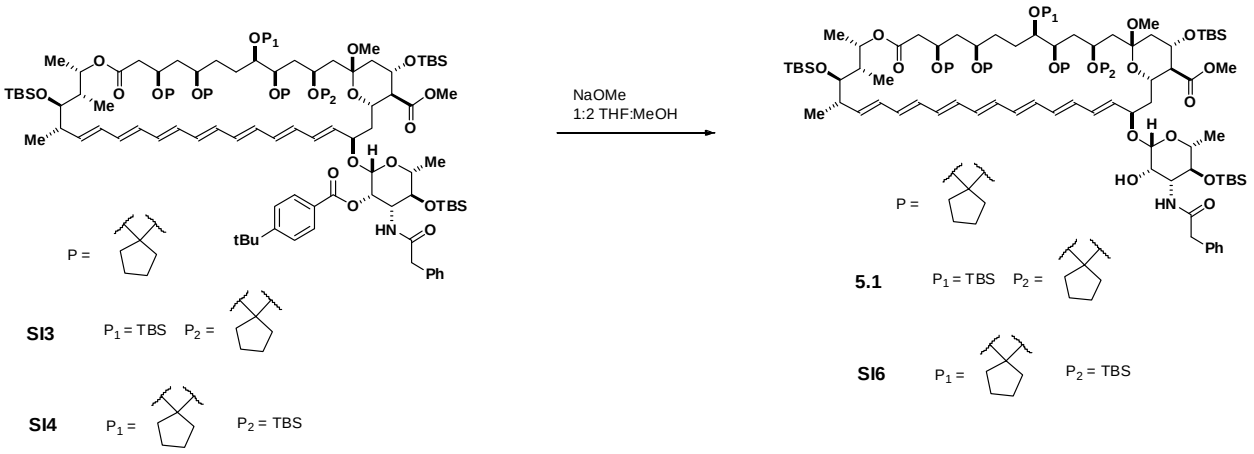

Alcohol 5.1

Prior to the reaction, **SI3/SI4** was azeotropically dried with acetonitrile followed by DCM and placed under vacuum for 8 hours. To a solution of **SI3/SI4** (130 mg, 71.4 μmol, 1 eq) in THF:MeOH 1:1 (1.8 mL) was added a solution of sodium methoxide (38.6 mg, 714 μmol, 10 eq) in MeOH (0.6 mL) dropwise. The reaction was allowed to stir at room temperature for 3 hours. The reaction was recharged with sodium methoxide (38.6 mg, 714 μmol, 10 eq) in MeOH (0.6 mL) dropwise. After stirring for 2 hours, the reaction solution was diluted with ethyl acetate

(200 mL) and washed twice with water (200 mL) followed by a wash with saturated sodium chloride (200 mL). The organic layer was dried over magnesium sulfate, filtered and concentrated *in vacuo*. **5.1** and **SI5** were separable by flash chromatography (SiO_2; hexane:ethyl acetate 4:1) purification yielded yellow-orange solids (104 mg, 62.8 μmol, 88 %).

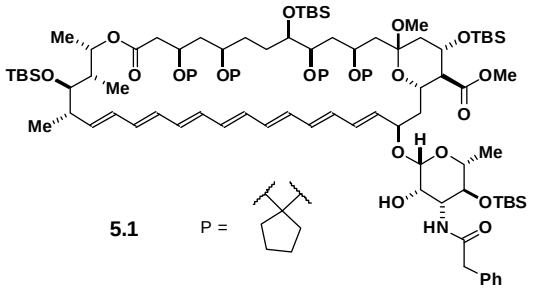

TLC (hexane:ethyl acetate 3:1)

R_f = **SI5** 0.18, **5.1** 0.25, stained by CAM

^{1}HNMR (500 MHz, acetone *d-6*)

δ 7.35 (m, 2H), 7.28 (m, 2H), 7.21 (m, 1H), 6.99 (d, *J* = 10 Hz, 1H), 6.39-6.15 (m, 11H) 6.08 (m, 1H), 5.84 (m, 1H), 5.76 (m, 1H), 4.81 (m, 1H), 4.63 (m, 1H), 4.61 (s, 1H), 4.22 (m, 1H), 4.04 (m, 2H), 3.85 (app t, *J* = 10 Hz, 2H), 3.75 (m, 1H), 3.71-3.52 (m, 9H), 3.48 (m, 1H), 3.32 (m, 1H), 3.00 (s, 3H), 2.41 (m, 1H), 2.31 (m, 1H), 2.23 (m, 2H), 2.16 (m, 1H), 1.97-1.71 (m, 9H), 1.70-1.38 (m, 12H), 1.34-1.24 (m, 8H), 1.22 (d, *J* = 6.5 Hz, 3H), 1.17 (d, *J* = 6.0 Hz, 3H), 1.10 (m, 1H), 1.02 (d, *J* = 7.0 Hz, 3H), 0.96 (d, *J* = 7.0 Hz, 3H), 0.93 (s, 9H), 0.91 (s, 9H), 0.85 (s, 9H), 0.83 (s, 9H), 0.13-(-0.02) (m, 24H)

^{13}CNMR (125 MHz, acetone *d-6*)

δ 173.4, 170.6, 169.9, 138.8, 137.1, 137.0, 134.5, 134.4, 134.3, 134.1, 133.9, 133.8, 133.6, 133.1, 132.5, 132.1, 130.8, 130.2, 129.3, 129.0, 127.2, 110.6, 100.8, 98.4, 75.3, 75.2, 74.6, 74.5, 73.2, 72.1, 71.6, 70.1, 68.9, 67.0, 66.7, 57.7, 55.5, 52.0, 48.4, 43.9, 43.8, 43.3, 41.5, 41.1, 40.8, 37.6, 36.8, 33.7, 32.7, 32.1, 31.7, 27.9, 26.4, 26.3, 25.9, 25.4, 24.9, 24.9, 23.3, 22.9, 19.1, 18.9, 18.7, 18.6, 18.3, 18.0, -3.3, -3.4, -4.0, -4.1, -4.2, -4.9.

HRMS (ESI)

Calculated for $C_{91}H_{151}NO_{18}Si_4$ $(M + Na)^+$:	1680.9906
Found:	1680.9905

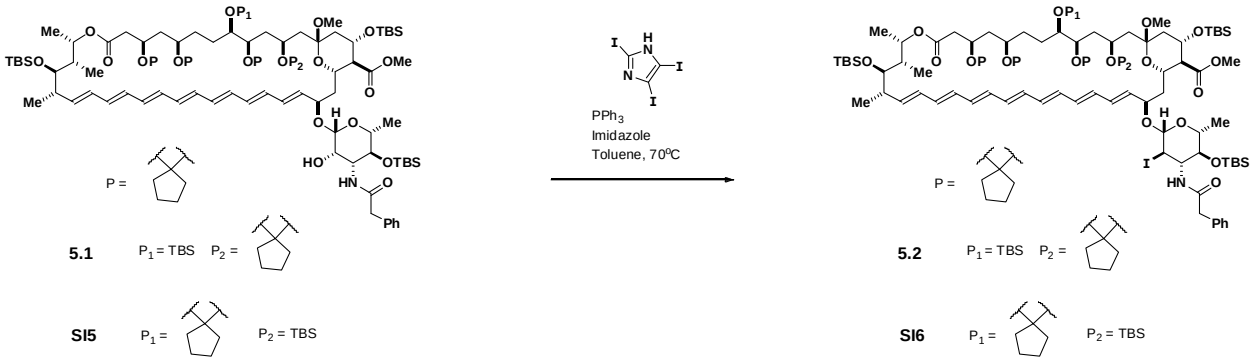

Iodide 5.2

Prior to the reaction, **5.1/SI6** was azeotropically dried with acetonitrile followed by DCM and placed under vacuum for 8 hours. A flask was charged with alcohol **5.1/SI6** (50 mg, 30 μmol, 1 eq), triiodoimidazole (13.4 mg, 30 μmol, 1 eq), imidazole (6.1 mg, 90 μmol, 3 eq), and triphenyl phosphine (15.7 mg, 60 μmol, 2 eq). The contents were dissolved in toluene (2 mL), and the reaction was allowed to stir at 70 °C for 6 hours. The reaction was then recharged with triiodoimidazole (13.4 mg, 30 μmol, 1 eq), imidazole (6.1 mg, 90 μmol, 3 eq), and triphenyl phosphine (15.7 mg, 60 μmol, 2 eq). After stirring for 2 hours at 70 °C, the reaction was diluted with ether (100 mL). The ether was washed twice with water (100 mL) followed by saturated sodium chloride (100 mL). The organic layer was dried over magnesium sulfate, filtered, and concentrated *in vacuo*. Flash chromatography (SiO_2; hexane:ethyl acetate 9:1) purification yielded a yellow-orange solid (42.5 mg, 24 μmol, 80 %).

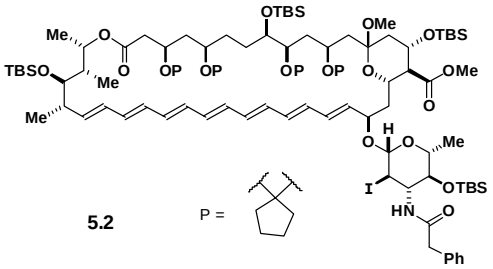

5.2

TLC (hexane:ethyl acetate 3:1)

R_f = 0.55, stained by CAM

^{1}HNMR (500 MHz, acetone *d-6*)

δ 7.37 (m, 2H), 7.29 (m, 2H), 7.21 (m, 1H), 6.37-6.25 (m, 9H), 6.23-6.08 (m, 3H), 5.83 (m, 2H), 4.79 (m, 1H), 4.71 (d, *J* = 8.5 Hz, 1H), 4.58 (m, 1H), 4.27 (m, 1H), 4.06 (m, 2H), 3.85, (app t, *J* = 5.0 Hz, 1H), 3.74 (m, 1H), 3.66 (s, 3H), 3.64- 3.51 (m, 8H), 3.42 (m, 1H), 3.03 (s, 3H), 4.2 (m, 1H), 2.28 (m, 3H), 2.15 (m, 1H), 2.02-1.92 (m, 3H), 1.87-1.73 (m, 6H), 1.70-1.38 (m, 15H), 1.34-1.25 (m, 5H), 1.21 (d, *J* = 6.0 Hz, 3H), 1.17(d, *J* = 6.0 Hz, 3H), 1.10 (m, 1H), 1.04(d, *J* = 7.0 Hz, 3H), 0.97 (d, *J* = 7.0 Hz, 3H), 0.93 (s, 9H), 0.91 (s, 9H), 0.86 (s, 9H), 0.83 (s, 9H), 0.11-(-0.01) (m, 24H)

^{13}CNMR (125 MHz, acetone *d-6*)

δ 173.0, 169.9, 138.5, 138.0, 136.4, 134.7, 134.6, 134.4, 134.3, 133.9, 133.8, 133.5, 133.0, 132.3, 131.8, 130.8, 130.7, 128.9, 128.4, 127.3, 110.7, 110.6, 102.6, 100.7, 76.6, 75.3, 75.2, 74.5, 72.1, 70.0, 68.9, 67.1, 67.0, 66.7, 57.6, 52.0, 48.5, 44.5, 44.1, 43.4, 41.4, 41.3, 40.8, 37.7, 37.4, 33.6, 32.8, 32.1, 31.7, 27.9, 26.5, 26.3, 25.9, 25.4, 24.9, 23.4, 22.9, 18.9, 18.7, 18.5, 18.3, 17.9, -3.6, -3.4, -3.9, -4.1, -4.2, -4.3, -4.9.

HRMS (ESI)

Calculated for $C_{91}H_{150}NO_{17}Si_4I$ $(M + Na)^+$: 1790.8923

Found: 1790.8929

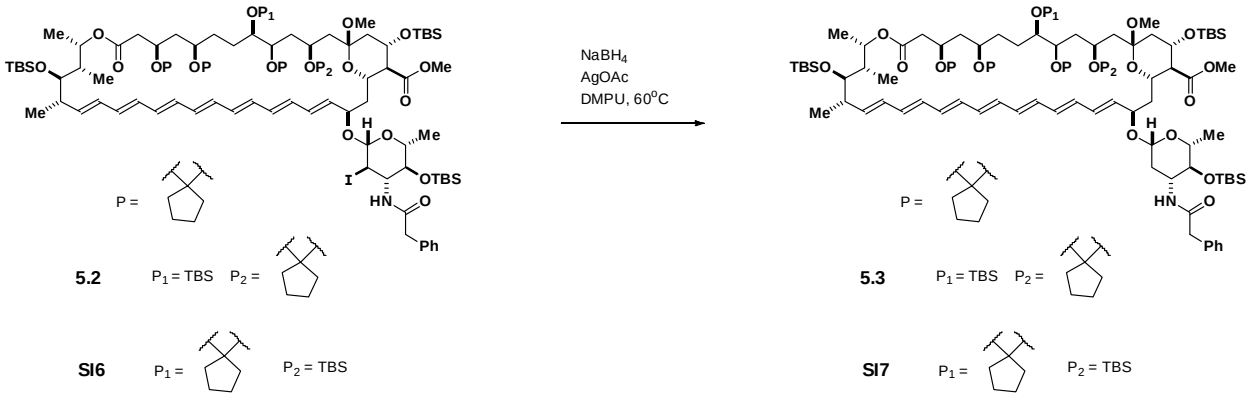

Methylene 5.3

To a solution of **5.2/SI6** (8 mg, 4.52 μmol, 1 eq) in DMPU (0.45 mL) was added sodium borohydride (1.4 mg, 36.2 μmol, 8 eq) and silver acetate (0.9 mg, 5.42 μmol, 1.2 eq). The reaction was heated to 60 ^{o}C for 3 hours. The reaction was diluted with ether (20 mL) and quenched with saturated sodium bicarbonate (20 mL). The ether layer was washed twice with water (20 mL) followed by a wash with saturated sodium chloride (20 mL). The combined aqueous layers were back extracted with ether (30 mL). The combined organic layers were dried over magnesium sulfate, filtered, and concentrated *in vacuo*. Flash chromatography (SiO_2; hexane:ethyl acetate 4:1) purification yielded a yellow-orange solid (4.5 mg, 2.76 μmol, 61 %).

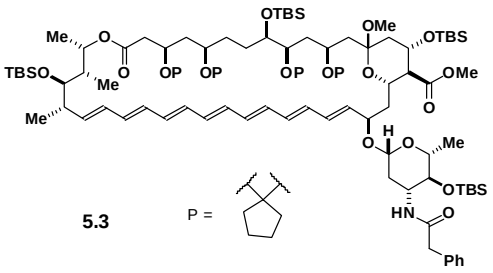

TLC (hexane:ethyl acetate 3:1)

R_f = 0.45, stained by CAM

^{1}HNMR (500 MHz, acetone *d-6*)

δ 7.30 (m, 5H), 6.56 (m, 1H), 6.39-5.99 (m, 12H), 5.80 (m, 1H), 5.63 (m, 1H), 5.16 (d, *J* = 4 Hz, 1H), 4.99 (m, 1H), 4.26 (m, 3H), 4.12 (m, 1H), 3.88 (m, 1H), 3.80 (m, 1H), 3.72 (m, 1H), 3.65 (m, 3H), 3.58 (m, 3H), 3.45 (m, 1H), 3.19 (m, 1H), 3.03 (s, 3H), 2.66 (m, 1H), 2.48-2.10 (m, 12H), 1.97-1.76 (m, 6H), 1.71-1.48 (m, 12H), 1.45-1.25 (m, 6H), 1.20-1.16 (m, 5H), 1.07-0.84 (m, 43H), 0.14-(-0.01) (m, 24H)

HRMS (ESI)

Calculated for $C_{91}H_{150}NO_{17}Si_4I$ $(M + Na)^+$: 1664.9957

Found: 1664.9896

diethylisopropyl silyl ether 5.4

4.6e (2.30 g, 1.57 mmol, 1 eq) was azeotropically dried with acetonitrile and left under vacuum overnight. DCM (40 mL) was added followed by hexane (40 mL) slowly while strirring to prevent **4.6e** from crashing out of solution. 2,6-lutidine (2.4 mL, 20.4 mmol, 13 eq) was added and the solution was cooled to 0 °C. Diethylisopropylsilyl triflate (DEIPSOTf) (2.5 mL, 12.5 mmol, 8 eq) was added dropwise at 0 °C over 20 min. The reaction was stirred for an additional 30 min. The reaction was diluted with diethyl ether and quenched with saturated sodium bicarbonate at 0 °C. The reaction was extracted with diethyl ether and washed with 1 M copper sulfate until no white precipitate was observed. The organic layers were washed twice with water and then once with saturated sodium chloride. The organic layers were then dried over sodium sulfate and filtered. The solvent was removed under reduced pressure and column chromatography (SiO_2; EtOAc:Hexane 1:9 → 1:4) purification yielded **5.4** as a yellow-orange solid (2.24 g, 1.13 mmol, 72 %).

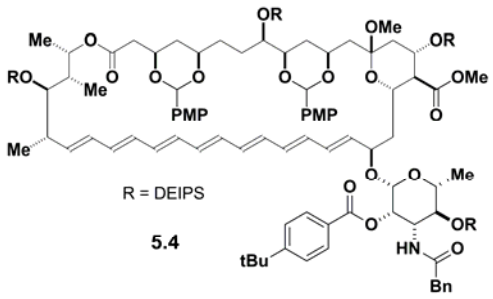

TLC (EtOAc:Hexane 1:3)

R_f = 0.25, stained by CAM

^{1}HNMR (500 MHz, $CD_3C(O)CD_3$)

δ 8.01 (d, *J* = 8.5 Hz, 2H), 7.63 (d, *J* = 8.5 Hz, 2H), 7.34 (m, 4H), 7.22 (m, 3H), 7.17 (m, 3H), 6.84 (m, 4H), 6.35-6.13 (m, 9H), 6.04 (m, 1H), 5.91 (m, 1H), 5.74 (m, 2H), 5.49 (m, 1H), 5.41 (s, 1H), 5.39 (s, 1H), 4.92 (app s, 1H), 4.75 (m, 1H), 4.66 (m, 1H), 4.31 (m, 1H), 4.25 (m, 1H), 4.12 (m, 1H), 3.84 (m, 1H), 3.81-3.77 (m, 9H), 3.68 (m, 4H), 3.64 (s, 3H), 3.57-3.45 (m, 3H), 2.74 (s, 3H), 2.45 (m, 2H), 2.26 (m, 1H), 2.17 (m, 1H), 2.09 (m, 1H), 1.90 (m, 2H), 1.73-1.59 (m, 4H), 1.51-1.34 (m, 18H), 1.26-1.11 (m, 6H), 1.08-0.76 (m, 54H), 0.73-0.39 (m, 19H).

^{13}CNMR (125 MHz, $CD_3C(O)CD_3$)

δ 173.1, 171.1, 169.8, 165.9, 160.7, 157.4, 138.2, 136.5, 134.6, 134.4, 134.2, 133.9, 133.8, 133.4, 132.8, 132.7, 132.5, 132.1, 131.1, 130.7, 130.6, 130.2, 129.0, 128.9, 128.8, 128.6, 128.2, 127.1, 126.2, 121.3, 117.9, 115.1, 113.8, 113.7, 101.7, 100.9, 100.5, 96.6, 81.3, 75.6, 74.7, 73.7, 73.2, 72.9, 72.7, 72.6, 68.6, 66.6, 58.1, 55.4, 54.5, 51.8, 48.3, 43.4, 41.0, 37.9, 36.8, 35.7, 31.4, 19.0, 18.0, 17.9, 17.8, 17.7, 17.6, 17.4, 14.0, 13.8, 13.4, 7.7, 7.6, 7.5, 7.4, 7.1, 5.1, 4.8, 4.7, 4.6, 4.4, 4.1.

HRMS (ESI)

Calculated for $C_{112}H_{171}NO_{21}Si_4$ $(M + Na)^+$: 2001.1318

Found: 2001.1221

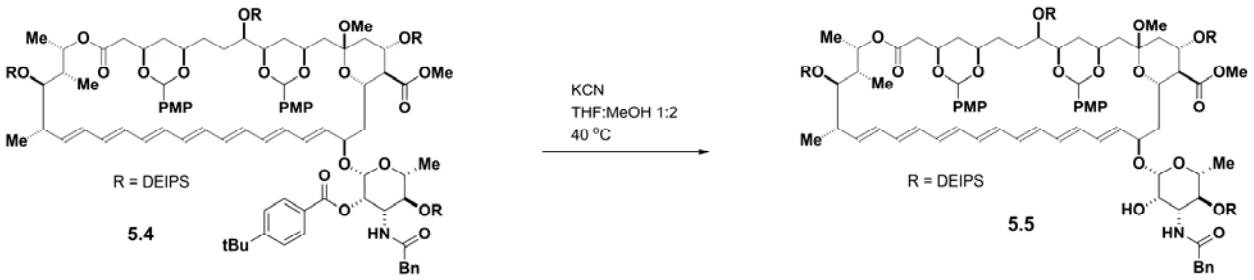

hydroxyl 5.5

5.4 (550 mg, 278 μmol, 1 eq) was dissolved in THF:MeOH 1:2 (13.5 mL), and KCN (27.0 mg, 417 μmol, 1.5 eq) was added. The reaction was heated to 40 °C for 2 days. The reaction was diluted with diethyl ether and washed with water three times followed by a wash of saturated sodium chloride. The organic layers were dried over sodium sulfate and filtered. The solvent was removed under reduced pressure and column chromatography (SiO_2; EtOAc:Hexane 1:4 → 3:7) purification yielded **5.5** as a yellow-orange solid (329 mg, 181 μmol, 65 %).

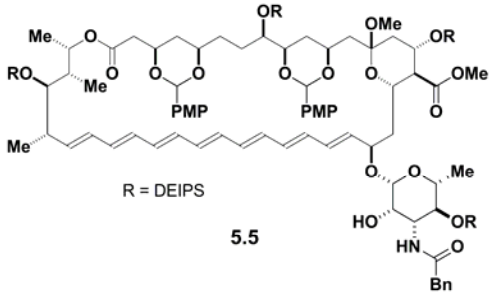

TLC (EtOAc:Hexane 3:7)

R_f = 0.22, stained by CAM

^{1}HNMR (500 MHz, $CD_3C(O)CD_3$)

δ 7.35 (m, 6H), 7.29 (m, 2H), 7.22 (m, 1H), 6.93 (d, *J* = 9.5 Hz, 1H), 6.85 (m, 4H), 6.40-6.17 (m, 11H), 6.09 (m, 1H), 5.82 (m, 1H), 5.77 (m, 1H), 5.43 (s, 1H), 5.42 (s, 1H), 4.80 (m, 1H), 4.62 (m, 1H), 4.60 (app s, 1H), 4.23 (m, 1H), 4.15 (m, 1H), 3.98 (m, 1H), 3.85 (m, 3H), 3.78 (m, 7H), 3.71 (m, 4H), 3.66 (m, 2H), 3.62 (s, 3H), 3.58-3.50 (m, 2H), 3.32 (m, 1H), 3.02 (s, 3H), 2.48 (m, 1H), 2.42 (m, 1H), 2.29-2.19 (m, 3H), 1.95-1.87 (m, 3H), 1.74 (m, 2H), 1.62-1.28 (m, 7H), 1.24-1.15 (m, 7H), 1.04-0.76 (m, 56H), 0.72-0.50 (m, 13H), 0.44-0.36 (m, 4H).

^{13}CNMR (125 MHz, $CD_3C(O)CD_3$)

δ 173.4, 170.8, 169.9, 160.8, 160.6, 137.2, 136.9, 134.6, 134.5, 134.1, 133.9, 133.8, 133.6, 133.2, 132.7, 132.6, 132.2, 130.9, 130.3, 129.5, 129.1, 128.7, 128.3, 127.3, 121.3, 117.9, 113.9, 113.8, 110.6, 101.8, 101.1, 100.8, 98.5, 81.4, 75.9, 75.0, 74.7, 74.6, 73.4, 73.0, 72.8, 71.5, 68.8, 67.1, 57.7, 55.8, 55.5, 52.0, 48.5, 43.8, 43.0, 41.2, 37.9, 36.7, 33.5, 32.7, 28.1, 18.9, 18.0, 17.9, 17.8, 17.4, 14.0, 13.9, 13.8, 13.5, 7.7, 7.6, 7.5, 7.2, 5.1, 4.9, 4.7, 4.6, 4.4, 4.1.

HRMS (ESI)

Calculated for $C_{101}H_{159}NO_{20}Si_4$ $(M + Na)^+$: 1841.0430

Found: 1841.0464

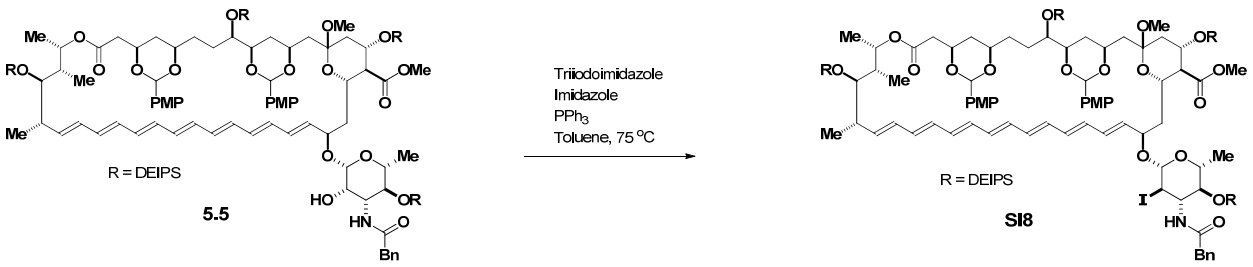

iodide SI8

5.5 (350 mg, 192 μmol, 1 eq), triiodoimidazole (130 mg, 288 μmol, 1.5 eq), triphenyl phosphine (152 mg, 378 μmol, 3 eq), and imidazole (60 mg, 866 μmol, 4.5 eq) were placed in a flask and dissolved in toluene (9.6 mL). The reaction was heated to 70 °C for 3 hrs. The reaction was diluted with diethyl ether and washed with saturated sodium bicarbonate followed by water four times. A final wash of saturated sodium chloride was performed, and the organic layers were dried over sodium sulfate and filtered. The solvent was removed under reduced pressure and column chromatography (SiO_2; EtOAc:Hexane 3:17) purification yielded **SI8** as a yellow-orange solid (296 mg, 154 μmol, 80 %).

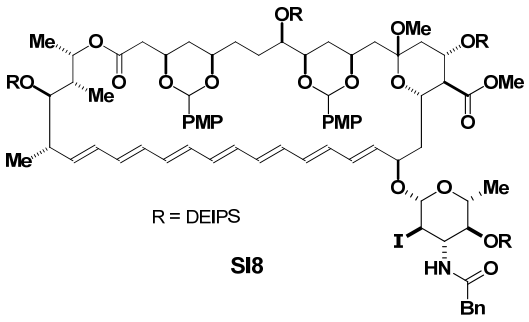

SI8

TLC (EtOAc:Hexane 3:7)

R_f = 0.55, stained by CAM

^{1}HNMR (500 MHz, $CD_3C(O)CD_3$)

δ 7.38-7.28 (m, 9H), 7.22 (m, 1H), 6.86 (m, 4H), 6.40-6.09 (m, 12H), 5.83 (m, 2H), 5.43 (s, 1H), 5.41 (s, 1H), 4.79 (m, 1H), 4.69 (app d, *J* = 7.5 Hz, 1H), 4.57 (m, 1H), 4.28 (m, 1H), 4.15 (m, 1H), 4.04 (m, 1H), 3.89 (m, 1H), 3.84 (m, 1H), 3.77 (m, 7H), 3.72 (m, 3H), 3.65 (s, 3H), 3.57 (m, 2H), 3.40 (m, 1H), 3.05 (s, 3H), 2.51-2.40 (m, 2H), 2.25 (m, 3H), 2.00 (m, 1H), 1.88 (m, 2H), 1.74 (m, 2H), 1.62-1.40 (m, 7H), 1.31-1.15 (m, 9H), 1.07-0.76 (m, 58H), 0.72-0.50 (m, 13H), 0.44-0.36 (m, 4H).

^{13}CNMR (125 MHz, $CD_3C(O)CD_3$)

δ 172.5, 169.3, 160.6, 160.2, 160.0, 158.4, 137.5, 134.2, 134.1, 133.9, 133.6, 133.4, 133.2, 132.9, 132.5, 132.1, 132.0, 131.9, 131.3, 130.2, 130.0, 128.3, 128.1, 127.7, 126.8, 113.3, 113.2, 102.1, 101.3, 100.5, 100.1, 94.2, 80.8, 76.3, 75.4, 74.4, 74.0, 72.5, 72.2, 68.1, 66.7, 57.0, 54.8, 51.4, 47.9, 43.8, 43.4, 42.5, 40.6, 37.3, 36.8, 32.9, 27.5, 18.1, 17.4, 17.3, 17.2, 16.8, 13.4, 13.2, 12.9, 7.1, 7.0, 6.9, 6.6, 4.5, 4.3, 4.2, 4.1, 3.8, 3.6.

HRMS (ESI)

Calculated for $C_{101}H_{158}NO_{19}Si_4I$ $(M + Na)^+$: 1950.9448

Found: 1950.9543

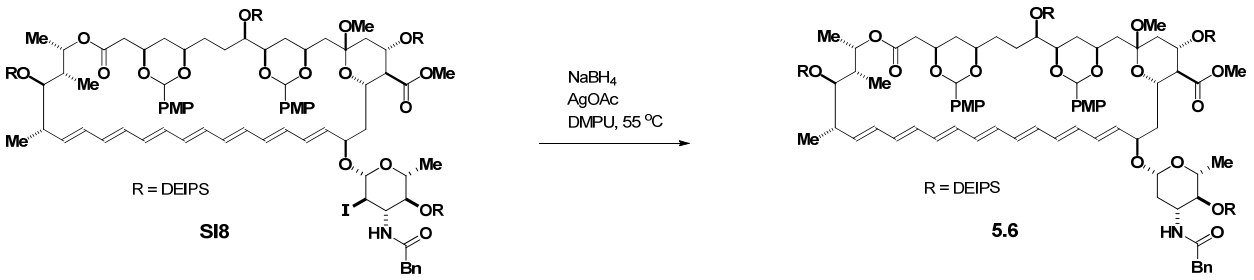

methylene 5.6

SI8 (320 mg, 166 μmol, 1 eq) was placed in a vial and azeotropically dried with toluene and placed under vacuum overnight. The vial was backfilled with argon and DMPU (6.6 mL) was added. Sodium borohydride (50 mg, 1.33 mmol, 8 eq) and silver(I) acetate (42 mg, 249 μmol, 1.5 eq) was added in a glovebox. The reaction was heated in the range of 50-55 °C for 3 hrs. After 3 hrs, an aliquot was removed in the glovebox every 30 min to monitor the reaction by TLC. The reaction was allowed to run to approximately 85 % conversion until the rate of decomposition exceeded conversion of the starting material. The reaction was cooled to room temperature and then diluted with dry diethyl ether that had been cooled to 0 °C. The reaction was quenched with saturated sodium bicarbonate cooled to 0 °C. Room temperature diethyl ether was used to extract the aqueous layer. The organic layer was then washed with water twice. A final wash of saturated sodium chloride was performed, and the organic layers were dried over sodium sulfate and filtered. The solvent was removed under reduced pressure and column chromatography (SiO_2; EtOAc:Hexane 3:17) purification yielded **5.6** as a yellow-orange solid (89.8 mg, 49.8 μmol, 30 %).

This reaction is quite sensitive to water and air. DMPU was obtained from Aldrich absolute over molecular sieves $H_2O \leq 0.03\%$. The product is unstable to the reaction conditions and decomposes over time; the best yields are obtained by stopping the reaction before complete conversion and recovering the starting material and product.

The reaction was found to be dependent upon the identity of the protecting group on the C3' amine. Extensive elimination or inactivity was observed for other protecting groups.

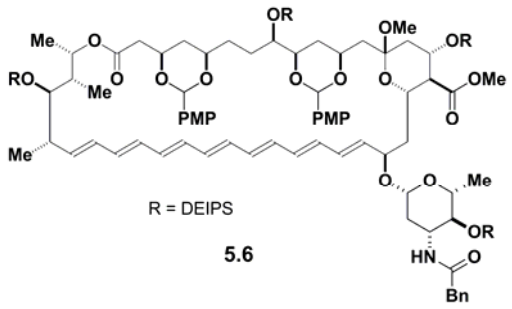

5.6

TLC (EtOAc:Hexane 1:3)

R_f = 0.47, stained by CAM

^{1}HNMR (500 MHz, $CD_3C(O)CD_3$)

δ 7.40-7.33 (m, 9H), 7.26 (m, 1H), 6.87 (m, 4H), 6.42-6.06 (m, 12H), 5.70 (m, 2H), 5.46 (s, 1H), 5.44 (s, 1H), 4.69 (app d, *J* = 5 Hz, 1H), 4.97 (m, 1H), 4.23 (m, 3H), 3.93 (m, 1H), 3.82-3.70 (m, 10H), 3.66 (m, 4H), 3.58 (m, 2H), 3.39 (m, 1H), 3.17 (m, 1H), 3.04 (s, 3H), 2.63 (m, 2H), 2.42 (m, 1H), 2.30 (m, 3H), 1.98 (m, 1H), 1.88 (m, 1H), 1.76-1.34 (m, 10H), 1.29-1.14 (m, 8H), 1.05-0.76 (m, 59H), 0.72-0.50 (m, 13H), 0.44-0.36 (m, 4H).

^{13}CNMR (125 MHz, $CD_3C(O)CD_3$)

δ 173.6, 170.0, 160.8, 160.7, 136.9, 134.6, 134.3, 133.6, 136.4, 133.0, 132.6, 132.5, 130.0, 129.4, 128.7, 128.4, 127.6, 113.9, 113.8, 102.0, 101.2, 81.7, 80.9, 76.5, 75.2, 73.4, 73.1, 55.5, 51.7, 44.1, 43.8, 42.7, 41.5, 37.9, 33.6, 32.6, 28.5, 18.0, 17.9, 17.8, 17.6, 17.4, 13.9, 13.5, 7.7, 7.6, 7.5, 7.4, 7.2, 4.8, 4.7, 4.4, 4.2.

HRMS (ESI)

Calculated for $C_{101}H_{159}NO_{19}Si_4$ $(M + Na)^+$: 1825.0481

Found: 1825.0496

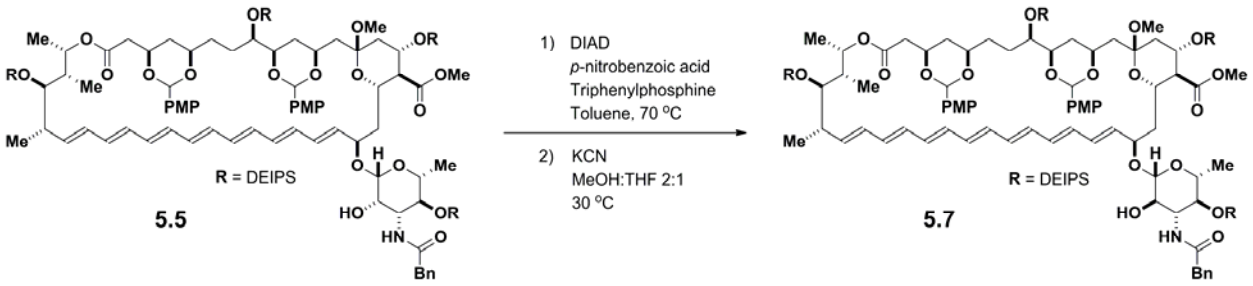

epi-alcohol 5.7

5.5 (18.2 mg, 10 μmol, 1 eq), triphenylphosphine (4.0 mg, 15 μmol, 1.5 eq), and *p*-nitrobenzoic acid (2.0 mg, 12 μmol, 1.15 eq) were placed in a flask and azeotroped in toluene to dryness (3x 0.5 mL). The reaction was then dissolved in toluene (0.3 mL) and cooled to 0 ^{o}C for the dropwise addition of DIAD (3.0 μl, 15 μmol, 1.5 eq). The reaction was stirred for 20 min at 0 ^{o}C then heated to 70 ^{o}C for 2 hrs. The reaction was diluted with diethyl ether (10 mL) and washed with saturated sodium bicarbonate (3.0 mL). The aqueous phase was extracted with diethyl ether (10 mL). A final wash of saturated sodium chloride was performed, and the organic layers were dried over sodium sulfate and filtered. The solvent was removed under reduced pressure and column chromatography (SiO_2; EtOAc:Hexane 5:95 to 1:3) purification yielded the C2' nitrobenzoate ester as a yellow-orange solid. Two reactions were run: (11.7 mg, 5.9 μmol, 59 %) (13.5 mg, 6.8 μmol, 68%)

The C2' *p*-nitrobenzoate ester was combined (25.2 mg, 12.8 μmol, 1.0 eq) and taken up in MeOH:THF 2:1 (435 μl). Potassium cyanide (2.5 mg, 38 μmol, 3.0 eq) was then added and the reaction was stirred for 72 hrs at 30 ^{o}C. The reaction was then diluted with diethyl ether (10 mL) and washed with saturated sodium bicarbonate (3.0 mL). The aqueous phase was extracted with diethyl ether (2x 10 ml). A final wash of saturated sodium chloride was performed, and the organic layers were dried over sodium sulfate and filtered. The solvent was removed under reduced pressure and column chromatography (SiO_2: EtOAc:Hexane 1:4 → 3:7) purification yielded **5.7** as a yellow-orange solid (15.8 mg, 8.7 μmol, 68 %).

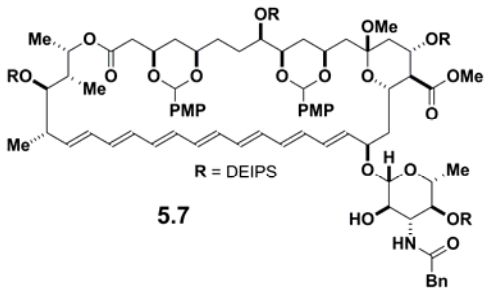

5.7

TLC (EtOAc:Hexane 3:7)

R_f = 0.2, stained by CAM

^{1}HNMR (500 MHz, $CD_3C(O)CD_3$)

δ 7.36 (m, 6H), 7.28 (m, 2H), 7.21 (m, 1H), 7.15 (m, 1H), 6.86 (m, 4H), 6.41-6.18 (m, 11H), 6.10 (m, 1H), 5.86 (m, 1H), 5.77 (m, 1H), 5.44 (s, 1H), 5.43 (s, 1H), 4.81 (m, 1H), 4.56 (m, 1H), 4.36 (app d, *J* = 7.5, 1H), 4.26 (m, 1H), 4.17 (m, 1H), 3.97-3.85 (m, 4H), 3.79 (m, 7H), 3.73 (m, 4H), 3.66 (s, 3H), 3.61-3.48 (m, 3H), 3.43 (m, 1H), 3.33 (m, 1H), 3.04 (s, 3H), 2.49 (m, 1H), 2.42 (m, 1H), 2.30-2.21 (m, 3H), 1.95-1.87 (m, 3H), 1.80-1.67 (m, 3H), 1.64-1.27 (m, 6H), 1.24-1.16 (m, 7H), 1.04-0.76 (m, 56H), 0.73-0.51 (m, 13H), 0.46-0.37 (m, 4H).

^{13}CNMR (125 MHz, $CD_3C(O)CD_3$)

δ 173.9, 172.1, 170.1, 161.0, 137.9, 137.0, 134.8, 134.7, 134.3, 134.1, 133.9, 133.7, 133.3, 132.9, 132.4, 131.1, 130.5, 129.7, 129.1, 128.9, 128.5, 127.3, 114.1, 114.0, 103.4, 102.0, 101.3, 100.9, 81.6, 76.5, 76.1, 75.2, 74.7, 73.3, 73.0, 69.0, 67.6, 57.8, 55.6, 52.1, 48.6, 44.3, 44.2, 38.1, 33.7, 32.9, 19.1, 18.2, 18.1, 18.0, 17.6, 14.3, 14.2, 14.1, 13.7, 7.8, 7.7, 7.6, 7.3, 5.4, 5.1, 5.0, 4.9, 4.6, 4.4

HRMS (ESI)

Calculated for $C_{101}H_{159}NO_{20}Si_4$ $(M + Na)^+$: 1841.0430

Found: 1841.0464

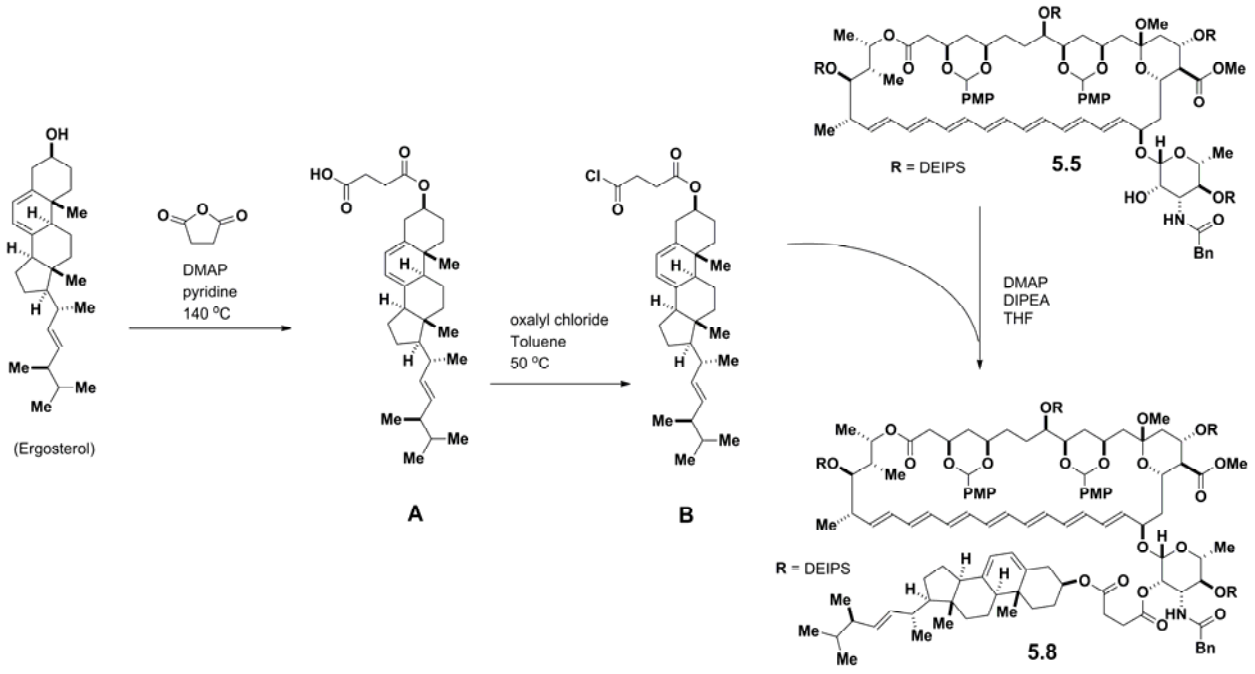

conjugate 5.8

Ergosterol (400 mg, 1.01 mmol, 1 eq) and succinic anhydride (1.01 g, 10.1 mmol, 10.0 eq) were azeotroped with toluene (3x 1.0 mL) in a 40 mL vial. Dry pyridine (20 mL 0.05 M) was then added followed by dimethylaminopyridine (DMAP) (154.2 mg, 1.26 mmol, 1.25 eq). The reaction was sealed with a teflon lined cap and heated to 140 °C for 16 hrs. The resulting black solution was extracted with HCl (10% v/v) and EtOAc. The organic phase was dried with sodium sulfate, filtered, and concentrated. Chromatography (SiO_2; EtOAc:Hexane 1:5 with 1% AcOH) purification yielded **A** as a white solid (282 mg, 0.57 mol, 56%).

A (12.5 mg, 25 μmol, 2.5 eq) was dissolved in toluene (0.3 mL) and oxalyl chloride (10.0 μL, 118 μmol, 4.75 eq) was added and the reaction was heated to 50 °C and stirred for 15 min. The resulting yellow solution was azeotroped with toluene (3x 0.3 mL) to dryness. The resulting off-white solid **B** was then dissolved in THF (0.3 mL) whereupon DMAP (3.1 mg, 25 μmol, 2.5 eq) was added to generate a cloudy white suspension. In a separate vial **5.5** (18.2 mg, 10 μmol, 1.0 eq) was dissolved in THF (0.15 mL) and diethylisopropyl amine (10 μL, 57 μmol, 5.7 eq) was added. The resulting yellow/orange solution was added dropwise via cannula to the first suspension and stirred for 3 hrs at room temperature. The reaction was diluted with diethyl ether

(10 mL) and washed with saturated sodium bicarbonate (3.0 mL). The aqueous phase was extracted with diethyl ether (2x 10 mL). A final wash of saturated sodium chloride was performed, and the organic layers were dried over sodium sulfate and filtered. The solvent was removed under reduced pressure and column chromatography (SiO_2; EtOAc:Hexane 5:95 → 1:3) purification yielded the **5.8** as a yellow-orange solid (14.5 mg, 6.3 μmol, 63 %)

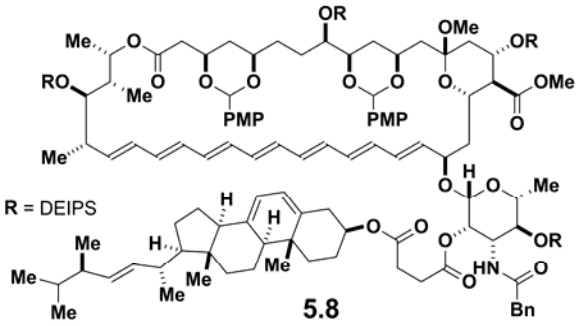

TLC (EtOAc:Hexane 1:3)

R_f = 0.76, stained by CAM

^{1}HNMR (500 MHz, $CD_3C(O)CD_3$)

δ 7.36 (m, 4H), 7.28 (m, 4H), 7.23 (m, 1H), 6.93 (m, 1H), 6.86 (m, 4H), 6.39-6.12 (m, 12H), 5.84(m, 2H), 5.61 (m, 1H), 5.41 (m, 3H), 5.26 (m, 3H), 5.83-4.61 (m, 4H), 4.29-4.13 (m, 3H), 3.90-3.81 (m, 3H), 3.79 (s, 3H), 3.78 (s, 3H), 3.72 (m, 2H), 3.67 (s, 3H), 3.56 (m, 2H), 3.47 (m, 2H), 3.00 (s, 3H), 2.71-2.34 (m, 9H), 2.31-2.08 (m, 5H), 2.00-1.45 (m, 30H), 1.41-0.38 (m, 98H)

^{13}CNMR (125 MHz, $CD_3C(O)CD_3$)

δ 173.4, 173.2, 172.3, 171.2, 170.1, 160.8, 142.3, 139.6, 137.8, 136.8, 136.7, 134.8, 134.5, 134.1, 133.7, 133.3, 132.9, 132.6, 132.1, 131.0, 130.5, 129.2, 128.9, 128.5, 127.5, 126.2, 121.4, 117.5, 114.1, 114.0, 102.0, 101.3, 100.9, 81.6, 76.2, 75.2, 75.1, 74.1, 73.9, 73.3, 73.1, 72.3, 68.9, 67.1, 58.1, 56.7, 55.7, 55.4, 54.6 52.1, 48.8, 47.1, 44.2, 43.9, 43.8, 43.7, 43.2, 41.4, 39.9, 38.8, 38.0, 37.6, 34.0, 33.8, 30.9, 29.1, 29.0, 28.4, 23.9, 21.7, 20.5, 20.2, 19.2, 18.3, 18.2, 18.1, 18.0, 17.9, 17.6, 16.6, 14.2, 14.1, 13.7, 12.6, 7.9, 7.8, 7.7, 7.6, 7.3, 5.4, 5.1, 5.0, 4.9, 4.7, 4.4, 1.5

MS (MALDI)

Calculated for $C_{133}H_{205}NO_{23}Si_4$ $(M + Na)^+$: 2319

Found: 2319

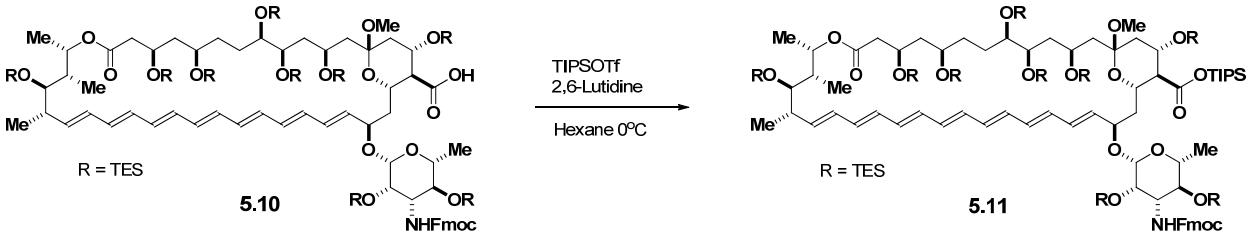

TIPS ester **5.11**

Intermediate **5.10** (15.8 g, 7.20 mmol, 1 eq) was azeotropically dried with toluene and placed under vacuum overnight. Hexane (240 mL) and 2,6-lutidine (2.9 mL, 25.2 mmol, 3.5eq) were added. The resulting solution was cooled to 0 ^oC and triisopropylsilyl triflate (2.9 mL, 10.8 mmol, 1.5eq) was added slowly over 15 min. The reaction was quenched after 1 hr with saturated aqueous sodium bicarbonate and extracted with ether. The organic layer was washed with copper sulfate, water, and finally saturated sodium chloride. The organic layer was dried with sodium sulfate and filtered. The solvent was removed under reduced pressure, and column chromatography (SiO_2; Ether:Hexane 5:95 → 1:4) purification yielded the **5.11** as a yellow-orange solid (15.2 g, 6.5 mmol, 90 %).

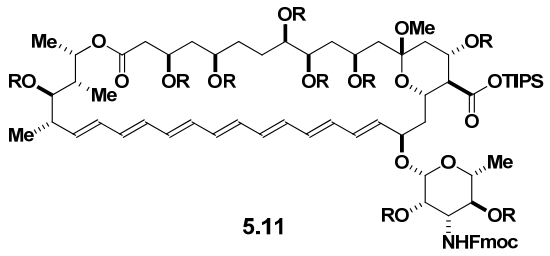

TLC (Ether:Hexane 0.1% Et_3N 3:7)

R_f = 0.72, stained by CAM

^{1}HNMR (500 MHz, $CD_3C(O)CD_3$)

δ 7.86 (d, *J* = 7.5 Hz, 2H), 7.69 (d, *J* = 7.5 Hz, 2H), 7.41 (t, *J* = 7.5 Hz, 2H), 7.33 (t, *J* = 7.5 Hz, 2H), 6.53-6.05 (m, 12H), 5.51 (m, 1H), 5.34 (m, 1H), 4.65 (m, 2H), 4.47 (m, 3H), 4.34 (m, 2H), 4.24 (m, 2H), 4.13 (m, 1H), 3.98 (m, 2H), 3.90 (m, 1H), 3.83 (m, 1H), 3.66 (m, 2H), 3.45 (m, 1H), 3.27 (m, 1H), 3.15 (s, 3H), 2.56 (m, 1H), 2.42 (m, 2H), 2.10-2.01 (m, 3H), 1.94-1.59 (m, 12H), 1.50 (m, 1H), 1.38-1.30 (m, 4H), 1.23 (m, 4H), 1.16 (m, 20H), 1.07-0.89 (m, 85H), 0.78-0.55 (m, 56H).

^{13}CNMR (125 MHz, $CD_3C(O)CD_3$)

δ 172.3, 170.5, 156.2, 145.0, 142.1, 139.0, 135.7, 135.3, 135.2, 134.7, 133.8, 132.9, 132.8, 132.7, 132.5, 131.4, 130.7, 130.6, 128.4, 127.8, 125.8, 125.7, 120.7, 101.2, 99.5, 76.7, 74.6, 74.0, 73.9, 73.2, 71.1, 69.4, 68.0, 67.5, 67.3, 67.2, 59.0, 58.2, 48.2, 48.0, 47.8, 44.3, 43.4, 42.1, 41.2, 37.2, 35.6, 27.4, 19.9, 19.2, 19.0, 18.4, 18.2, 12.9, 11.3, 7.6, 7.5, 7.4, 7.3, 6.4, 6.2, 6.1, 6.0, 5.9, 5.8.

LRMS (ESI)

Calculated for $C_{126}H_{231}NO_{19}Si_{10}$ $(M + Na)^+$: 2365.5

Found: 2365.1

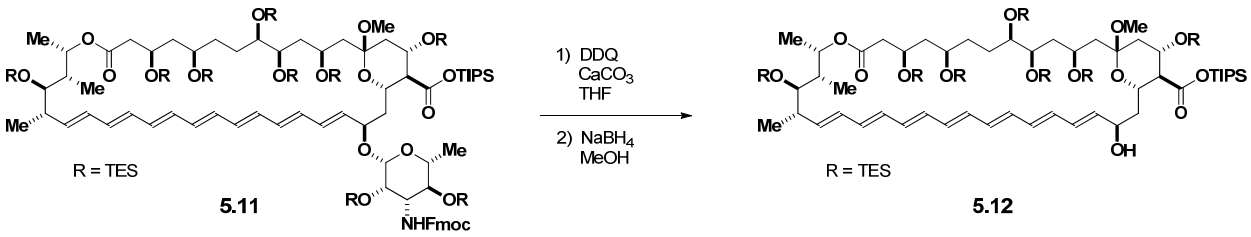

allylic alcohol **5.12**

Intermediate **5.11** (12.5 g, 5.35 mmol, 1 eq) was azeotropically dried with toluene and placed under vacuum overnight. THF (100 mL) was added. The resulting solution was cooled to 0 ^oC, and DDQ (1.82 g, 8.03 mmol, 1.5eq) and $CaCO_3$ (5.3 g, 53.5 mmol, 10 eq) were added. The reaction was warmed to room temperature and quenched after 30 min with saturated aqueous sodium bicarbonate and extracted with ether. The organic layer was washed with water

and then saturated sodium chloride. The organic layer was dried with sodium sulfate and filtered. The solvent was removed under reduced pressure, and flash column chromatography (SiO_2; Ether:Hexane 1:4) purification yielded the enone as a dark red solid. This intermediate is sensitive to silica gel and was immediately subjected to the next reaction conditions.

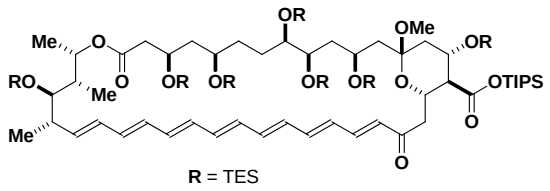

TLC (Ether:Hexane 3:17)

R_f = 0.35, stained by CAM

LRMS (ESI)

Calculated for $C_{93}H_{180}NO_{14}Si_8$ $(M + Na)^+$: 1768.1

Found: 1768.0

The enone intermediate was azeotropically dried with toluene. THF (10 mL) and MeOH (20 mL) was added. The resulting solution was cooled to 0 ^oC, and $NaBH_4$ (1.08 g, 28.6 mmol, 5.3 eq) was added. The reaction was quenched after 30 min with 1M aqueous ammonium chloride and extracted with ether. The organic layer was washed with water and then saturated sodium chloride. The organic layer was dried with sodium sulfate and filtered. The solvent was removed under reduced pressure, and flash column chromatography (SiO_2; Ether:Hexane 1:9 → 1:4) purification yielded the **5.12** as a yellow-orange solid. This intermediate is not stable to long term storage and extended periods on silica gel. (4.5 g, 2.57 mmol, 48 % 2 steps).

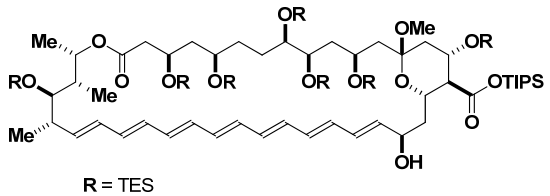

5.12

TLC (Ether:Hexane 1:4)

R_f = 0.44, stained by CAM

^{1}HNMR (500 MHz, $CD_3C(O)CD_3$)

δ 6.49-6.10 (m, 13H), 5.53 (m, 1H), 4.68 (m, 1H), 4.50 (m, 2H), 4.22 (m, 1H), 4.15 (m, 1H), 4.06 (m, 1H), 4.00 (m, 1H), 3.91 (d, *J* = 4 Hz, 1H), 3.83 (m, 1H), 3.68 (m, 1H), 3.63 (m, 1H), 3.15 (s, 3H), 2.55 (m, 2H), 2.42 (m, 1H), 2.36 (m, 1H), 2.13 (m, 1H), 2.01 (m, 2H), 1.95-1.70 (m, 8H), 1.63 (m, 3H), 1.49 (m, 1H), 1.31 (m, 3H), 1.18-1.14 (m, 20H), 1.07-0.96 (m, 69H), 0.77-0.61 (m, 43H).

^{13}CNMR (125 MHz, $CD_3C(O)CD_3$)

δ 172.2, 170.5, 139.6, 138.6, 134.8, 134.7, 134.0, 133.3, 133.1, 133.0, 132.8, 132.7, 131.7, 131.6, 130.8, 127.9, 101.1, 76.7, 74.0, 73.2, 71.0, 69.3, 69.1, 67.4, 67.3, 59.2, 48.0, 47.8, 44.4, 43.5, 41.8, 41.3, 40.6, 35.5, 27.4, 19.8, 19.2, 18.4, 18.3, 12.8, 11.2, 7.7, 7.6, 7.5, 7.4, 7.3, 6.4, 6.2, 6.1, 5.9, 5.8.

LRMS (ESI)

Calculated for $C_{93}H_{182}NO_{14}Si_8$ $(M + Na)^+$: 1770.2

Found: 1770.2

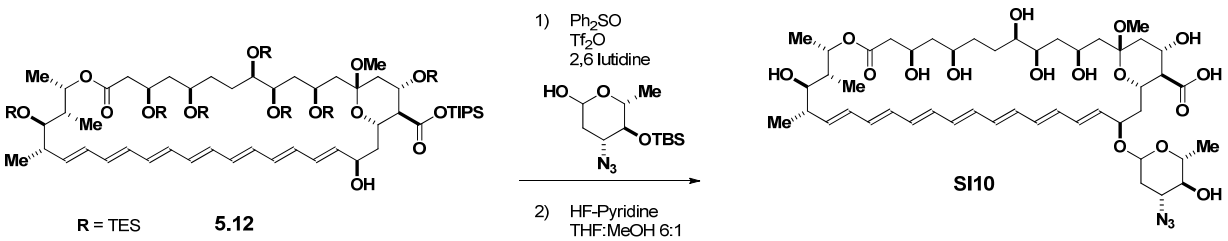

octaol **SI10**

Intermediate **5.12** (2.5 g, 1.29 mmol, 1 eq) was azeotropically dried with toluene and placed under vacuum overnight. Hexane (80 mL) was added followed by activated 4 angstrom molecular sieves. The resulting solution was allowed to stir at room temperature while the sugar donor was prepared. The sugar donor (739 mg, 2.57 mmol, 2.0 eq) was dissolved in DCM (26 mL). Diphenyl sulfoxide (911 mg, 4.50 mmol, 3.5 eq) and activated 4 angstrom molecular sieves

were added. The reaction was stirred for 4 hours at room temperature. 2,6-lutidine (675 μL, 5.79 mmol, 4.5 eq) was added, and the reaction was cooled to -60 °C. Triflic anhydride (1M in DCM) (2.57 mL, 2.57 mmol, 2 eq) was added slowly. The reaction was warmed to -20 °C and stirred for 1.5 hrs. 2,6-lutidine (600 μL, 5.15 mmol, 4.0 eq) was added to the solution of **5.12**, and it was cooled to -30 °C. The sugar donor reaction was cannulated over to the solution of **5.12**. The reaction was warmed to 0 °C for 1hr. The reaction was quenched with saturated aqueous sodium bicarbonate and extracted with ether. The organic layer was washed with copper sulfate, water, and saturated sodium chloride. The organic layer was dried with sodium sulfate and filtered. The solvent was removed under reduced pressure, and column chromatography (SiO_2; Ether:Hexane 3:47) purification yielded the glycosidated product as a mixture of isomers ranging from 1:1 to 2:1 α:β (2.12 g, 1.06 mmol, 82 %). The isomers were inseparable at this stage and were taken directly on the next reaction.

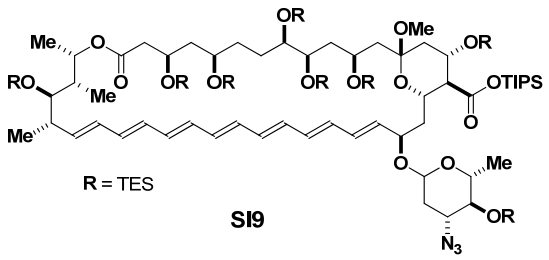

SI9

TLC (Ether:Hexane 1:19)

R_f = 0.25, stained by CAM

LRMS (ESI)

Calculated for $C_{105}H_{205}N_3O_{16}Si_9$ $(M + Na)^+$: 2039.3

Found: 2039.9

The glycosidated product **SI9** (710 mg, 352 μmol, 1 eq) was azeotropically dried with toluene in a teflon vial. THF (3 mL) was added, and the solution was cooled to 0 °C. Pyridine (3 mL) in a teflon vial was cooled to 0 °C, and MeOH (0.5 mL) was added. 70% HF-pyridine was added slowly to the pyridine-MeOH solution at 0 °C. This solution was transferred slowly to the THF solution of glycosylated intermediate. The reaction was allowed to stir for 12 hours at room

temperature. The reaction was quenched at 0 °C with excess MeOTMS and diluted with toluene. The solution was concentrated under reduced pressure and diluted again with toluene. This process was repeated 3 times to remove all of the pyridine. The product is base sensitive, especially if water is present, – care must be taken not to concentrate directly to solid with pyridine present. Reversed phase HPLC purification (C18 SiO_2; MeCN:5 mM NH_4OAc in H_2O 1:19 → 19:1 over 30 minutes) allowed the α and β isomers to be separated and yielded 260 mg, 275 μmol, 78 %.

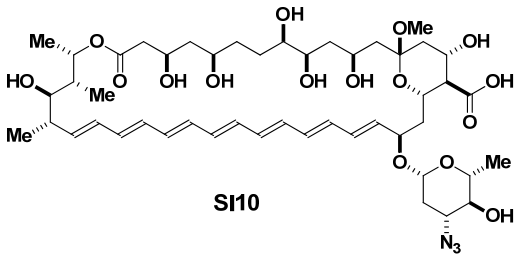

SI10

HPLC (C18 SiO_2; MeCN:5 mM NH_4OAc in H_2O 1:19 → 19:1 over 30 minutes)

t_r = 17.1 min, α

t_r = 16.2 min, β

^{1}HNMR (500 MHz, $CD_3S(O)CD_3$)

δ 6.32-6.05 (m, 12H), 5.81 (m, 1H), 5.60 (m, 1H), 4.97 (m, 1H), 4.58 (m, 1H), 4.43 (m, 1H), 3.99 (m, 1H), 3.84 (m, 1H), 3.73 (m, 2H), 3.52 (m, 2H), 3.32 (m, 1H), 3.21 (m, 1H), 3.10 (m, 1H), 3.00 (s, 3H), 2.93 (m, 2H), 2.29 (m, 1H), 2.16 (m, 2H), 2.01 (m, 2H), 1.76 (m, 1H), 1.68 (m, 1H), 1.52-1.23 (m, 14H), 1.15 (d, *J* = 5.5 Hz, 3H), 1.11 (d, *J* = 5.5 Hz, 3H), 1.03 (d, *J* = 6 Hz, 3H), 0.89 (d, *J* = 7 Hz, 3H).

HRMS (ESI)

Calculated for $C_{48}H_{73}N_3O_{16}$ $(M + Na)^+$: 970.4889

Found: 970.4897

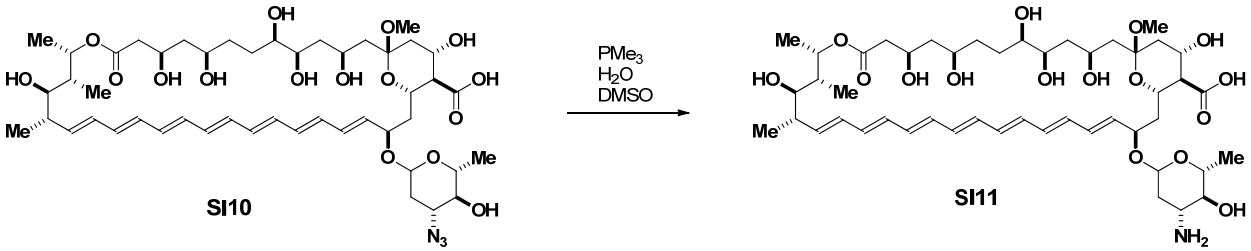

amine **SI11**

SI10 (19 mg, 20 µmol, 1 eq) was dissolved in DMSO (657 µL). Added water (36 µL, 200 µmol, 100 eq) and trimethyl phosphine (1M) (60 µL, 60 µmol, 3 eq). The reaction was heated to 55 °C for 3 hrs. Reversed phase HPLC purification (C18 SiO_2; MeCN:5 mM NH_4OAc in H_2O 1:19 → 19:1 over 30 minutes) yielded **SI11** (10.5 mg, 11.4 µmol, 57 %).

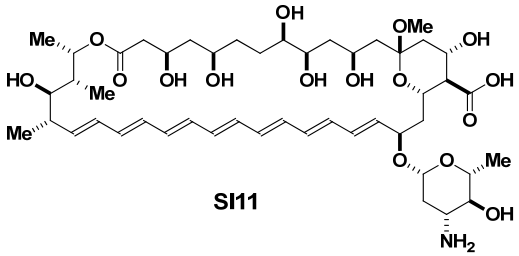

HPLC (C18 SiO_2; MeCN:5 mM NH_4OAc in H_2O 1:19 → 19:1 over 30 minutes)

t_r = 14.3 min

^{1}HNMR (500 MHz, $CD_3S(O)CD_3$)

δ 6.34-6.06 (m, 12H), 5.90 (m, 1H), 5.62 (m, 1H), 4.94 (m, 1H), 4.63 (m, 1H), 4.52 (m, 1H), 3.97 (m, 1H), 3.90 (m, 1H), 3.73 (m, 2H), 3.56 (m, 1H), 3.38 (m, 1H), 3.30 (m, 1H), 3.25 (m, 1H), 3.15 (m, 1H), 2.95 (m, 5H), 2.25 (m, 4H), 2.03 (m, 1H), 1.77 (m, 3H), 1.53-1.24 (m, 13H), 1.17 (d, *J* = 5 Hz, 3H), 1.11 (d, *J* = 6 Hz, 3H), 1.03 (d, *J* = 6 Hz, 3H), 0.89 (d, *J* = 6.5 Hz, 3H).

HRMS (ESI)

Calculated for $C_{48}H_{75}NO_{16}$ $(M + H)^+$: 922.5164

Found: 922.5169

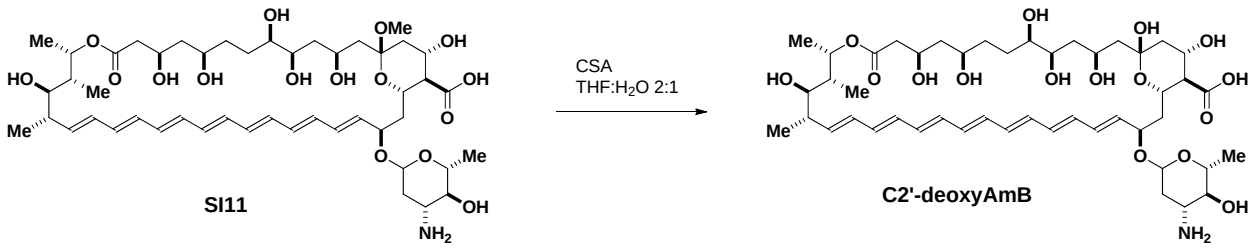

C2'-deoxyAmB

SI11 (5 mg, 5.42 μmol, 1 eq) was placed in a vial. 180 μL of a 180 mM solution of CSA in 2:1 THF:H_2O was added. The reaction was stirred for 30 min. Reversed phase HPLC purification (C18 SiO_2; MeCN:5 mM NH_4OAc in H_2O 1:19 → 19:1 over 30 minutes) yielded **C2'-deoxyAmB** (3.9 mg, 4.34 μmol, 80 %).

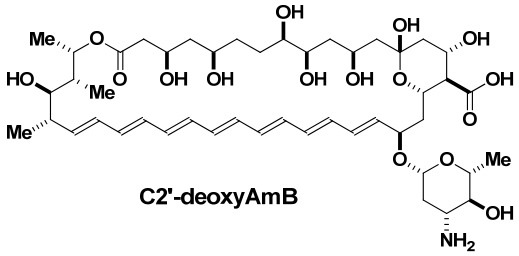

HPLC (C18 SiO_2; MeCN:5 mM NH_4OAc in H_2O 1:19 → 19:1 over 30 minutes)

t_r = 15.1 min

^{1}HNMR (500 MHz, $CD_3S(O)CD_3$)

δ 6.47-5.94 (m, 11H), 5.73 (m, 1H), 5.42 (m, 2H), 5.23 (m, 1H), 4.77 (m, 1H), 4.61 (m, 1H), 4.38 (m, 1H), 4.26 (m, 1H), 4.15 (m, 1H), 4.06 (m, 1H), 3.99 (m, 1H), 3.70-3.20 (m, 4H), 3.09 (m, 1H), 2.92 (m, 1H), 2.36-2.16 (m, 5H), 1.99 (m, 1H), 1.83-1.72 (m, 4H), 1.56-1.51 (m, 4H), 1.39-1.23 (m, 7H), 1.15 (d, *J* = 5.5 Hz, 3H), 1.11 (d, *J* = 6 Hz, 3H), 1.03 (d, *J* = 6 Hz, 3H), 0.91 (d, *J* = 6.5 Hz, 3H).

HRMS (ESI)

Calculated for $C_{47}H_{73}NO_{16}$ $(M + H)^+$: 908.5008

Found: 908.5007

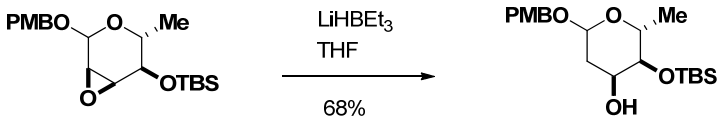

SI12

alcohol **SI12**

Epoxide intermediate (8 g, 21 mmol, 1 eq) was dissolved in THF (263 mL). The resulting solution was cooled to 0 ^{o}C, and $LiHBEt_3$ (1M in THF) (105 mL, 105 mmol, 5eq) was added slowly. The reaction heated to 60 ^{o}C for 2.5 hrs. The reaction was cooled to 0 ^{o}C and quenched with 1M ammonium chloride. The mixture was extracted with ether. The organic layer was washed with water and saturated sodium chloride. The organic layer was dried with sodium sulfate and filtered. The solvent was removed under reduced pressure, and column chromatography (SiO_2; Ether:Hexane 1:4 → 1:3) purification yielded **SI2** as an oil (5.47 g, 14.3 mmol, 68 %).

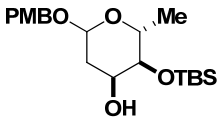

SI12

TLC (Ether:Hexane 3:7)

R_f = 0.38, stained by CAM

^{1}HNMR (500 MHz, $CDCl_3$)

δ 7.27 (d, *J* = 8.5 Hz, 2H), 6.88 (d, *J* = 9 Hz, 2H), 4.87 (d, *J* = 4 Hz, 1H), 4.66 (d, *J* = 12 Hz, 1H), 4.44 (d, *J* = 11.5 Hz, 1H), 4.04 (m, 1H), 3.92 (m, 1H), 3.81 (s, 3H), 3.32 (dd, *J* = 3 Hz, *J* = 9.5 Hz, 1H), 3.19 (m, 1H), 2.14 (dd, *J* = 3.5 Hz, *J* = 15 Hz, 1H), 1.89 (td, *J* = 3.5 Hz, *J* = 14.5 Hz, 1H), 1.26 (d, *J* = 6.5 Hz, 3H), 0.93 (s, 9H), 0.12 (s, 6H).

^{13}CNMR (125 MHz, $CDCl_3$)

δ 159.5, 129.9, 114.0, 95.7, 75.1, 68.9, 68.0, 63.7, 55.5, 35.7, 26.1, 18.4, -4.0, -4.4.

HRMS (ESI)

Calculated for $C_{20}H_{34}O_5Si$ $(M + Na)^+$: 405.2073

Found: 405.2078

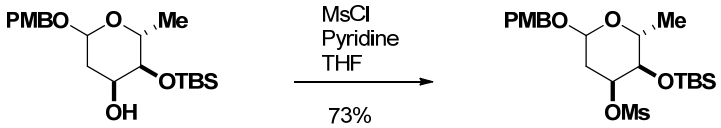

SI12 **5.14**

mesylate **5.14**

SI12 (4.83 g, 12.6 mmol, 1 eq) was dissolved in THF (15 mL). Pyridine (10.2 mL, 126 mmol, 10 eq) and MsCl (3.17 mL, 41 mmol, 3.25 eq) were added. The reaction was stirred overnight. The reaction was then quenched with saturated aqueous sodium bicarbonate and extracted with ether. The organic layer was washed with 1M ammonium chloride, water, and saturated sodium chloride. The organic layer was dried with sodium sulfate and filtered. The solvent was removed under reduced pressure, and column chromatography (SiO_2; Ether:Hexane 2:3) purification yielded **5.14** as a solid (4.24 g, 9.2 mmol, 73 %).

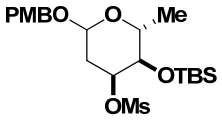

5.14

TLC (Ether:Hexane 2:3)

R_f = 0.27, stained by CAM

^{1}HNMR (500 MHz, $CDCl_3$)

δ 7.27 (d, *J* = 9 Hz, 2H), 6.88 (d, *J* = 8.5 Hz, 2H), 4.90 (dd, *J* = 3 Hz, *J* = 8 Hz, 2H), 4.66 (d, *J* = 11.5 Hz, 1H), 4.35 (d, *J* = 11 Hz, 1H), 4.13 (m, 1H), 3.80 (s, 3H), 3.43 (dd, *J* = 3 Hz, *J* = 9 Hz, 1H), 2.91 (s, 3H), 2.41 (dd, *J* = 3 Hz, *J* = 15 Hz, 1H), 1.96 (m, 1H), 1.23 (d, *J* = 6.5 Hz, 3H), 0.93 (s, 9H), 0.14 (s, 3H), 0.11 (s, 3H).

^{13}CNMR (125 MHz, $CDCl_3$)

δ 159.4, 130.2, 129.6, 113.9, 94.8, 77.5, 72.7, 69.1, 64.3, 55.5, 39.9, 34.5, 26.0, 18.3, -3.9, -4.6.

HRMS (ESI)

Calculated for $C_{21}H_{36}O_5SiS$ $(M + Na)^+$: 483.1849

Found: 483.1848

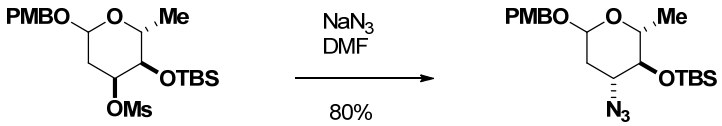

5.14 **SI13**

azide **SI13**

5.14 (1.6 g, 3.47 mmol, 1 eq) was dissolved in DMF (15 mL). Sodium azide (1.6 g, 24.3 mmol, 7 eq) was added. The reaction heated to 160 °C for 1.5 hrs. The reaction was cooled to room temperature. The reaction was quenched with saturated aqueous sodium bicarbonate and extracted with ether. The organic layer was washed with water, and saturated sodium chloride. The organic layer was dried with sodium sulfate and filtered. The solvent was removed under reduced pressure, and column chromatography (SiO_2; Ether:Hexane 1:19) purification yielded **SI13** as a solid (1.13 g, 2.78 mmol, 80 %).

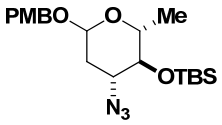

SI13

TLC (Ether:Hexane 1:19)

R_f = 0.30, stained by CAM

^{1}HNMR (500 MHz, $CDCl_3$)

δ 7.29 (d, *J* = 9 Hz, 2H), 6.91 (d, *J* = 8.5 Hz, 2H), 4.91 (d, *J* = 3 Hz, 2H), 4.61 (d, *J* = 11.5 Hz, 1H), 4.39 (d, *J* = 11 Hz, 1H), 3.82 (s, 3H), 3.71 (m, 2H), 3.10 (t, *J* = 9 Hz, 1H), 2.19 (dd, *J* = 5 Hz, *J* = 13.5 Hz, 1H), 1.73 (td, *J* = 4 Hz, *J* = 12.5 Hz, 1H), 1.27 (d, *J* = 6 Hz, 3H), 0.94 (s, 9H), 0.22 (s, 3H), 0.13 (s, 3H).

^{13}CNMR (125 MHz, $CDCl_3$)

δ 159.6, 129.9, 129.8, 114.1, 95.4, 76.7, 68.9, 68.8, 61.8, 55.5, 35.9, 26.2, 18.7, 18.4, -3.9, -4.0.

HRMS (ESI)

Calculated for $C_{20}H_{33}N_3O_4Si$ $(M + Na)^+$: 430.2138

Found: 430.2156

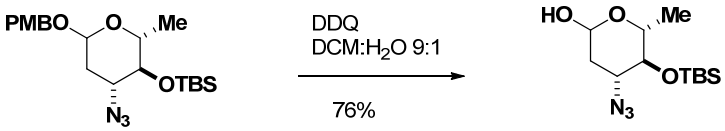

SI13 **5.15**

alcohol **5.15**

SI13 (6.5 g, 15.9 mmol, 1 eq) was dissolved in DCM:H_2O 9:1 (160 mL). The solution was cooled to 0 °C, and DDQ (4.3 g, 19.1 mmol, 1.2 eq) was added. The reaction was warmed to

room temperature and stirred for 2 hrs. The reaction was quenched with saturated aqueous sodium bicarbonate and extracted with ether. The organic layer was washed with water, and saturated sodium chloride. The organic layer was dried with sodium sulfate and filtered. The solvent was removed under reduced pressure, and column chromatography (SiO_2; Ether:Hexane 1:19) purification followed by (C18 SiO_2, water:MeCN 1:4) yielded **5.15** as a solid (3.47 g, 12.1 mmol, 76 %).

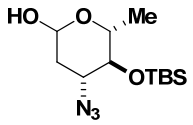

5.15

TLC (EtOAc:Hexane 1:4)

R_f = 0.31, stained by CAM

(H_2O:MeCN 1:4)

R_f = 0.50, stained by CAM

HRMS (ESI)

Calculated for $C_{12}H_{25}N_3O_3Si$ $(M + Na)^+$: 310.1563

Found: 310.1566

5-7 References

1. Silberstein, A. *J. Membr. Biol.* **1998**, *162*, 117-126.
2. Baran, M.; Mazerski, M. *Biophys. Chem.* **2002**, *95*, 125-133.
3. Neumann, A.; Czub, J.; Baginski, M. *J. Phys. Chem. B* **2009**, *113*, 15875-15885.
4. Matsumori, N.; Sawada, Y.; Murata, M. *J. Am. Chem. Soc.* **2005**, *127*, 10667-10675.
5. Croatt, M. P.; Carreira, E. M. *Org. Lett.* **2011**, *13*, 1390-1393.
6. Barton, D.; Serebryakov, E. *Proc. Chem. Soc.* **1962**, 309.
7. Garegg, P.; Samuelsson, B. *J. Chem. Soc., Perkin Trans. 1* **1980**, 2866-2869.

8. Hutchins, R.; Kandasamy, D.; Dux, F.; Maryanoff, C.; Rotstein, D.; Goldsmith, B.; Burgoyne, W.; Cistone, F.; Dalessandro, J.; Puglis, J. *J. Org. Chem.* **1977**, *43*, 2259-2267.
9. Nicolaou, K. C.; Chakraborty, T. K.; Ogawa, Y.; Daines, R. A.; Simpkins, N. S.; Furst, G. T. *J. Am. Chem. Soc.* **1988**, *110*, 4660-4672.
10. Nicolaou, K. C.; Daines, R. A.; Ogawa, Y.; Chakraborty, T. K. *J. Am. Chem. Soc.* **1988**, *110*, 4696-4705.
11. Tsuchikawa, H.; Matsushita, N.; Matsumori, N.; Murata, M.; Oishi, T. *Tetrahedron Lett.* **2006**, *47*, 6187-6191.
12. Wilcock, B. C.; Uno, B. E.; Bromann, G. L.; Clark, M. J.; Anderson, T. M.: Burke, M. D. *Nature Chemistry* **2012**, *4*, 996-1003.
13. Mitsunobu, O.; Yamada, M. *Bull. Chem. Soc. Jpn.* **1967**, *40*, 2380-2382.
14. Matsumori, N. *et al*. *Chem. Biol.* **2004**, *11*, 673-679.
15. Palacios, D. S.; Anderson, T. M.; Burke, M. D. *J. Am. Chem. Soc.* **2007**, *129*, 13804-13805.
16. Guo, H.; O'Doherty, G. A. *Angew. Chem. Int. Ed.* **2007**, *46*, 5206.
17. Wu, X.; Li, X.; Zanotti-Gerosa, A.; Pettman, A.; Liu, J.; Mills, A. J.; Xiao, J. *Chem. Eur. J.* **2008**, *14*, 2209.
18. Nicolaou, K. C.; Daines, R. A.; Chakraborty, T. K.; Ogawa, Y. *J. Am. Chem. Soc.* **1987**, *109*, 2821-2822.
19. Szpilman,A. M.; Cereghetti, D. M.; Manthrope, j. M.; Wurtz, N. R.; Carreira, E. M. *Chem. Eur. J.* **2009**, *15*, 7117-7128.
20. Hou, D.; Lowary, T. L. *Carbohydr. Res.* **2009**, *344*, 1911-1940.
21. Marzabadi, C. H.; Franck, R. W. *Tetrahedron* **2000**, *56*, 8385-8417.
22. Tanaka, T.; Yoshizawa, A.; Takahashi, T. *Angew. Chem. Int. Ed.* **2007**, *46*, 2505-2507.
23. Chao, C.; Yen, Y.; Hung, W.; Mong, K. T. *Adv. Synth. Catal.* **2011**, *353*, 879-884.
24. Nguyen, H. M.; Poole, J. L.; Gin, D. Y. *Angew. Chem. Int. Ed.* **2001**, *40*, 414-417.
25. Codee, J.; Hossain, L.; Seeberger, P. *Org. Lett.* **2005**, *7*, 3251-3254.
26. Pangborn, A.B.; Giardello, M.A.; Grubbs, R.H.; Rosen, R.K.; Timmers, F.J. *Organometallics* **1996**, *15*, 1518-1520.